

Ogata, K., Weert, A., Betlem, P., Birchall, T., and Senger, K., 2023, Shallow and deep subsurface sediment remobilization and intrusion in the Middle Jurassic to Lower Cretaceous Agardhfjellet Formation (Svalbard): *Geosphere*, v. 19, <https://doi.org/10.1130/GES02555.1>.

Shallow and deep subsurface sediment remobilization and intrusion in the  
Late Jurassic Agardhfjellet Formation (Svalbard)

---

Supplemental material

---

*by*

Kei Ogata, Annelotte Weert, Peter Betlem, Thomas Birchall, Kim Senger

2023

# Contents

<b>1</b>	<b>Fieldwork data</b>	<b>2</b>		
<b>2</b>	<b>Optical microscopy</b>	<b>4</b>		
2.1	Upper complex . . . . .	4	3.1.1	I1S2 . . . . . 33
2.1.1	Injectite 1 . . . . .	4	3.1.2	I2S2 . . . . . 34
2.1.2	Injectite 2 . . . . .	8	3.2	Lower complex . . . . . 37
2.2	Lower complex . . . . .	9	3.2.1	I3S1-1 . . . . . 37
2.2.1	Injectite 3 . . . . .	9	3.2.2	I4S1 . . . . . 39
2.2.2	Injectite 4 . . . . .	13	3.2.3	M6 . . . . . 42
2.2.3	M6 . . . . .	14	3.2.4	I5S1 . . . . . 43
2.2.4	Injectite 5 . . . . .	14	3.2.5	I6S1-2 . . . . . 47
2.2.5	Injectite 6 . . . . .	15	3.2.6	I7S1 . . . . . 48
2.2.6	Injectite 7 . . . . .	18	3.2.7	I7S2 . . . . . 49
2.2.7	M13 . . . . .	18	3.2.8	M13 . . . . . 51
2.3	Formations . . . . .	18	3.3	Formations . . . . . 54
2.3.1	Brentskardhaugen Bed . . . . .	18	3.3.1	F6 - Carolinefjellet Formation . . . . . 54
2.3.2	Slottsmøya Member . . . . .	18	3.3.2	F8 - Brentskardhaugen Bed . . . . . 55
2.3.3	Rurikfjellet Formation . . . . .	18	3.4	Mounds . . . . . 58
2.3.4	Carolinefjellet Formation . . . . .	22	3.4.1	M3-1 . . . . . 58
2.4	Mounds . . . . .	22	3.4.2	M4 . . . . . 59
2.4.1	M1 . . . . .	24	3.4.3	M8-2 . . . . . 60
2.4.2	M2 . . . . .	24	3.4.4	M12-1 . . . . . 61
2.4.3	M3 . . . . .	24	3.4.5	K1 . . . . . 63
2.4.4	M4 . . . . .	24	3.5	Lenses . . . . . 64
2.4.5	M5 . . . . .	24	3.5.1	L2-2 . . . . . 64
2.4.6	M7 . . . . .	24	<b>4</b>	<b>Micromorphology</b>
2.4.7	M8 . . . . .	28		<b>66</b>
2.4.8	M9 . . . . .	28	4.1	Upper Complex . . . . . 66
2.4.9	M10 . . . . .	28	4.1.1	Injectite 1 . . . . . 66
2.4.10	M11 . . . . .	28	4.1.2	Injectite 2 . . . . . 70
2.4.11	M12 . . . . .	28	4.2	Lower Complex . . . . . 71
2.4.12	K1 . . . . .	28	4.2.1	Injectite 3 . . . . . 71
2.5	Lenses . . . . .	31	4.2.2	Injectite 4 . . . . . 73
2.5.1	L1 . . . . .	31	4.2.3	M6 . . . . . 73
2.5.2	L2 . . . . .	31	4.2.4	Injectite 5 . . . . . 74
2.5.3	L3 . . . . .	31	4.2.5	Injectite 6 . . . . . 75
			4.2.6	Injectite 7 . . . . . 76
<b>3</b>	<b>SEM-EDS</b>	<b>33</b>	4.2.7	M13 . . . . . 77
3.1	Upper complex . . . . .	33	4.3	Formations . . . . . 77
			4.3.1	Brentskardhaugen Bed . . . . . 77
			4.3.2	Carolinefjellet Formation . . . . . 78



# 1 Fieldwork data

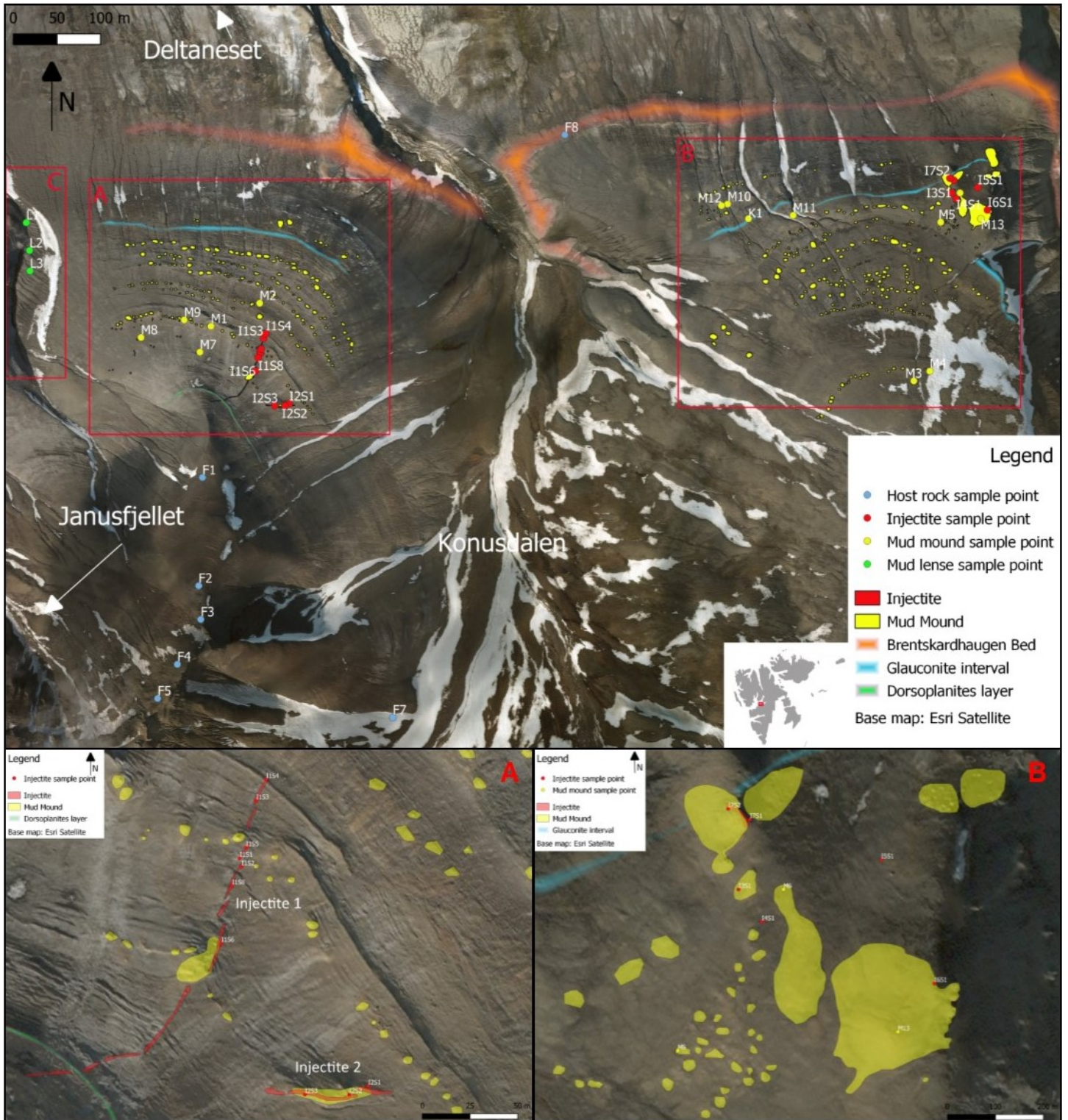


Figure S1: Map of the study area with the sample locations and interpret stratigraphic beds. The red squares mark three area's; (A): Upper injectite complex, (B): Lower complex, and (C): Micadalen. Below, two zoomed in maps with the locations of the injectites in the Upper complex (A) and Lower complex (B) areas are given

Sample nr.	Coordinates		Notes
	Latitude (°)	Longitude (°)	
I1S1	78.33892	15.85627	Upper complex, I1
I1S2	78.33888	15.85631	Upper complex, I1
I1S3	78.33919	15.85665	Upper complex, I1
I1S4	78.33929	15.85688	Upper complex, I1
I1S5	78.33897	15.85641	Upper complex, I1
I1S6	78.33852	15.85584	Upper complex, I1
I1S8	78.33879	15.85609	Upper complex, I1
I2S1	78.33785	15.85925	Upper complex, I2
I2S2	78.33781	15.85881	Upper complex, I2
I2S3	78.33781	15.85778	Upper complex, I2
M1	78.33944	15.85132	Mudflake + coal/wood
M2	78.33991	15.85626	Sample for comparison
M3	78.33832	15.92252	Big clasts + coal/wood
M4	78.33852	15.92413	Big quartz clast
M5	78.34157	15.92525	
I3S1	78.34217	15.92637	Lower complex, I3
I4S1	78.34205	15.92680	Lower complex, I4
M6	78.34217	15.92720	Lower complex, sill structure next to I4
I5S1	78.34228	15.92900	Lower complex, I5
I6S1	78.34182	15.92998	Lower complex, I6
I7S1	78.34243	15.92658	Lower complex, I7
I7S2	78.34247	15.92618	Lower complex, I7
M13	78.34164	15.92931	Lower complex, sand volcano
L1	78.34071	15.82561	Mica dalen lens
L2	78.34051	15.82491	Mica dalen lens
L3	78.34026	15.82713	Mica dalen lens
F1	78.33634	15.85046	Slottsmoya member
F2	78.33412	15.85008	Slottsmoya member/Rurik formation
F3	78.33343	15.85029	Rurik formation/top Agardhfjellet formation
F4	78.33251	15.84792	Rurik formation
F5	78.33181	15.84592	Rurik formation
F6	78.22691	15.60296	Caroline formation
F7	78.33142	15.86973	Agardhfjellet silt layer
F8	Sample not in situ		Brentskardhaugen Bed
M7	78.33891	15.85020	Isolated mount
M8	78.33921	15.84424	Isolated mount
K1	78.34164	15.90577	Glauconite interval
M9	78.33957	15.84861	Aligned mound
M10	78.34194	15.90366	Carbonate mound with large wood fragments
M11	78.34171	15.91030	Bioturbated bed
M12	78.34191	15.90304	

Table S1: GPS coordinates of all sample locations. Due to the abrupt ending of the fieldwork, sample F6 was collected along Vei 600 in Longyearbyen afterwards.

## 2 Optical microscopy

Here, short descriptions for the thin sections are given. Because the thin sections from the injectites (...) For the injectites, a bar diagram showing the overall grain content can be found below, in Figure S2. The data regarding the bulk sample composition: mineralogy, size, sphericity and roundness, can be found in section 4.

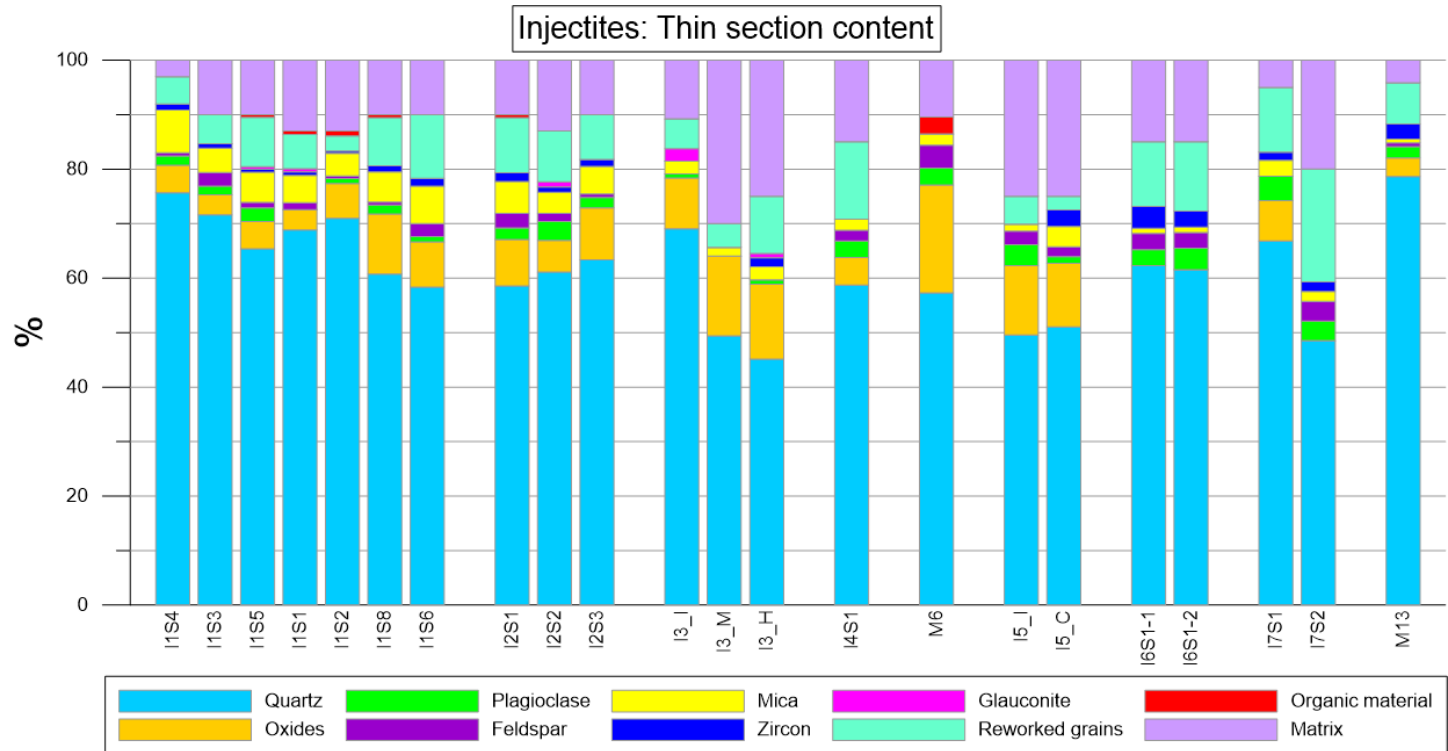


Figure S2: Bar diagram displaying the average content of all studied samples collected from the injectites. The samples of I1 and I2 are displayed from bottom (left) to top (right), I3 is divided into zones: host rock (H), transition host rock to injectite (M) and the injectites interior (I), I5 has two zones: the injectites interior (I) and zone with a clast (C).

### 2.1 Upper complex

#### 2.1.1 Injectite 1

Seven thin sections from Injectite 1 were studied. From the bottom to the top of the injectite: I1S4, I1S3, I1S5, I1S1, I1S2, I1S8 and I1S6 (Fig. S3). The thin sections are mainly composed of quartz grains (up to 70%), plagioclase, feldspar, mica's, zircon, glauconite, oxides and reworked grains (Fig.S2). Some thin sections also show small (<0,1 mm) fragments of shell fossils and carbon flakes with structures reminiscent of plants (referred to as organic material in Fig. S2) (Fig. S4.B & C). All grains have varying sizes (<0,1 - 3 mm), are sub- to well-rounded, poorly sorted, not oriented and lay in a fine-grained matrix (<0,1 mm) (Fig. S4.A). The matrix is composed of small particles of the same material filling the injectite. The quartz grains appear in different forms: with an undulose birefringence (70%), a normal birefringence (30%). Most quartz crystals are mono-crystalline, but around 10% of all quartz grains are poly-crystalline. Furthermore, apart from the grains displayed in Figure S2, chalcedony and chert were identified (Fig. S5.B). Cataclastic deformation bands were observed in samples I1S5 and I1S1 (Fig. S4.D & F), which are located in the middle part of the injectite. Quartz overgrown by feldspar with illite inclusions was observed, as well as feldspar grains that have the same illite inclusions. This was observed in samples I1S2 and I1S6 (Fig. S5.A).

Towards the top of the injectite, the grains seem to be more packed, with less matrix present. When looking at the edges of the injectites, some things are noticed. Going away from the edge of the injectite, into the injectites interior, the amount of big quartz grains (>0,5 mm) increases (Fig. S4.E). Also, the clay minerals, mainly glauconite, is present near the edges of the injectites, disappearing when moving into the injectites interior. Secondary infilling by calcite crystals is also observed (Fig. S4.D).

One thin section was taken from the unconsolidated material at the bottom of the injectite (I1S4). This thin section contains the same grain content as the other thin sections from Injectite 1. Overall, the matrix is missing, but some grains are still attached to each other by minor amounts of matrix (Fig. S5E & F).



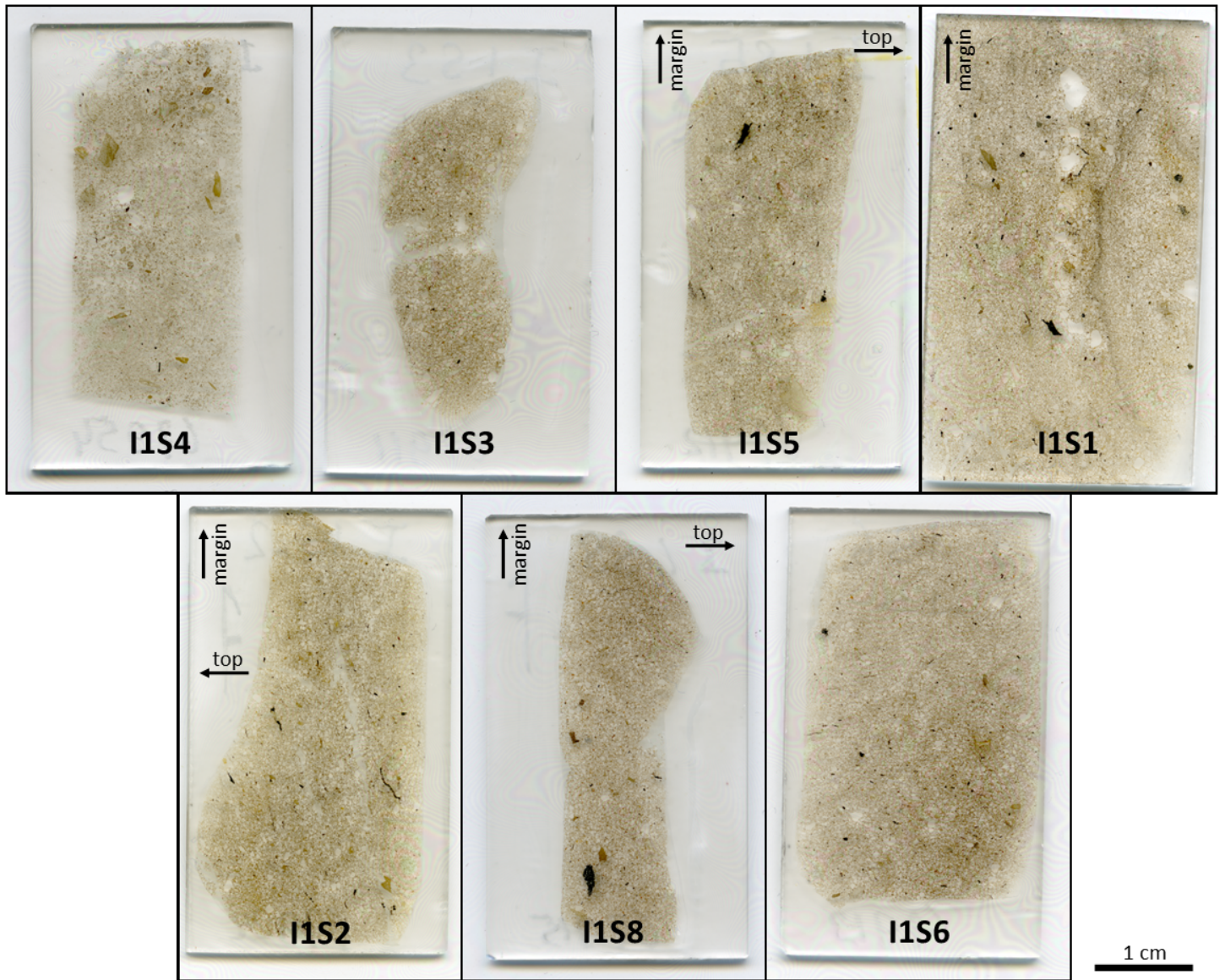


Figure S3: Scans from the thin sections of Injectite 1. The thin sections are arranged from the bottom to the top of the injectite: I1S4, I1S3, I1S5, I1S1, I1S2, I1S8, I1S6. Where available, the direction of the injectites top and margin are displayed.



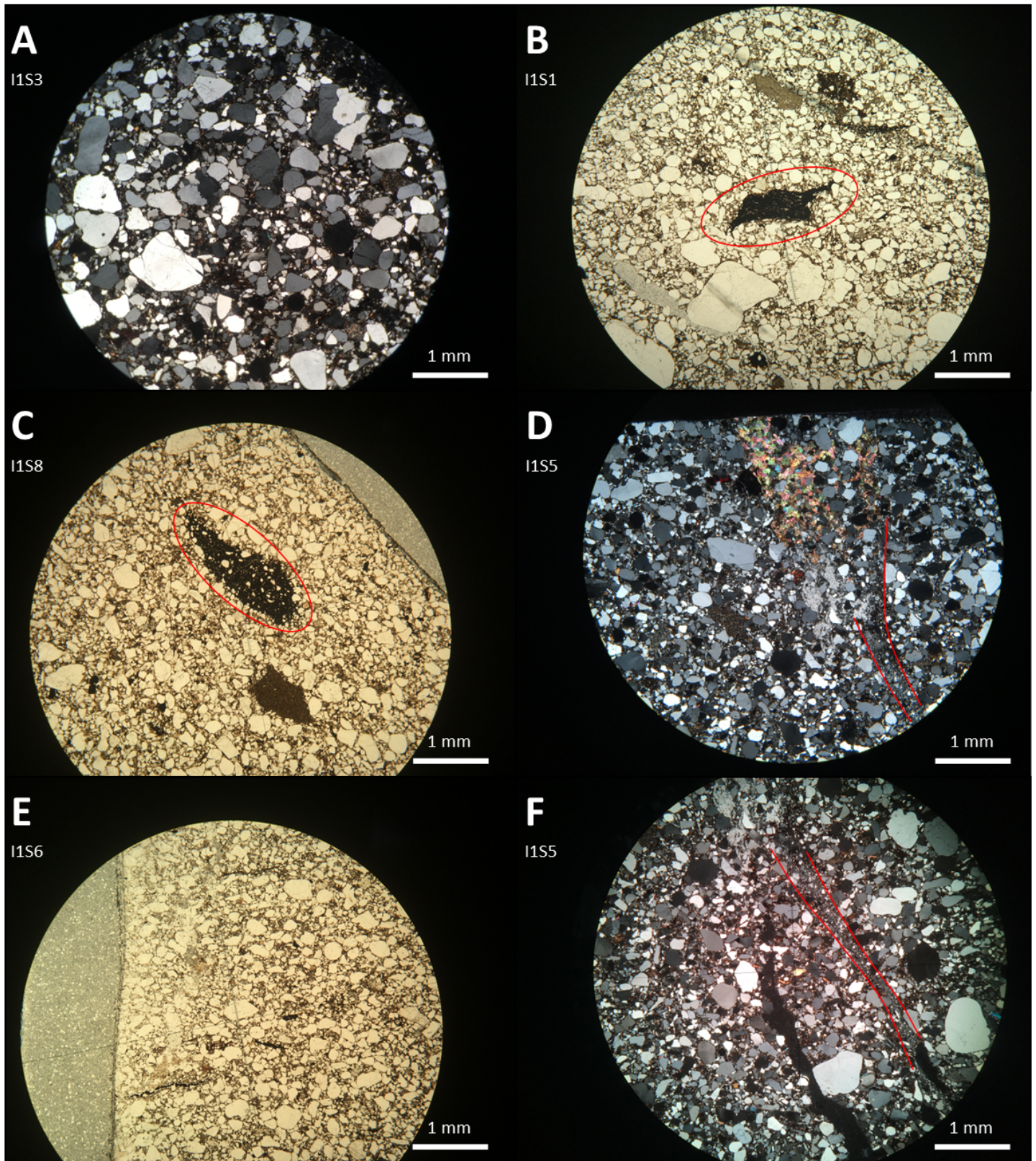


Figure S4: (A): XPL image of the interior, showing the different roundness of the clasts; (B, C): PPL images, with in the red circles the carbon clasts; (D): XPL image with the top of the image being the top of the injectite. The colored crystals are secondary calcites and the red stripes mark a cataclastic deformation band; (E): PPL image of the margin of the injectite on the left side of the image; (F): XPL image showing the continuation of the cataclastic deformation band of image D.



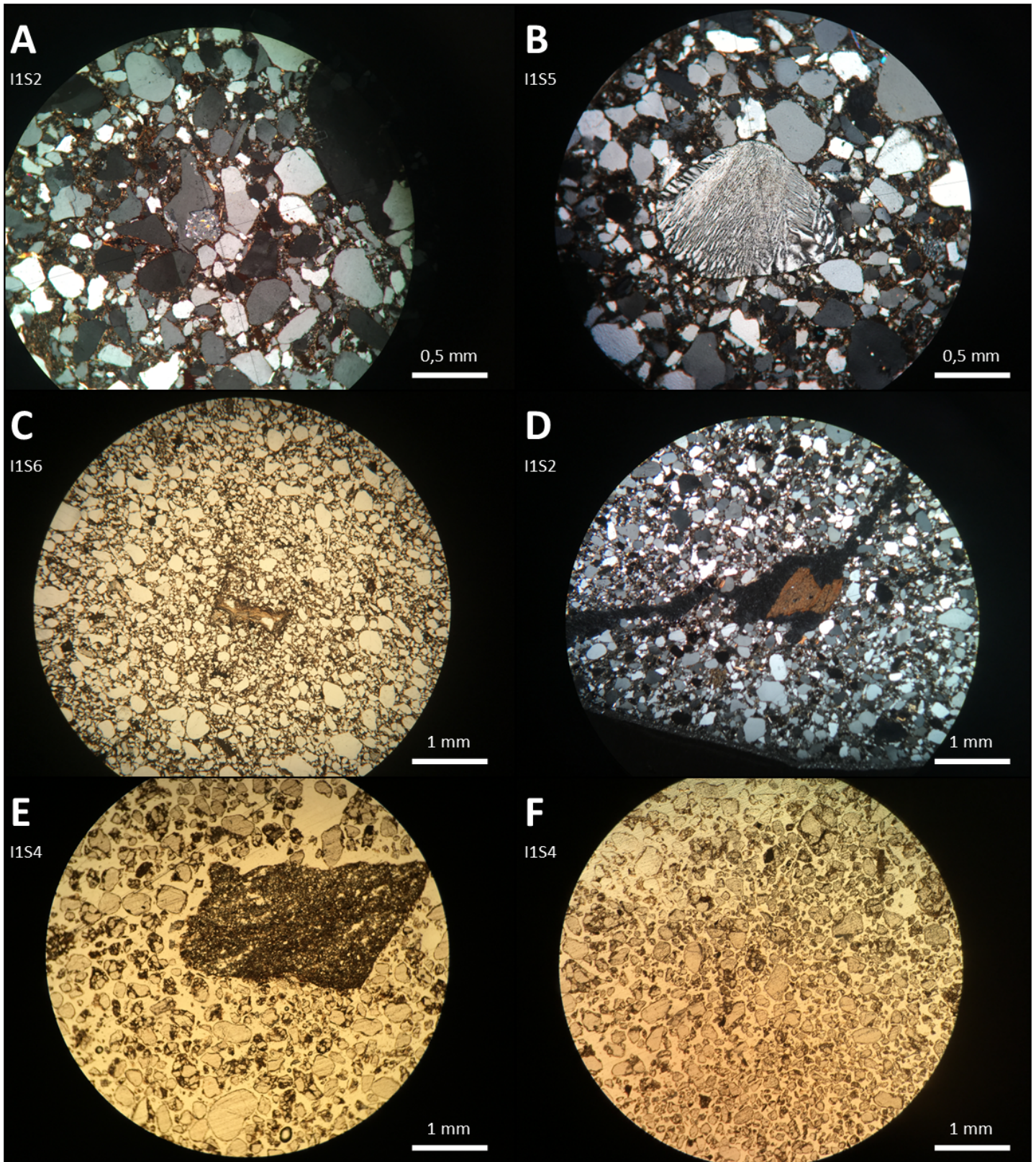


Figure S5: (A): XPL image showing feldspar with illite, overgrowing a quartz grain, SEM point B in sample I1S2; (B): XPL image of a chalcedony grain; (C): PPL image with some sort of reworked grain in the middle; (D): XPL image showing a crack (black material) through the thin section and a reworked grain (orange); (E, F): PPL images showing the unconsolidated material at the bottom of Injectite 1.



### 2.1.2 Injectite 2

Three thin sections were made originating from Injectite 2. From bottom to top of the injectite: I2S1, I2S2 and I2S3 (Fig. S7). The content and structure of the interior of Injectite 2 is very alike Injectite 1. Quartz makes up the biggest part of the composition (up to 65%). Plagioclase, feldspar, mica's, zircon, glauconite, oxides and reworked grains were observed (Fig. S2, as well as small ( $<0,1$  mm) fragments of shell fossils and carbon flakes (referred to as organic material in Fig. S2) (Fig. S6.B). Again, the grains have varying sizes ( $<0,1$  - 3 mm), are sub- and well-rounded, poorly sorted, not oriented and lay in a fine-grained matrix ( $<0,1$  mm) (Fig. S6A & D). The matrix is composed of clays and small particles of the same material filling the injectite. The quartz grains appear in different forms: with an undulose birefringence (70%), a normal birefringence (30 %). Most quartz crystals are mono-crystalline, but around 10% of all quartz grains are poly-crystalline. Furthermore, apart from the grains displayed in figure S2, chalcedony and chert were identified. Some quartz grains have cracks filled by secondary calcite (Fig. S6.C).

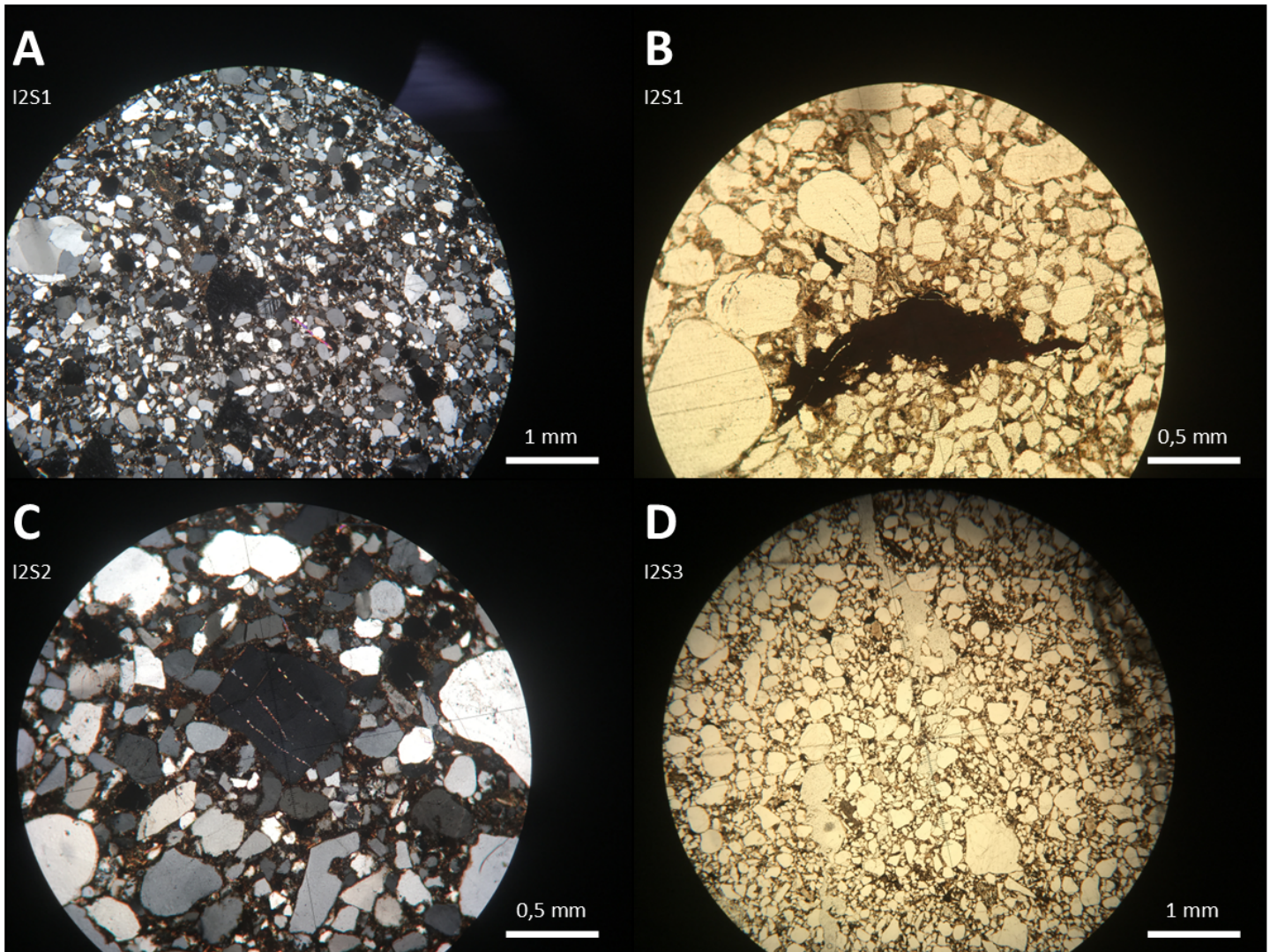


Figure S6: (A): XPL image showing the different clasts in the interior of Injectite 2; (B): PPL image of one of the carbon grains; (C): XPL image of a quartz grain with cracks, filled by secondary calcite; (D): PPL image of the interior of Injectite 2.



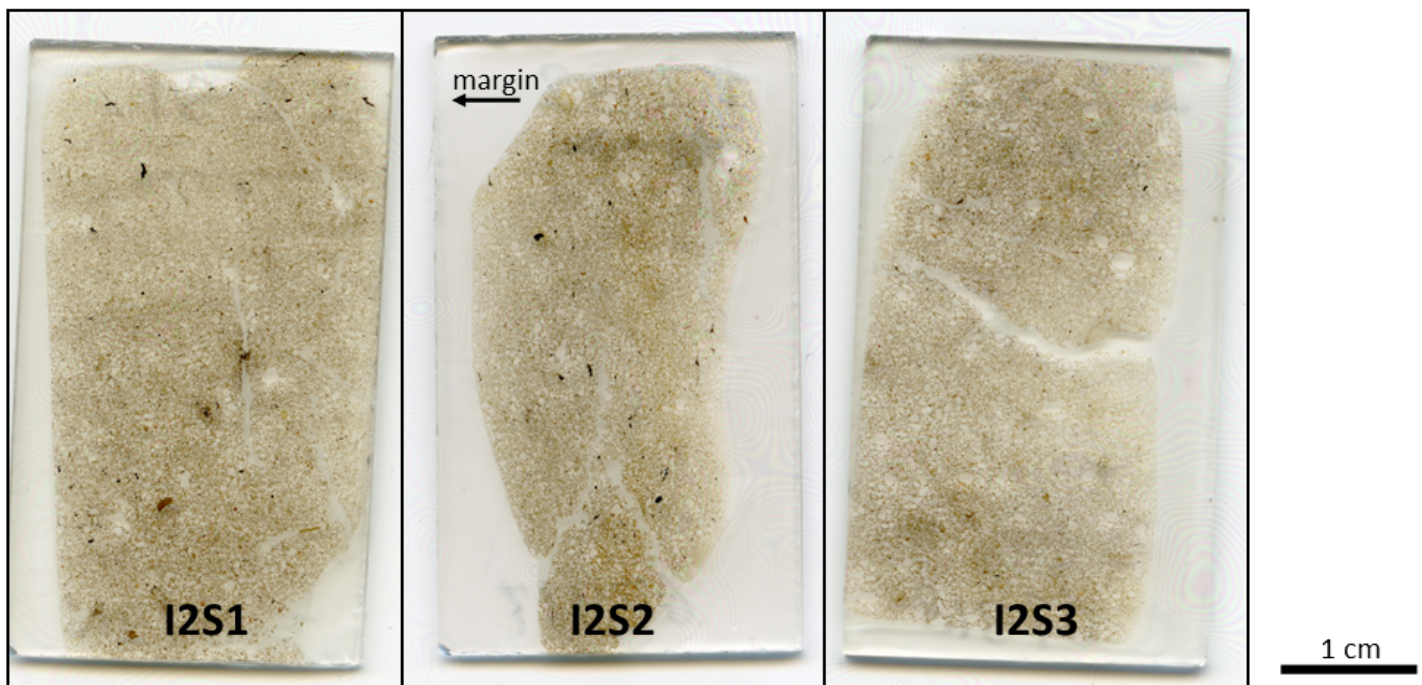


Figure S7: Scans from the thin sections of Injectite 2. The thin sections are arranged from the bottom to the top of the injectite: I2S1, I2S2, I2S3. Where available, the direction of the injectites top and margin are displayed.

## 2.2 Lower complex

### 2.2.1 Injectite 3

Four thin sections were made from samples of Injectite 3: 67633, 67634, I3S1-1 and I3S1-2. Samples 67633 and 67634 were taken during a previous fieldwork. Because Injectite 3 is thin (up to 5,5 cm in the field), all thin sections include the injectite interior (I), the margin (M) and the host rock (H) (Fig. S8, S9, S10.A). These will be described separately.

**Injectite interior:** The interior of Injectite 3 has some differences, compared with Injectites 1 and 2, which will be described below. Yet, the grain composition is about the same; about 70% of the grains is composed of quartz. Furthermore, similar amounts of plagioclase, feldspar, mica and reworked grains can be found. Quartz appears mono- and poly-crystalline (Fig. S10.B), with 45% of the quartz grains having an undulose extinction. Chert and chalcedony are present as well. This injectite contains some more glauconite and oxides and less zircon and organic material than Injectites 1 and 2 (Fig. S2, I3.I). Especially more pyrite crystals were observed, mainly as subhedral crystals, but the oxides also comprise barite crystals, framboidal pyrite or pyrite overprints organic remnants (Fig. S10.D). Thin section I3S1-1 contains a big (0,5 cm) chert grain, which has an accumulation of smaller grains at one of its edges (Fig. S10.F). Thin section I3S1-2 contains a big (2 cm) chert grain, crosscut by fractures, which are filled by calcite (Fig. S11.C). Like Injectite 1 and 2, the grains are well-to sub-rounded, poorly sorted and have varying sizes (<0,1 mm - 2 cm). Contrasting to Injectite 1 and 2, the grains seem to be oriented along the injectites margins and the space between the grains is filled by a yellow-brownish colored sparite cement. Around some grains, mainly quartz and reworked grains, a fibrous rim of cement is present (Fig. S10.C). Sample 67634 also shows some sort of carbon staining within the cement (Fig. S10.E). Three sorts of fractures were seen within the injectite interior: fractures only crosscutting grains (Fig. S11.D), fractures crosscutting both grains and cement (Fig. S11.A) and fractures that continue in the injectites margin and host rock (Fig. S10.A). The first two types of fractures are filled by cement and are oriented along the injectites margin. The fractures that crosscut the whole thin section have edge of isopachous cement with no further filling or uniform direction. Most of these fractures crosscut the thin sections in the length of the thin section. Apart from the fractures, also compressional crack were found (Fig. S10.B) oriented parallel to the injectite and filled with calcite crystals and material from the injectites interior.

**Margin:** Next to the injectites interior, the margin can be found, having an average thickness of 0,4 cm (Fig. S8, S11.B). The margin shows a gradual transition towards the injectites interior, but appear abrupt towards the host rock, with a sharp contact. Contrasting to the injectites interior, the margin of the injectite contains about 20% more cement. The present grains are smaller than the ones observed in the injectites interior (<0,1 mm - 1 mm) and only quartz grains, oxides, mica's and reworked grains make up the grain composition (Fig. S2, I3.M). Especially more oxides (about 5-10% more) were observed at the margins, mainly barite crystals that are attached to the edges of quartz crystals and framboidal pyrite



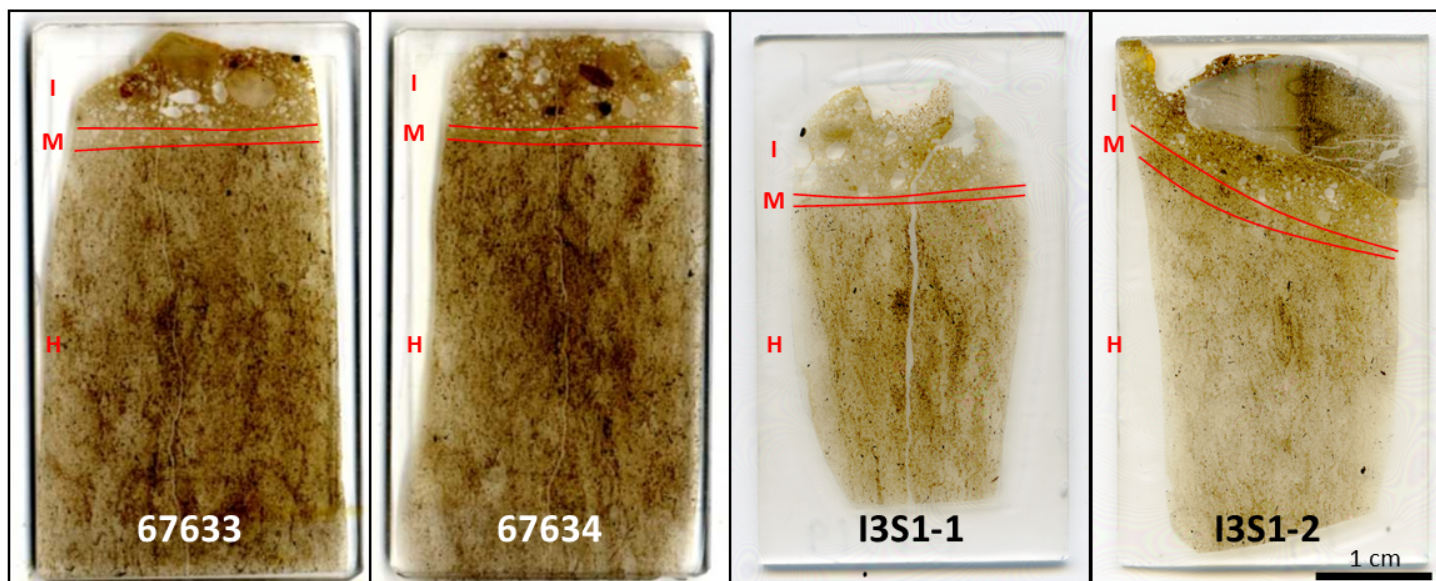


Figure S8: Scans from the thin sections of Injectite 3: 67633, 67634, I3S1-1 and I3S1-2. The scans of 67633 and 67634 have a lesser quality, due to the use of a different scanning device. For all thin sections, the locations of the host rock (H), injectites margin (M) and the injectite interior (I) are displayed.

structures. The grains are sub- to well-rounded, poorly sorted and are oriented parallel with the margin. The same type of fractures and cracks as found in the injectites interior, were found in the injectites margin.

**Host rock:** The host rock comprises material from the Agardhfjellet Formation. The material comprises well sorted, small (<0,1 - 0,2 mm), subangular grains in a blocky cement (Fig. S11.E, F). The grain composition is dominated by quartz, supplemented by oxides, plagioclase, feldspar, mica, zircon, glauconite, reworked grains and some fossils (Fig. S2, I3.H). Also here, quartz has some different appearances, but not all that are observed within the injectites; only mono-crystalline quartz is present, from which 20% have an undulose birefringence. Also, some chert grains were observed. The present fossils are remnants of shells, composed of calcite or pyrite and carbon flakes. Around these carbon remnants, the cement has a darker yellow-brownish color. A few grains show concave-cortex contacts, referring to some pressure solution. Within the host rock, only the fractures that crosscut the whole thin section were found.

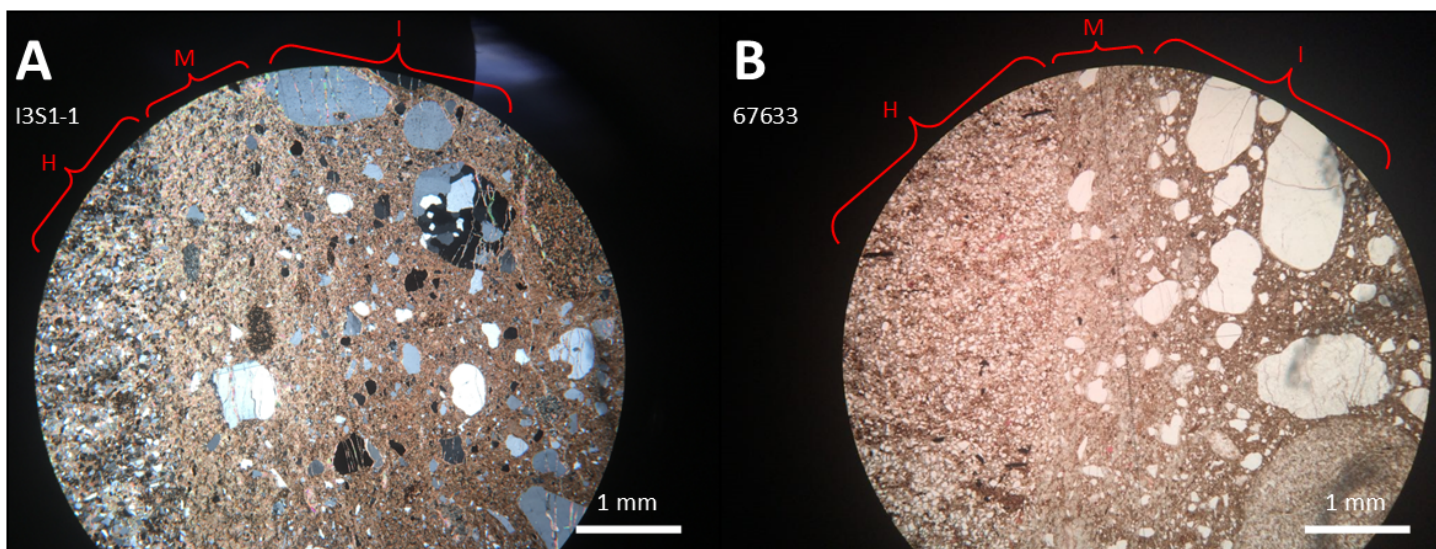


Figure S9: Pictures showing the injectites interior (I), injectites margin (M) and host rock (H). (A): XPL picture of thin section I3S1-1; (B): PPL picture of thin section 67633.



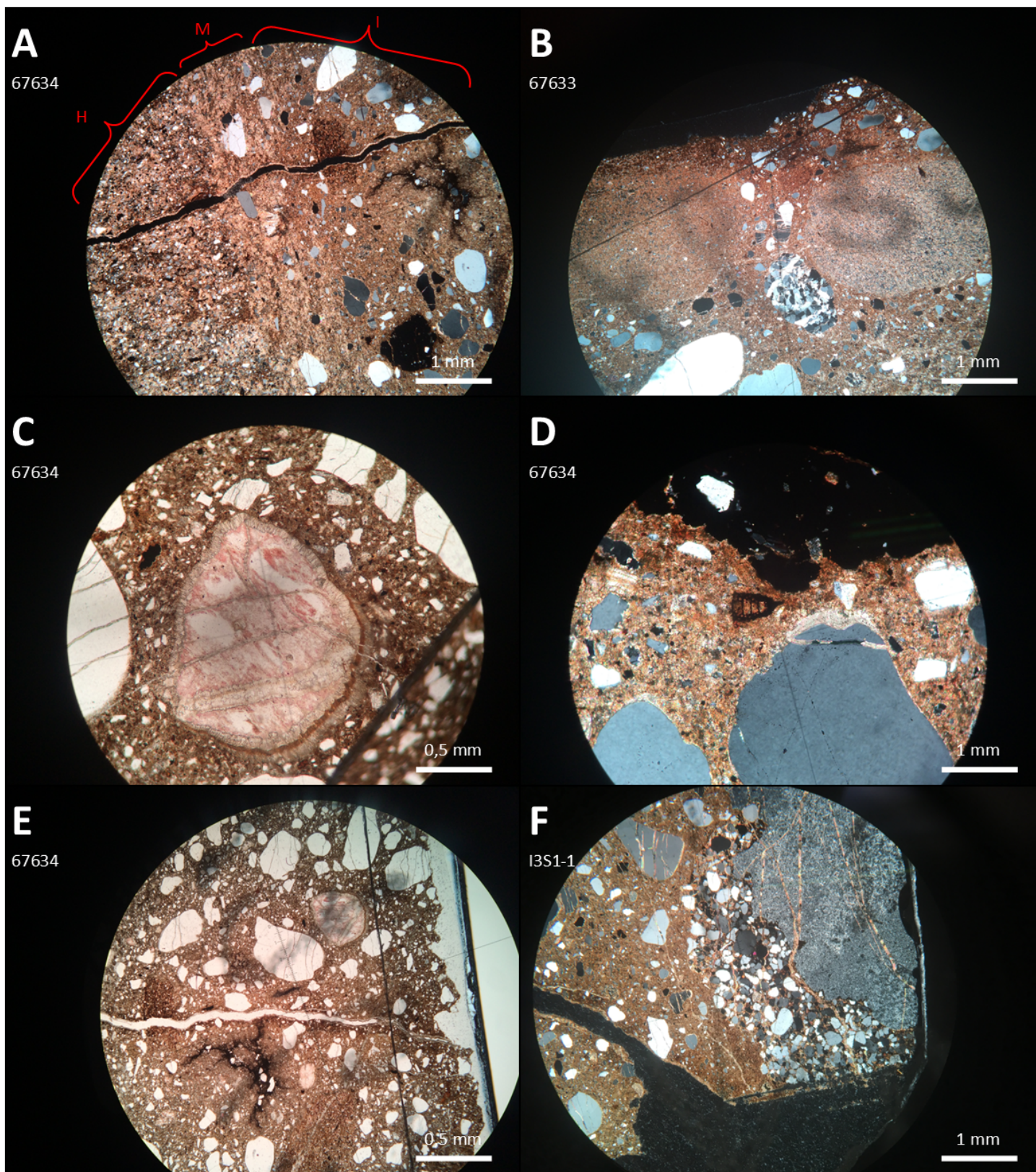


Figure S10: (A): XPL picture showing the injectites interior (I), injectites margin (M) and host rock (H), with a fracture going through all three zones; (B): XPL picture the injectites interior, showing two big reworked grains and a poly-crystalline quartz grain with a compressional crack connecting the two grains; (C): PPL picture a reworked grain in the injectites interior with fibrous cement around it; (D): XPL picture of the injectites interior, showing fibrous cement around the quartz grain and an organic remnant, overprinted by oxides; (E): PPL picture of some sort of carbon staining (black material= in the cement of the injectites interior; (F): An accumulation of smaller grains behind a bigger chert grain in the injectites interior.



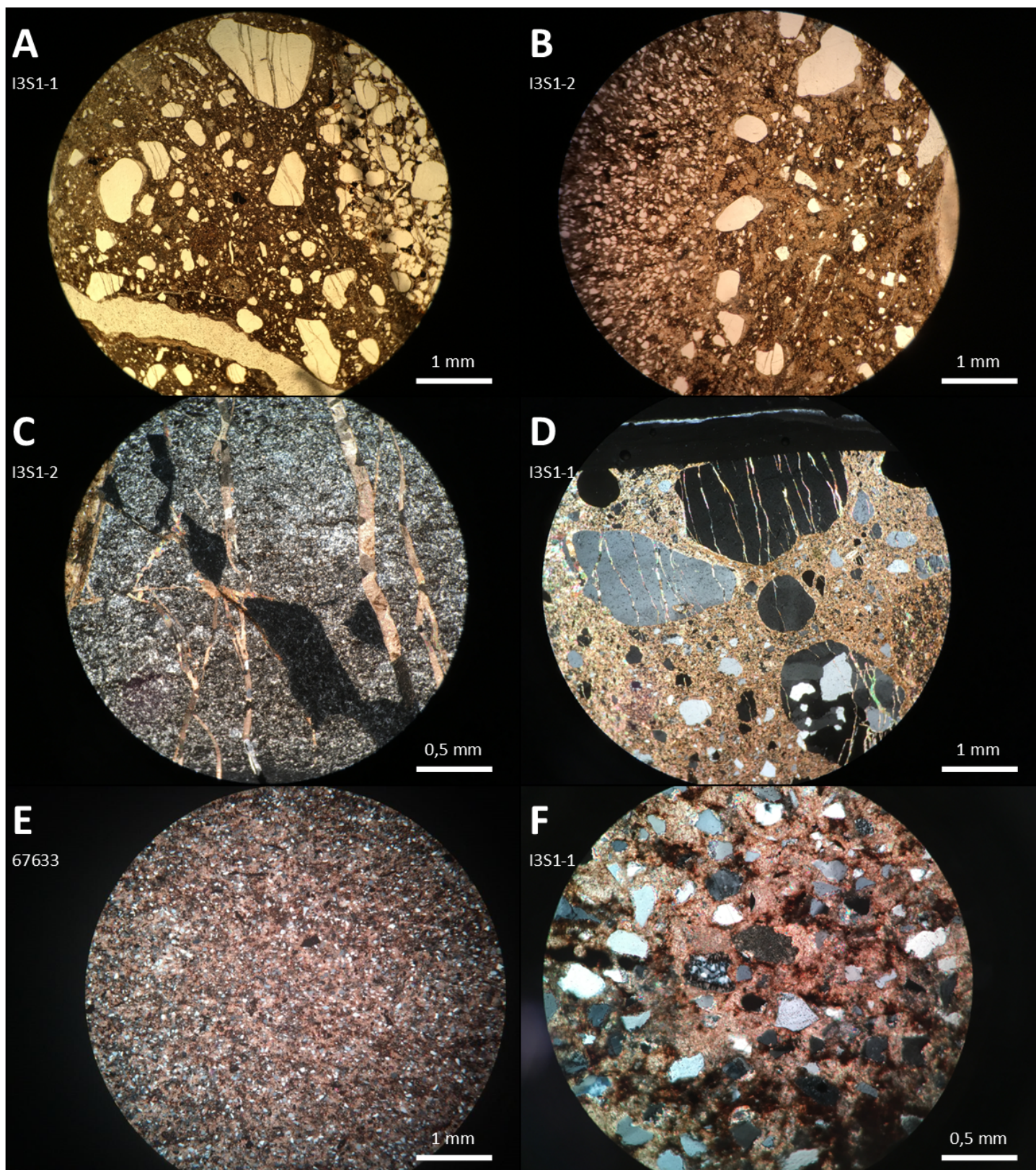


Figure S11: (A): PPL picture showing the different sort of fractures found within the injectites interior; (B): PPL picture showing mainly the injectites margin; (C): XPL picture of the big chert grain of sample I3S1-2 with the fractures crosscutting the grain; (D): XPL picture of the injectites interior, showing the fractures crosscutting the grains; (E): XPL picture of the host rocks material; (F): XPL picture showing the different sort of grains within the host rock.



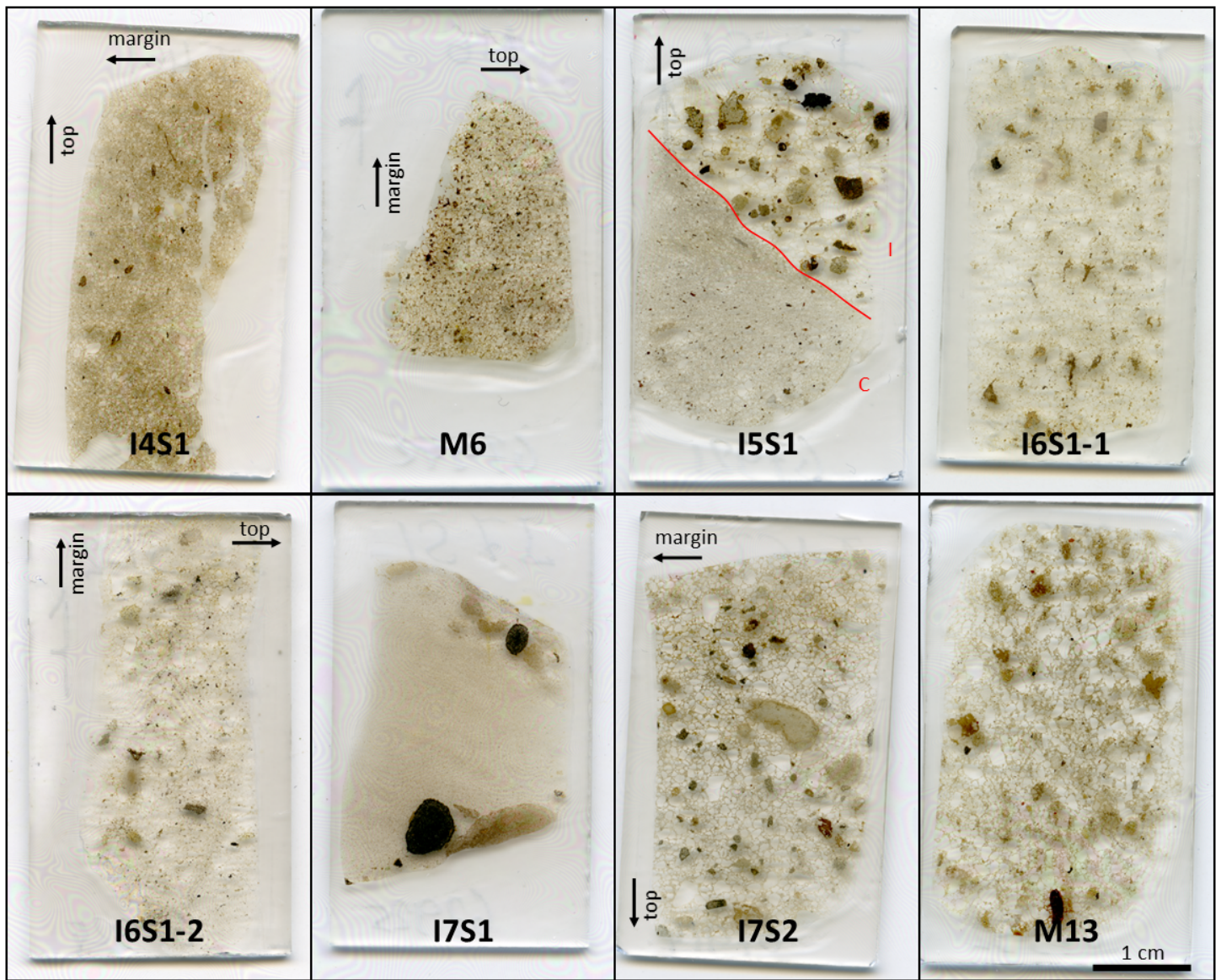


Figure S12: Scans from the thin sections of Injectites 4, 5, 6 and 7, M6 and M13. For Injectite 5, the location of the injectites interior (I) and the mudstone clast (C) are displayed. The thin sections are arranged in the order they will be described. Where available, the direction of the injectites top and margin are shown.

### 2.2.2 Injectite 4

From Injectite 4, only one thin section was studied: I4S1 (Fig. S12). The interior of Injectite 4 is very similar to the interior of Injectite 3; the grains are well- to sub-rounded, poorly sorted and have varying sizes ( $<0,1$  mm -  $0,5$  cm) (Fig. S13.A). The sparite cement between the grains has better developed crystals than the cement of Injectite 3, having the same yellow-brownish color. Like in all previous injectites, quartz dominates the grain composition (around 60%), complemented by oxides, plagioclase, feldspar, mica and reworked grains (Fig. S2). Quartz appears mono- and poly-crystalline, and about 70% of the grains has an undulose extinction. Chert and chalcedony were observed as well. The oxides are mainly subhedral barite crystals and framboidal pyrite clusters. The grains seem to be slightly elongated along the injectites margin. Small cracks within grains are observed, oriented parallel to the injectites margins.



### 2.2.3 M6

M6 is located next to Injectite 4 and is, because of similarities in structure and composition, supposed to be part of the Lower Injectite complex (Fig. S12, S13.D). One thin section was made from the sample taken at location M6. The sample contains well- to sub-rounded, poorly sorted grains in varying sizes (<0,1 mm - 0,5 cm). The grains lay in a brownish-colored sparite cement, similar to the observed cement of Injectite 4 (Fig. S13.B). The grain composition is dominated by quartz (55%) and furthermore oxides, plagioclase, feldspar, mica and organic material were observed (Fig. S2). Quartz appears mono- and poly-crystalline, with 40% of the grains having an undulose extinction. Also chert and chalcedony were observed (Fig. S13.C).

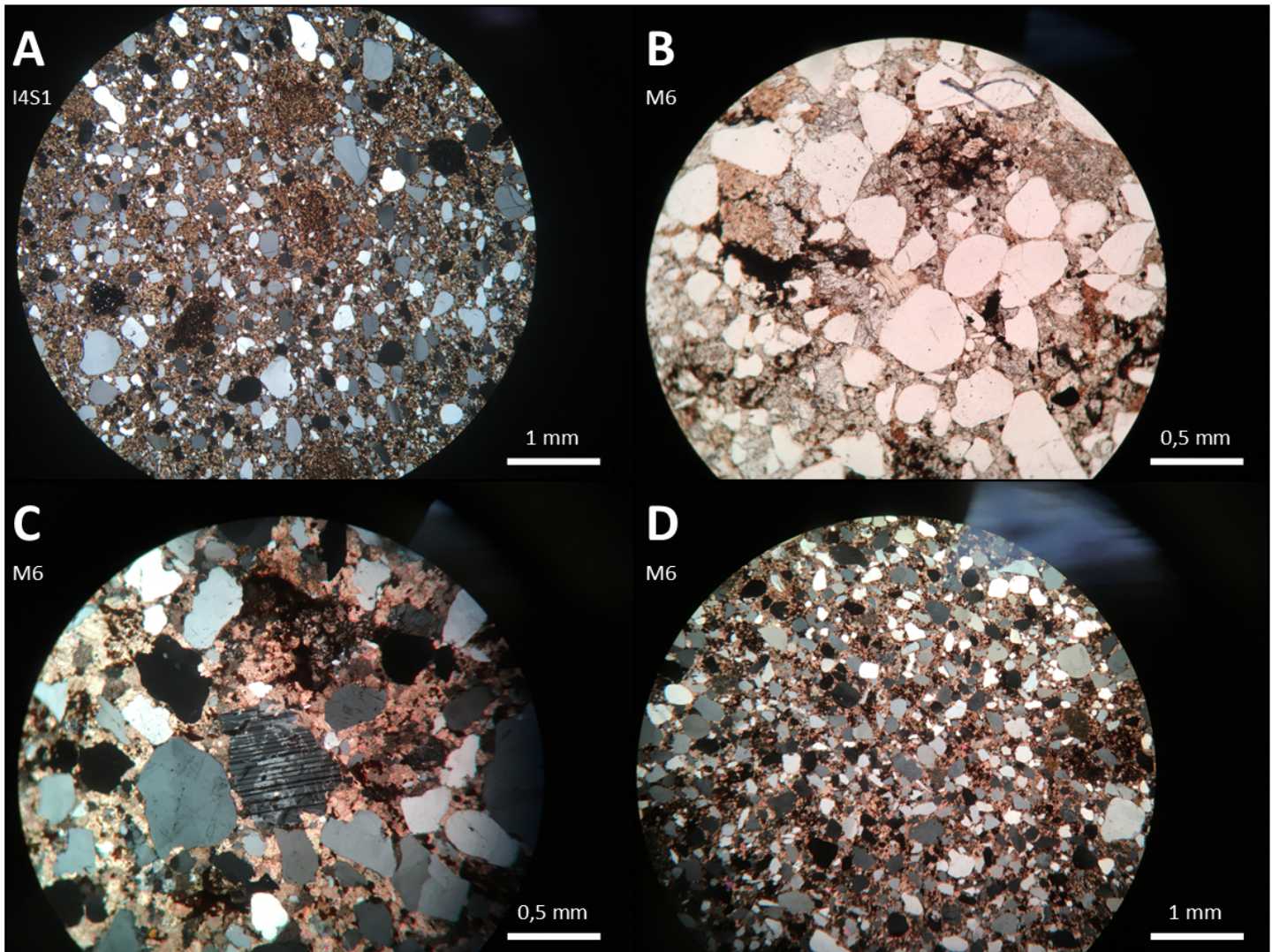


Figure S13: Pictures from samples I4S1 and M6. (A): XPL picture of the interior of Injectite 4; (B): PPL picture of the interior of M6, showing the cement between the grains; (C): XPL picture of an silica grain with an interesting pattern in the interior of M6; (D): XPL picture of the interior of M6.

### 2.2.4 Injectite 5

From Injectite 5, one thin section was made: I5S1. The outcrop of Injectite 5 contains mudstone clasts (Fig. S14.A), from which one is incorporated in the thin section (Fig. S12, S14.B). The injectites interior and mudstone clast will be described separately.

**Interior:** The interior of Injectite 5 is composed of sub- to well-rounded, poorly sorted, non-oriented grains with different sizes (<0,1 mm - 0,8 cm). The grains lay in a sparry cement that has the same yellow-brownish color as the other injectites of the Lower Complex. The grain composition is dominated by quartz (50%), complemented by oxides, plagioclase, feldspar, mica and reworked grains (Fig. S2, S14.D). Both mono- and poly-crystalline quartz crystals were observed, from which 80% has an undulose birefringence. Chert and chalcedony were also observed. The oxides mainly comprise barite and pyrite crystals, framboidal pyrite structures and rutile overprinting organic structures (Fig. S14.C).



**Mudstone clast:** The mudstone clast contains moderately sorted, subangular, small grains (0,1 - 0,3 mm) (Fig. S14.B). The grains seem to be slightly elongated along the boundary with the injectites interior, which is abrupt. The grain composition of the mudstone clast is also dominated by quartz (50%), complemented by oxides, plagioclase, feldspar, mica, zircon and reworked grains (Fig. S2). Mono- and poly-crystalline quartz crystals were observed, from which 80% has an undulose extinction. Compared to the injectites interior, the clast contains more mica and zircon and less plagioclase, feldspar and reworked grains (Fig. S2, I5\_I and I5\_C). Also here, rutile overprints organic remnants. The same sort of brownish sparite cement can be found between the grains, however, the cement crystals within the injectites interior are better developed and bigger.

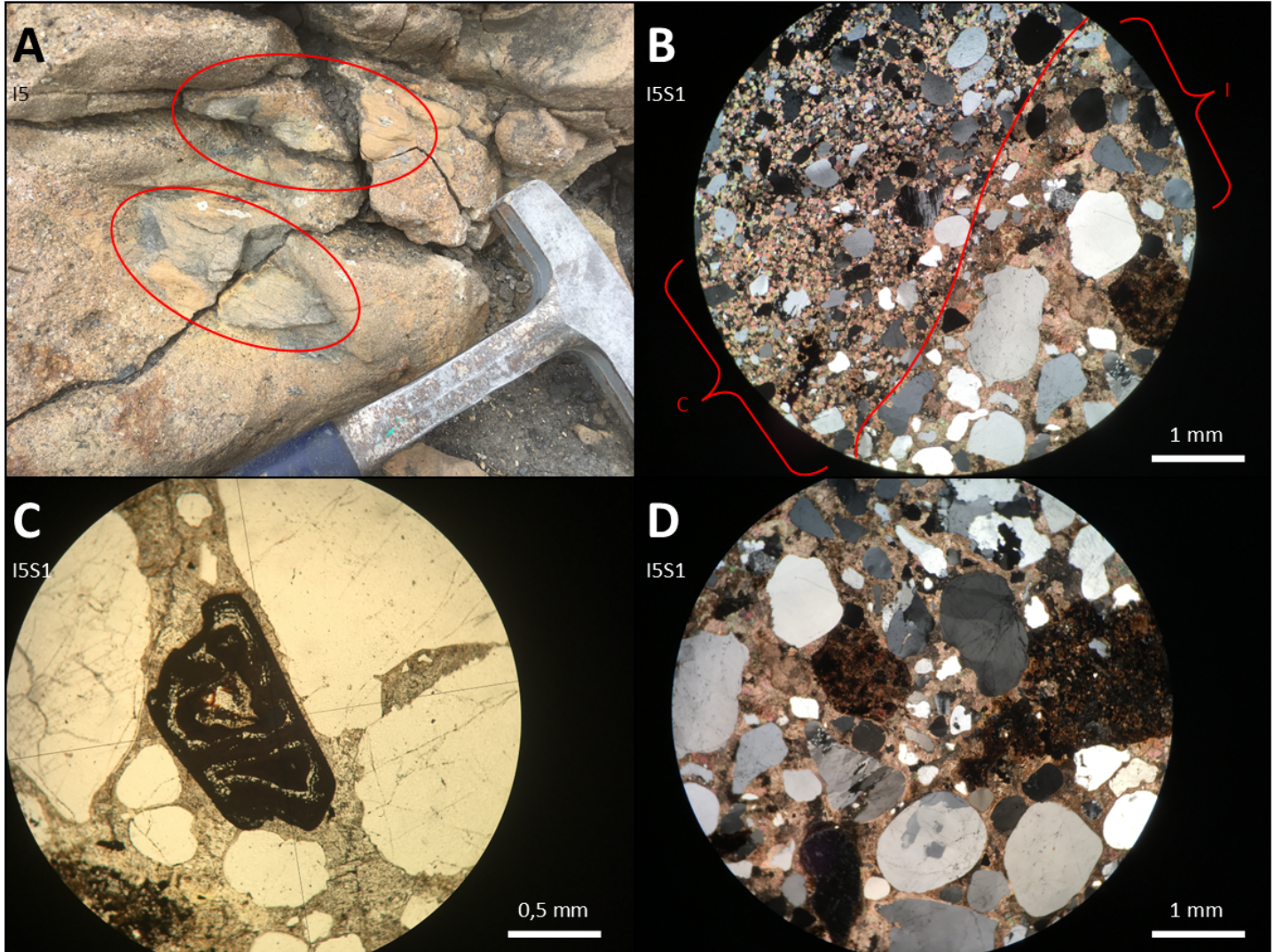


Figure S14: All pictures originate from Injectite 5. (A): Picture from the field, showing Injectite 5 and the present mudstone clasts (in the red circles); (B): XPL picture showing the injectite interior (I) and mudstone clast (C); (C): PPL picture of rutile overgrowing an organic structure; (D): XPL picture showing the interior of Injectite 5.

### 2.2.5 Injectite 6

Two thin sections were made from samples originating from Injectite 6: I6S1-1 and I6S1-2 (Fig. S12). The samples contain sub- to well-rounded, unsorted grains with different sizes (<0,1 - 1 mm) within a yellow-brownish sparite cement (Fig. S15.A, B, C). The composition of the grains is dominated by quartz (60%), supplemented by plagioclase, feldspar, mica, zircon and reworked grains (Fig. S2). Quartz appear both mono- and poly-crystalline, with 40% of the crystals having an undulose extinction. Chert and chalcedony was observed as well. The grains seem to be slightly elongated along the margin of the injectite.



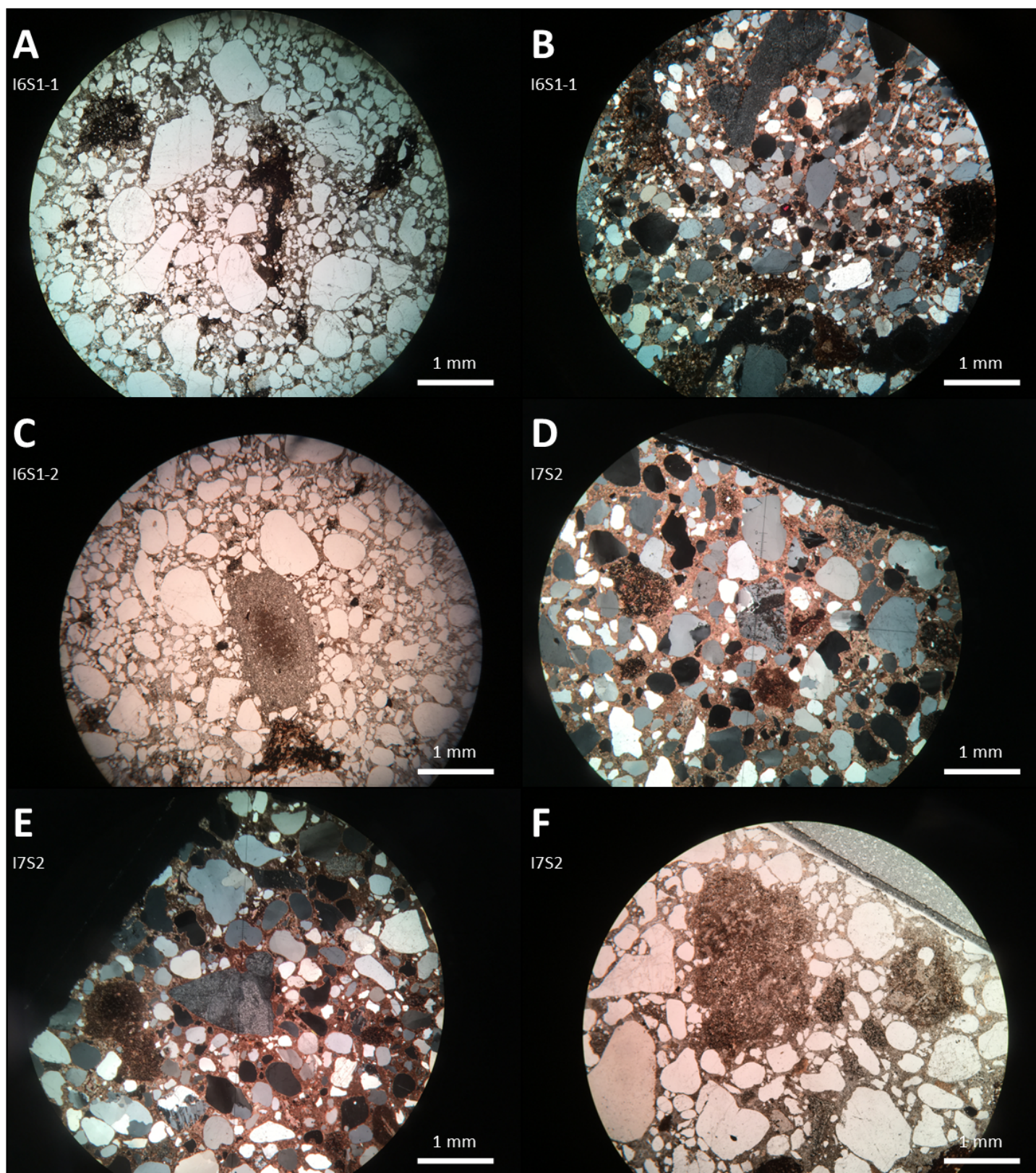


Figure S15: Pictures from Injectite 6 and Injectite 7 (sample I7S2). (A): PPL picture showing the interior of Injectite 6; (B): XPL picture showing the injectite interior of Injectite 6; (C): PPL picture showing a reworked grain in the interior of Injectite 6; (D) XPL picture showing the interior of I7S2; (E) XPL picture showing a chalcedony grain within the interior of I7S2; (F): PPL picture showing the interior of I7S2.



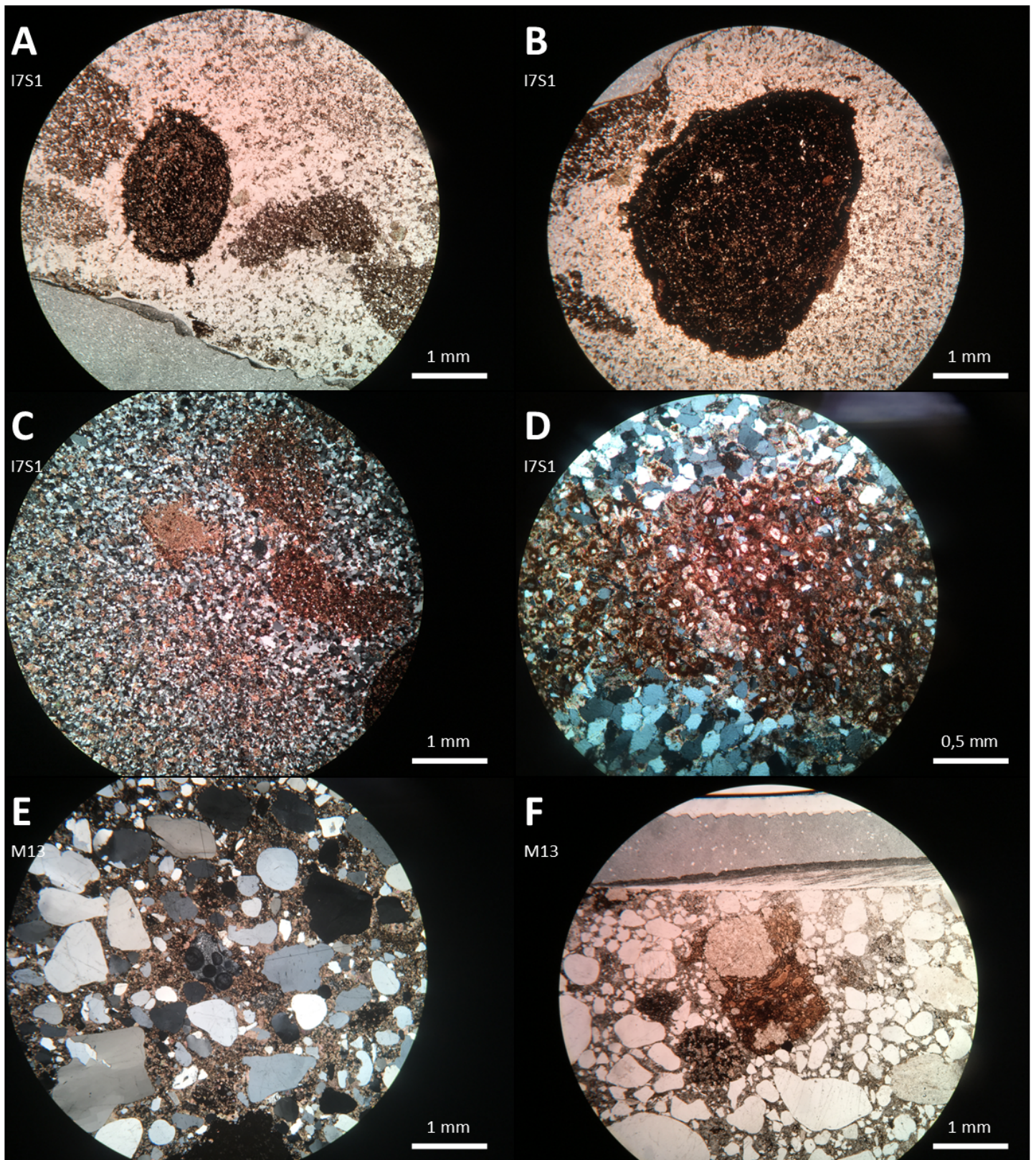


Figure S16: Pictures from I7S1 and M13. (A): PPL picture showing the bigger grains present in I7S1; (B): PPL picture showing another big grain present in I7S1; (C): XPL picture of the bigger grains of I7S1; (D): XPL picture with a zoom in on the interior of the bigger grains; (E): XPL picture of M13, showing the interior and in the middle of the picture the chalcedony grain that contains ooids; (F): PPL picture of the interior of M13.



### 2.2.6 Injectite 7

From Injectite 7, two thin sections were made: I7S1 and I7S2 (Fig. S12). The two thin sections were made from different parts of the outcrop: I7S2 originates from the lower consolidated part of the injectite, while I7S1 comes from the upper, less cohesive part of the injectite. Both thin sections show grains in a yellow-brownish sparite cement. The grain composition is similar to the previous described injectites: quartz dominates the grain composition (roughly 60%), complemented with oxides, plagioclase, feldspar, mica, zircon and reworked grains (Fig. S2). Quartz appear both mono- and poly-crystalline, with 50% of the crystals having an undulose extinction. Chert and chalcedony was observed as well. I7S1 seems to contain more quartz and oxide grains, compared to I7S2, which contains more feldspar and reworked grains (Fig. S2). The structure of both thin sections differs. I7S2 has a structure similar to the other injectites interior; poorly sorted, sub- to well-rounded grains of differing sizes (<0,1 mm - 1 mm) (Fig. S15.D, E, F). The grains seem slightly elongated along the injectites margin and the grain size increases, going further away from the margin. The structure of I7S1 differs from previous observed injectite interiors. The thin section contains moderately-sorted, subangular grains with different sizes (0,1 - 0,3 mm). The grains appear packed, with concave-cortex contacts (Fig. S16.D). There are about 10 bigger, well-rounded grains (up to 1,5 cm), which are composed of carbon, clay and small grains (<0,1 mm) (Fig. S16.A, B, C).

### 2.2.7 M13

Sample M13 was taken from the interpret sand volcano. The interior of the thin section looks most similar to the injectite interiors of I5S1 and I7S2 (Fig. S12). M13 contains sub- to well-rounded, non-sorted grains of different sizes (<0,1 mm - 0,5 cm) in a yellow-brownish sparite cement (Fig. S16.E, F). The grain composition is dominated by quartz (80%), supplemented by oxides, plagioclase, feldspar, mica, zircon and reworked grains (Fig. S2). Quartz appear both mono- and poly-crystalline, with 80% of the crystals having an undulose extinction. Chert and chalcedony was observed as well. Reworked grains within this thin section comprise mudstone clasts, composed of small quartz and pyrite crystals (<0,1 mm), darker clasts enriched in carbon and reworked silica grains. Also a chalcedony grain, containing ooids was observed (Fig. S16.E).

## 2.3 Formations

### 2.3.1 Brentskardhaugen Bed

One thin section of the Brentskardhaugen bed was analyzed (F8, Fig. S17). The rock contains a conglomerate with angular to rounded grains in a cement (crystals up to 0.5 mm). The cement appears in two manners; there is yellow colored ankerite cement (Fig. S18.C) with two big spots of dark-brown colored carbonate-fluorapatite cement, which are the phosphatic nodules, typical for the Brentskardhaugen Bed (Fig. S18.A, D). About 80% of the grains are small (0.2-0.5 mm), with some bigger grains (up to 1 cm). Quartz dominates the composition of the grains (50% of the grains). Furthermore, glauconite, siderite, pyrite, alumino-silicates, muscovite, orthoclase, albite, apatite, carbon, chert grains and fossils have been observed. The minerals seem to be equally divided between the two cement types. Only observed in the yellow-colored cement are a few bigger grains with a thin rim (<0.1 mm thick) of darker colored cement and benthic foraminifera, composed of siderite. In the dark brown colored cement most grains appear with a fibrous cement rim around them (Fig. S18.B). Between the carbonate-fluorapatite cement, ankerite and calcite crystals have been found.

### 2.3.2 Slottsmøya Member

Three thin sections from the Slottsmøya Member of the Agardhfjellet Formation have been analyzed (F1, F2 and F7, Fig. S17). The formation is characterized by small grains (<1 mm, 30% of the thin sections) in a muddy matrix (70 % of the thin sections). The muddy matrix comprises micrite and some spots of pseudosparite. Where micrite fills the space between the grains, cracks with iron staining on the sides have been observed (Fig. S18.E, F). The cracks seem to be filled with calcite cement. Shell fragments, pellets and bioturbation marks are present in all the analyzed samples. Most bigger fossils (up to 0,5 cm) occur broken (Fig. S18.E) and contain small pores filled with isopachous calcite cement. Last, clusters of pyrite crystals, surrounded by calcite blocky cement were observed.

### 2.3.3 Rurikfjellet Formation

From the Rurikfjellet Formation, four thin section were analyzed (F3, F4, F5-1 and F5-2, Fig. S17). Some structural differences between the samples were observed. The stratigraphical lowest sample shows banding, with elongated grains along the bedding plane (Fig. S19.C). The bands can be distinguished by their composition; there are bands with mainly colorless minerals, like quartz, and bands with mainly darker colored minerals, like oxide-minerals. Looking at the samples collected higher in the stratigraphy, the bands disappear and slumped structures become visible (Fig. S19.D). The overall composition of the samples are roughly the same; a well sorted siltstone dominated by quartz grains. Furthermore, mica's, oxides, glauconite, rutile and feldspar grains with the same size as the quartz grains have been identified. All grains have a size of about 0,1 to 0,3 mm and are angular to sub-angular.

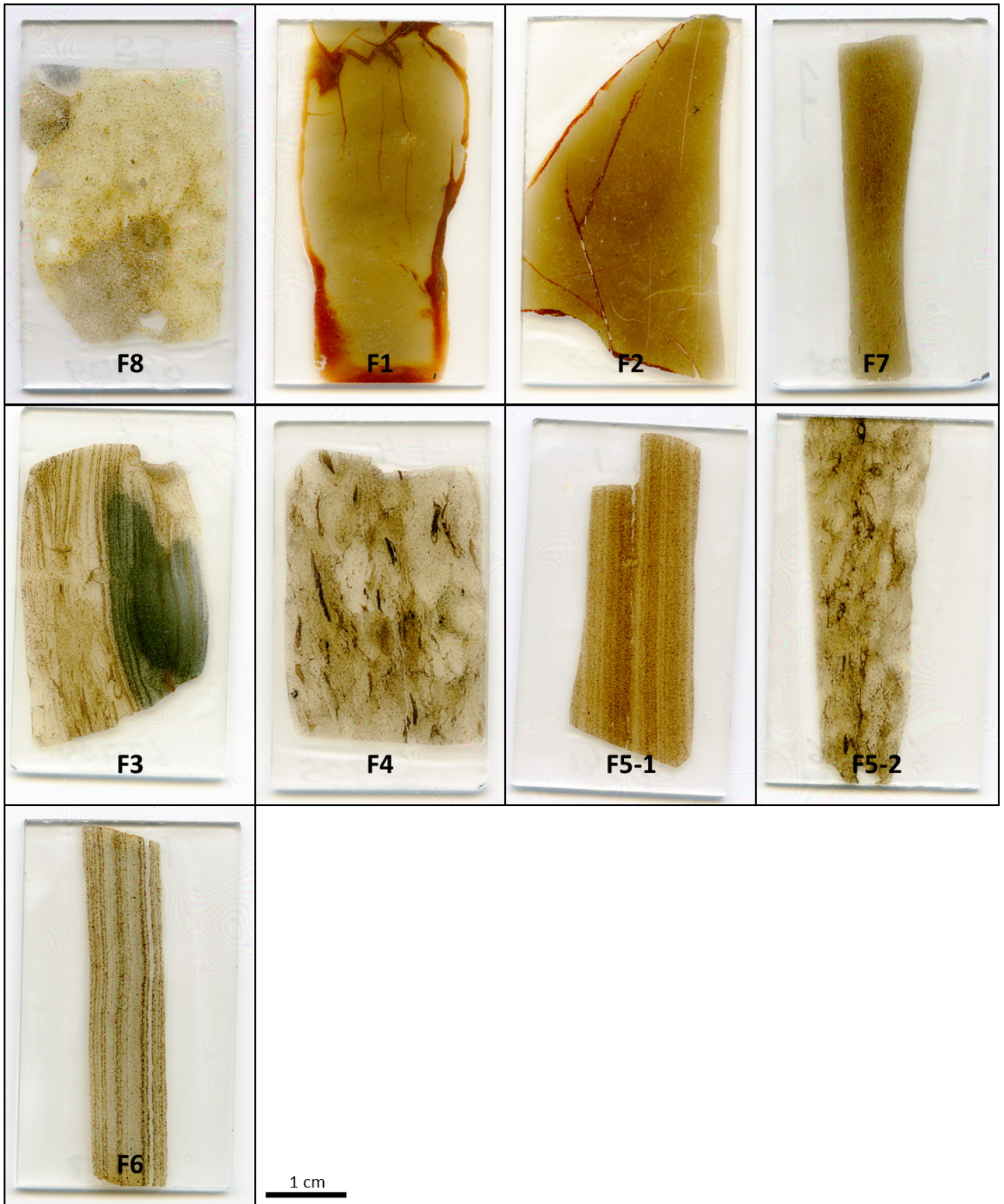


Figure S17: Scans from the thin sections of the samples from the formations. The thin sections are arranged in the order they will be described: the Brentskardhaugen Bed (F8), the Slottsmøya Member (F1, F2 and F7), the Rurikfjellet Formation (F3, F4, F5-1 and F5-2) and the Carolinefjellet Formation (F6).



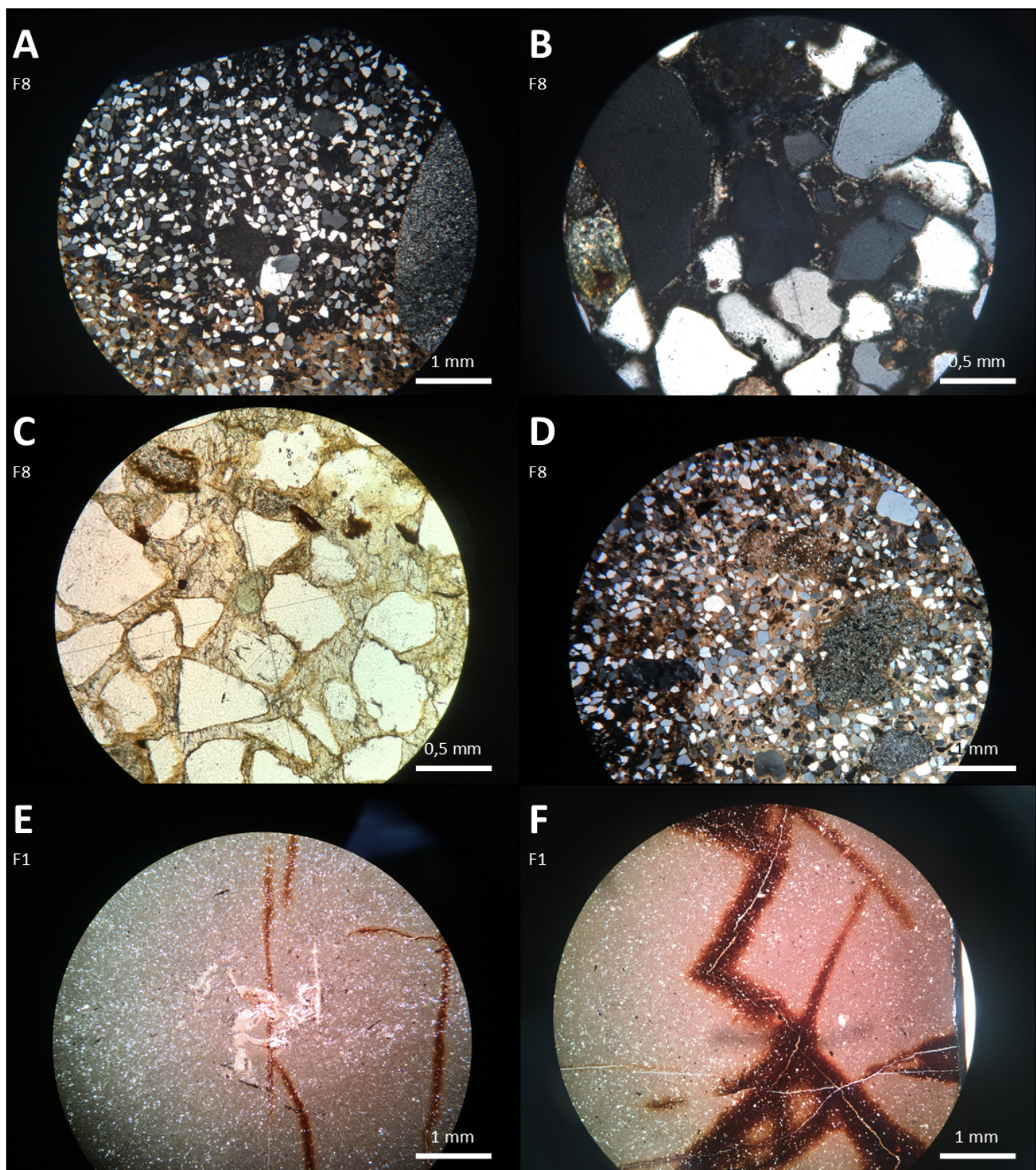


Figure S18: Scans from the thin sections of the samples from the formations. The thin sections are arranged in the order they will be described: the Brenskardhaugen Bed (F8), the Slottsmøya Member (F1, F2 and F7), the Rurikfjellet Formation (F3, F4, F5-1 and F5-2) and the Carolinefjellet Formation (F6).



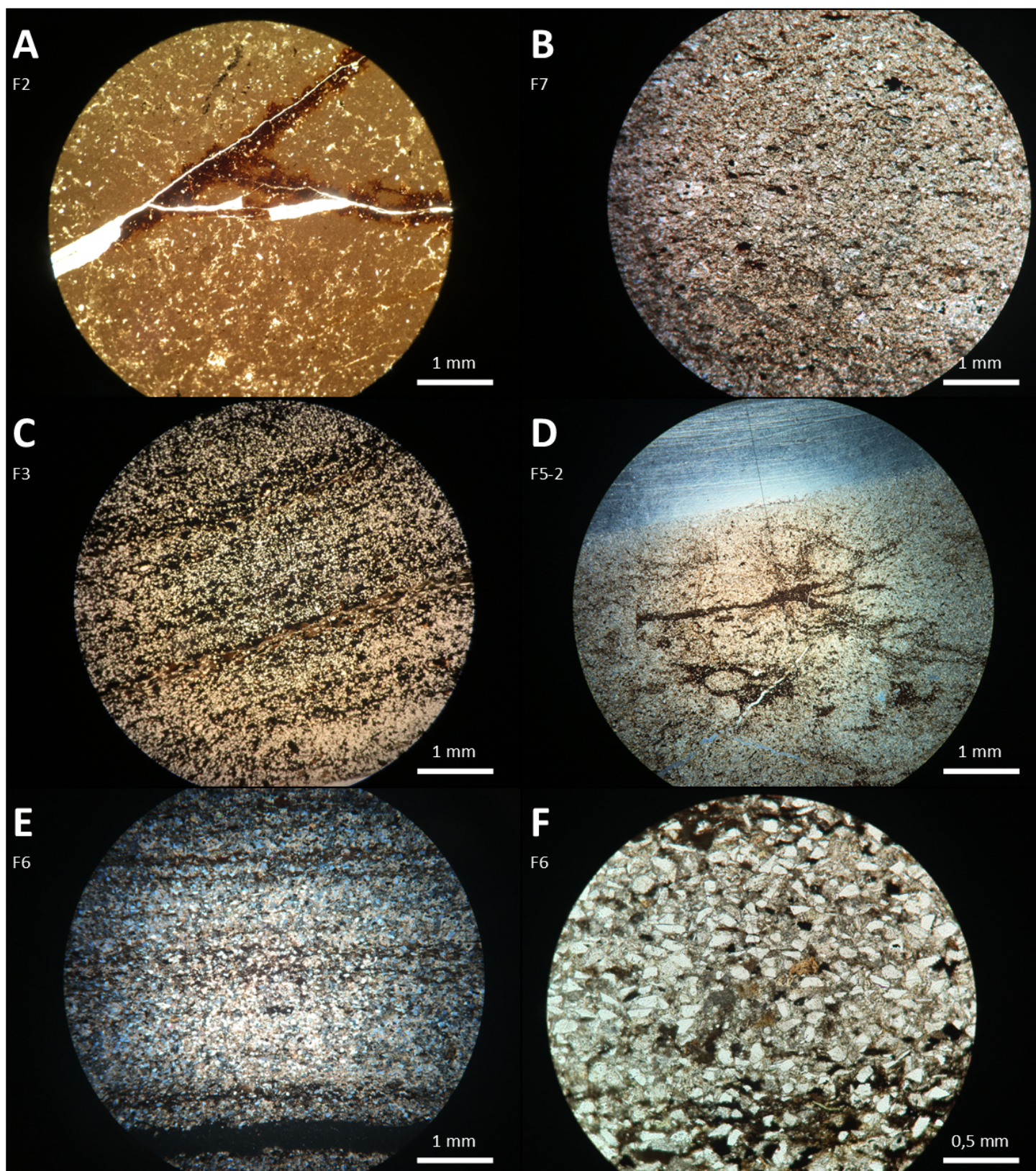


Figure S19: Scans from the thin sections of the samples from the formations. The thin sections are arranged in the order they will be described: the Brentskardhaugen Bed (F8), the Slottsmøya Member (F1, F2 and F7), the Rurikfjellet Formation (F3, F4, F5-1 and F5-2) and the Carolinefjellet Formation (F6).



### 2.3.4 Carolinefjellet Formation

From the Carolinefjellet Formation, one sample was analyzed (F6, Fig. S17). Due to the abrupt ending of the fieldwork, it was not possible to collect a sample from this formation during the field campaign, wherefore it was collected along Vei 600 in Longyearbyen afterwards. The sample contains small, angular grains (about 0.1 mm) in a muddy matrix (Fig. S19.E, F). The matrix comprises pseudosparite, ankerite cement and micrite. The grain content is dominated by quartz. Furthermore, siderite, pyrite, albite, orthoclase, glauconite, colorless mica's (probably muscovite) and plagioclase grains were recognized. Also, fossils (up to 0,5 mm) were observed; shells, pellets and gastropoda. Pores within these fossils are filled with a calcite cement. The grains appear in bands, having the same orientation as the bedding plane of the outcrop the sample originates from (Fig. S19.E).

### 2.4 Mounds

Different types of samples from the mounds were taken during the fieldwork. The mounds are composed of a yellow-brown colored siltstone that is mainly composed of quartz grains that lay within a microsparite cement. Some mounds contained one or more bigger (>0,5 cm) grains (thin sections ) or fossilised wood (thin sections ) that were sampled. Also some samples from the glauconite interval were taken (thin sections M10, M11, M12 and K1).

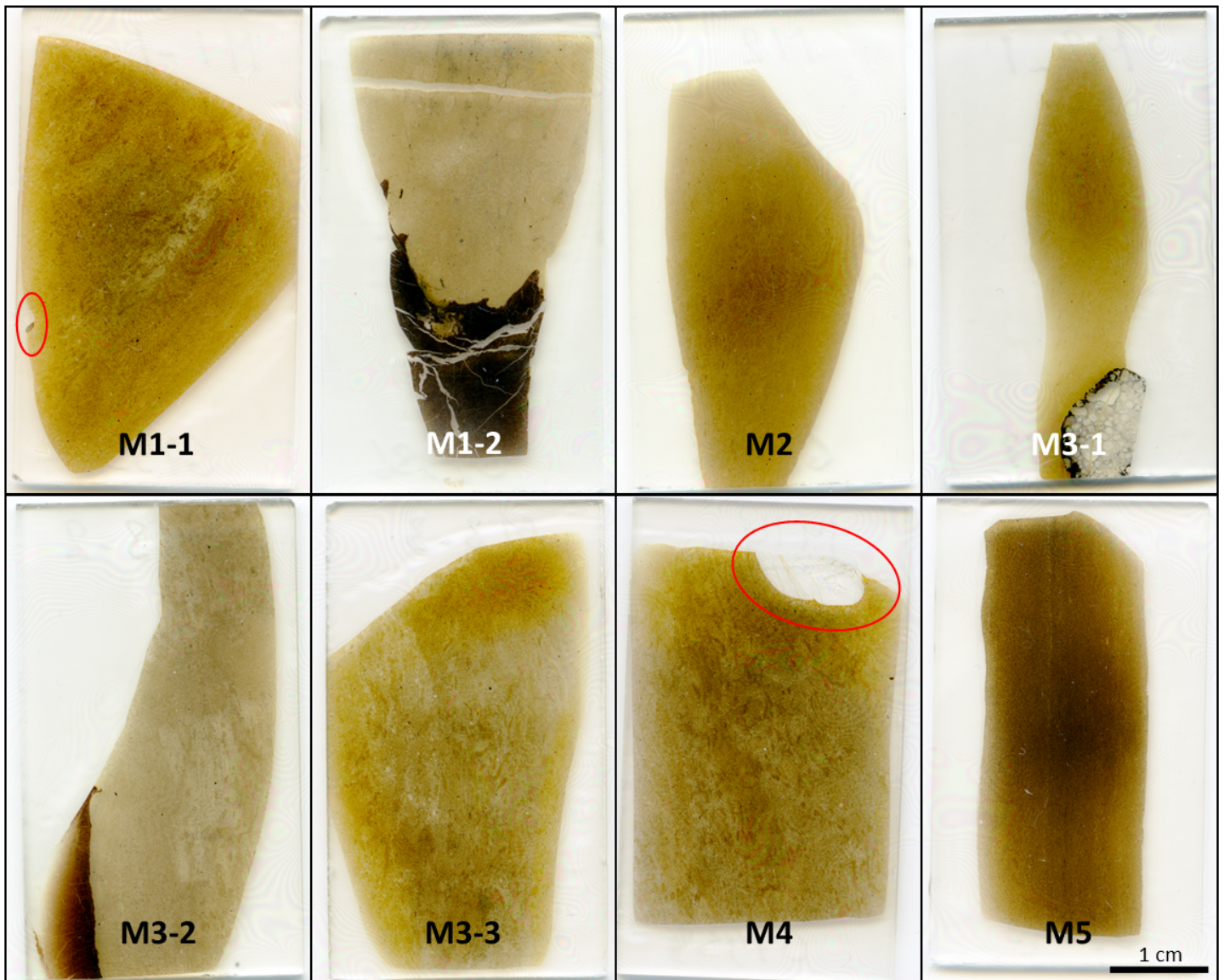


Figure S20: Scans from the thin sections of the samples from M1 to M5. The thin sections are arranged in the order they will be described. The red circles mark the targeted bigger grains of thin sections M1-1 and M5.



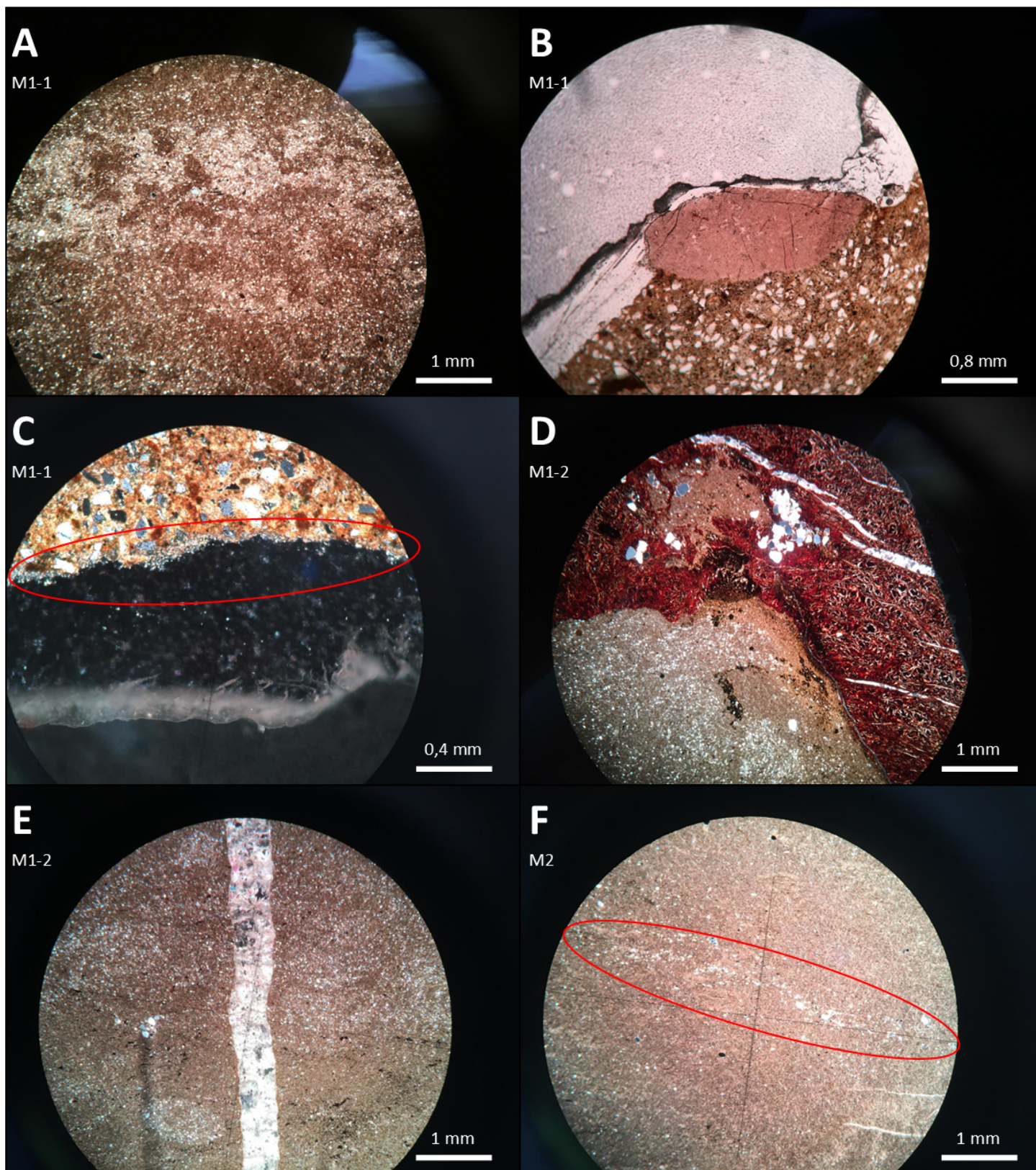


Figure S21: Pictures from samples M1 and M2. (A): PPL pictures, showing an overview of M1-1 with possible bioturbation marks; (B): PPL picture of the bigger mudstone clast present in sample M1-1; (C) XPL picture of the rim of calcite crystals present around the mudstone clast of M1-1; (D): XPL picture of the fossilised wood (brown-reddish material) of sample M1-2; (E): XPL picture of the crack crosscutting M1-2 and filled with calcite crystals; (F): PPL picture of M2, showing a band of quartz grains.

#### 2.4.1 M1

Two thin sections were made from M1: M1-1 and M1-2 (Fig. S20). M1-1 contains a bigger (0,2 cm) grain, while M1-2 contains a fragment of fossilised wood (black material on the thin section scan). Both thin sections contain small ( $<0,1 - 0,2$  mm), moderately-sorted, angular, non-oriented grains in a cement that has partly been transformed into micrite. Also traces of bioturbations seem present (Fig. S21.A) Quartz dominates the grain composition, which further comprises glauconite, oxides and mica. The bigger grain found in thin section M1-1 (red circle on Fig. S20 and Fig. S21.B), is a mudstone. The grain is bordered by calcite crystals, which form a rim around the grain (Fig. S21.C). Thin section M1-2 contains a crack, crosscutting the thin section, which is filled with calcite (S21.E). The present fossilised wood within this thin section contains cracks that have a similar infilling of calcite. Some quartz grains are recognized within the interior of the fossilised wood and a higher amount of oxides seems present in the material surrounding the piece of fossilised wood (Fig. S21.D).

#### 2.4.2 M2

Sample M2 contains similar material as found within M1; small ( $<0,1 - 0,2$  mm), moderately-sorted, angular, non-oriented grains in a cement that has partly been transformed into micrite. Quartz dominates the grain composition, which further comprises glauconite, oxides and mica. Contrasting to the thin sections of M1, here bands of bigger (up to 0,5 mm) quartz grains can be found (Fig. S21.F).

#### 2.4.3 M3

Three thin sections were made from M3: M3-1, M3-2 and M3-3 (Fig. S20). M3-1 contains a bigger (up to 1 cm) silica grain and M3-2 contains a piece of fossilised wood. All three thin section contain a small ( $<0,1 - 0,2$  mm), moderately-sorted, angular, non-oriented grains in a cement that has partly been transformed into micrite. Quartz dominates the grain composition, which further comprises glauconite, oxides, chert and mica. The cement of thin section M3-1 seems less micritised than the cement in M3-2 and M3-3. The grain found in M3-1 contains oncoids and ooids, overprinted by silica (Fig. S22.A, B, C). On the edges of the grain, accumulations of oxide crystals are present (Fig. S22.A, B). Around the big grain, the small grains of the host rock seem elongated around the big grain (Fig. S22.B). The big silica grain also contains a crack, which is filled by calcite, that doesn't continue in the surrounding host rock (Fig. S22.A). The piece of fossilised wood found in M3-2 looks similar to the fossilised wood found in M1-2 (Fig. S22.D, E). Also here, an increased amount of oxide crystals is present in the host rock around the wood. Thin section M3-3 contains some structures that look like bioturbation marks and some bigger quartz grains (up to 0,4 mm) (Fig. S22.F).

#### 2.4.4 M4

Sample M4 looks very similar to M3-3; small ( $<0,1 - 0,2$  mm), angular, moderately-sorted, non-oriented grains in a cement that has partly been transformed into micrite, where some sort of bioturbation marks are still visible (Fig. S23.B). The grain content is dominated by quartz, supplemented by glauconite, oxides and mica. This thin section contains a big quartz grain (1 cm, red circle S20 and Fig. S23.A). The big quartz grain has calcite cracks that do not continue in the host rock. Also, the quartz grain has an undulose birefringence, a small calcite rim like observed with the mudclast of M1-1 and two inclusions of smaller quartz grains.

#### 2.4.5 M5

Sample M5 looks similar to sample F7 (Fig. S17), but the cement of M5 has a darker appearance. The thin section contains small ( $<0,1 - 0,1$  mm), moderately-sorted, angular grains in a brown cement (Fig. S23.C). The grain composition is dominated by quartz, but oxides, glauconite and mica were also found. The grains seem to be elongated along the length of the thin section. Furthermore, the thin section contains shell fragments and some grains made of calcite crystals.

#### 2.4.6 M7

Sample M7 looks most similar to the host rock of M1, M2 and M3-1, containing small ( $<0,1 - 0,2$  mm), moderately-sorted, angular, non-sorted grains in a partly micritised cement. This cement covers about 70 to 80% of the thin section. The grain composition is dominated by quartz, supplemented by oxides, glauconite and mica. The oxides appear as black dots. Furthermore, shell fragments and a pore filled with calcite cement were found (Fig. S23.D). Around the pore, an increased amount of oxide dots is present.



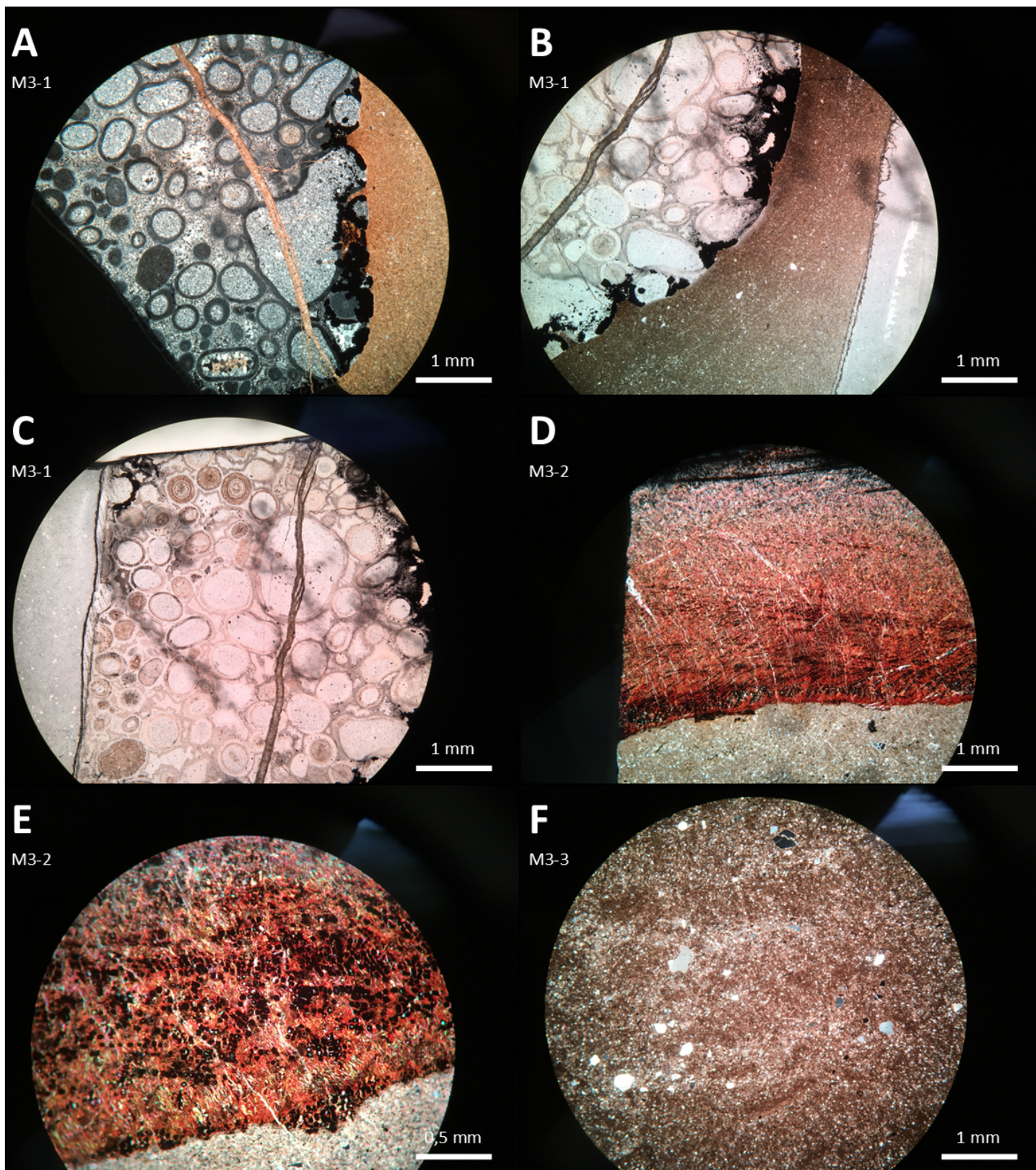


Figure S22: Pictures from samples M3. (A): XPL picture of the silica grain of M3-1, showing the ooids, oncoids and oxide crystals; (B): PPL picture of the silica grain of M3-1, showing the edge with oxides and grains that seem elongated around the grain; (C): PPL picture of the silica grain of M3-1, showing the ooids and oncoids; (D): XPL picture of the fossilised wood of M3-2; (E): XPL picture zoomed in on the fossilised wood, showing the structure of the wood and black oxide dots; (F): XPL picture of M3-3, showing an overview of the thin section and the possible bioturbation marks.



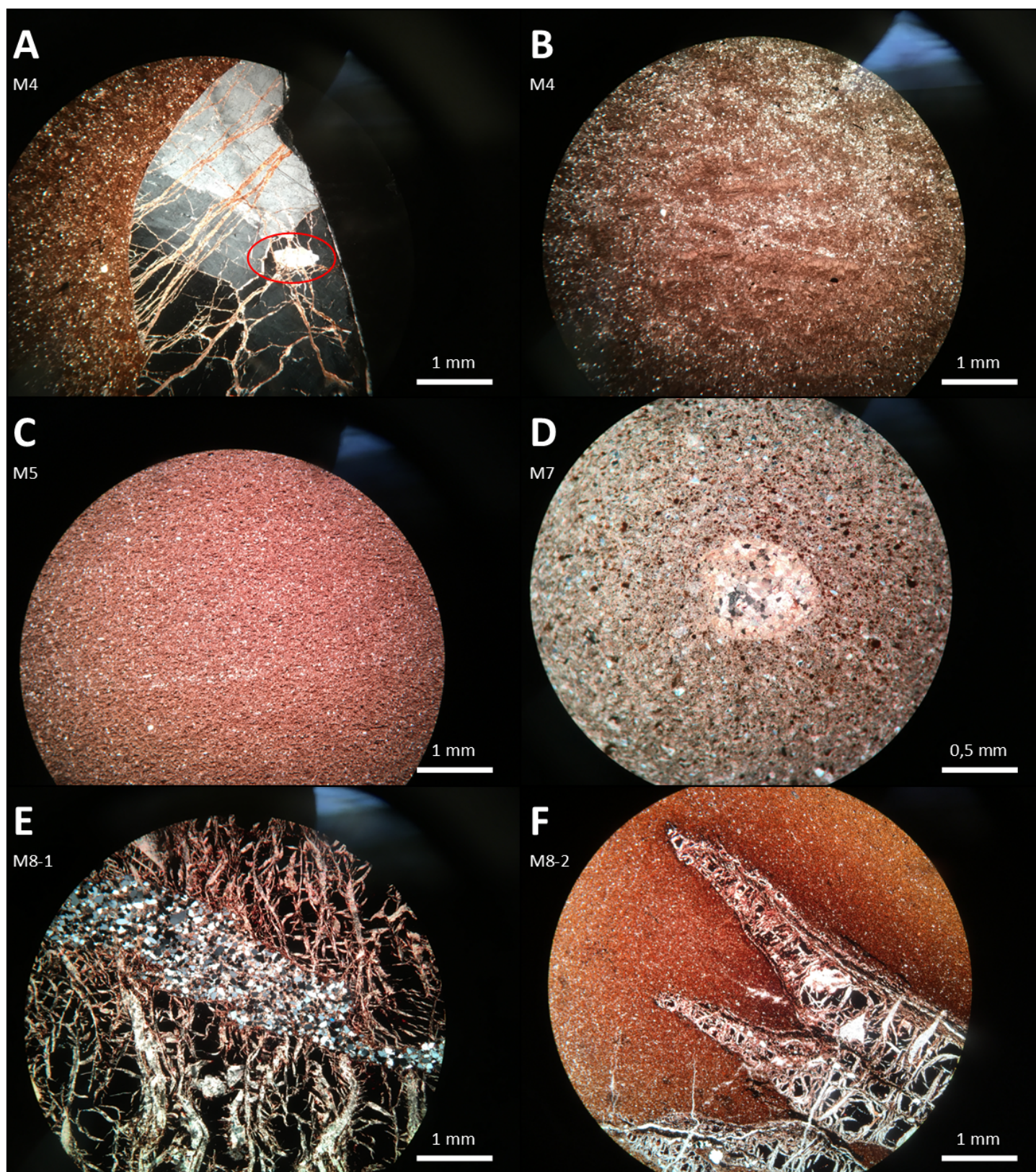


Figure S23: Pictures from samples M<sub>4</sub>, M<sub>5</sub>, M<sub>7</sub> and M<sub>8</sub>. (A): XPL picture the big quartz grain of M<sub>4</sub>, with in the red circle one of the quartz inclusions; (B): XPL picture of M<sub>4</sub> showing the possible bioturbation marks; (C): PPL picture of M<sub>5</sub>; (D): XPL picture of M<sub>7</sub>, showing the pore filled by calcite crystals; (E) XPL picture showing the quartz grains and calcite crystals that fill up cracks in the wood fossil of M<sub>8-1</sub>; (F): PPL picture of M<sub>8-2</sub>, showing the black material and cell-like structure (red-brownish material).



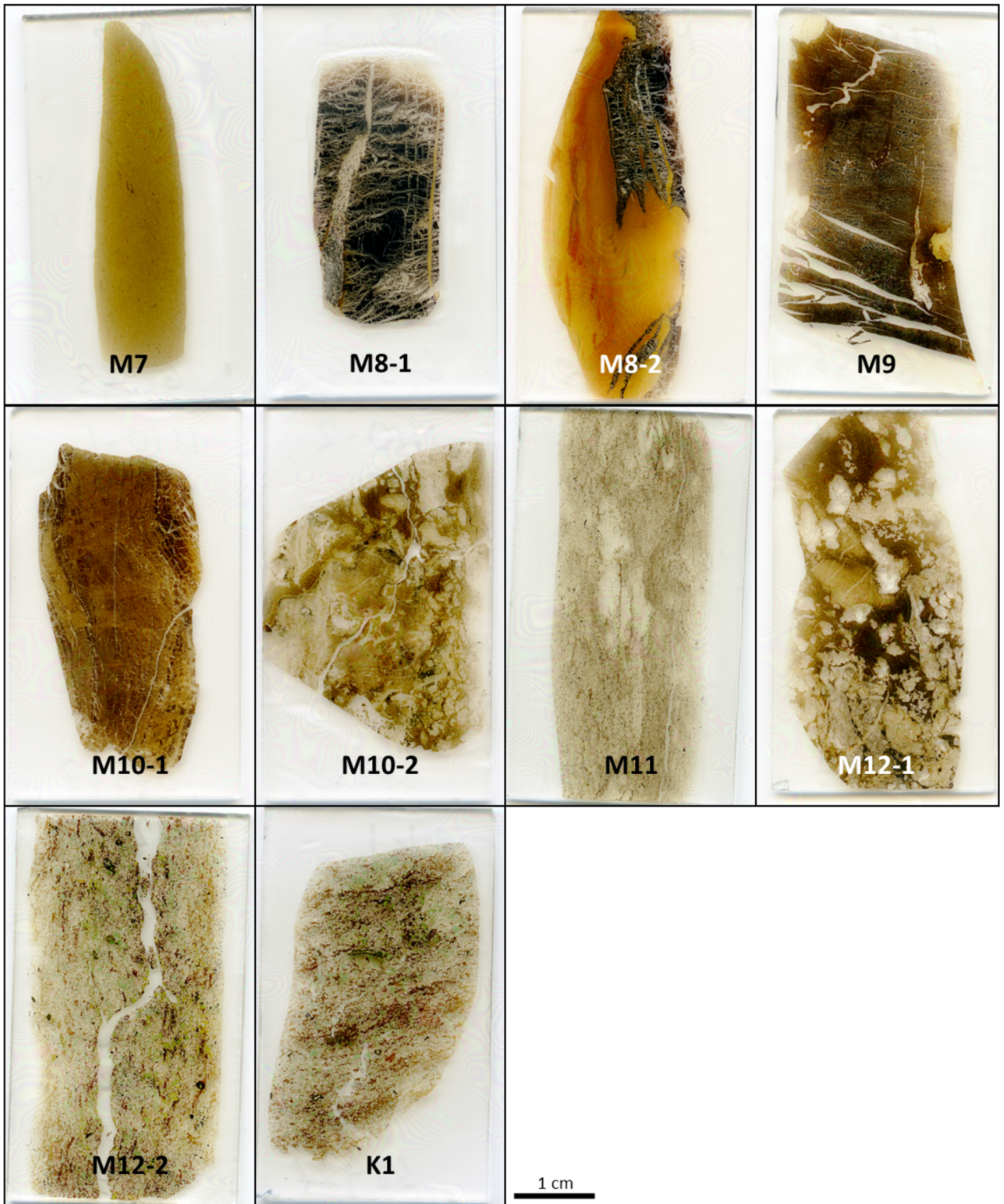


Figure S24: Scans from the thin sections of the samples from M8 to M12 and K1. The thin sections are arranged in the order they will be described.

#### 2.4.7 M8

From M8, two thin sections were made: M8-1 and M8-2 (Fig. S24). Both thin sections contain fossilised wood. The black material (Fig. S23.E) is similar to the observed fossilised wood of M1-2 and M3-2. This black material contains cracks filled with quartz grains and calcite crystals (Fig. S23.E). Sample M8-2 contains also a red-brown colored cell-like structure with some present quartz grains and oxide dots (Fig. S23.F). The cell-like part of the thin section also contains some structures that can be interpreted as nerves or veins originating from the tree or plant (Fig. S25.A). These structures are not found in the part of the fossilised wood made of the black material. It can be assumed that the black material may be the skin of the tree, while the cell-like structure found in M8-2 originates from the inside of the tree.

#### 2.4.8 M9

Sample M9 also contains fossilised wood, similar to black skin-like material observed in the previous thin section containing fossilised wood (M1-2, M3-2, M8-1 and M8-2). Also here, quartz grain and calcite crystals fill in cracks within the wood structure (Fig. S25.B, C). The piece of fossilised wood of this sample looks more altered than the previous described samples, as this sample contains more cracks crosscutting the wood-structure and more red alteration-like material is present. Also, this sample contains a spot with muddy material and quartz grains, that seems incorporated into the wood-structure (Fig. S25.B).

#### 2.4.9 M10

Two thin sections were made from sample M10; M10-1 and M10-2. Both thin sections contain fossilised wood, but in different states. M10-1 looks like the previous described thin sections with the black skin-like wood structure (M1-2, M3-2, M8-1, M8-2 and M9), but within this sample, the cell structure is better visible (Fig. S25.D). Contrasting to the previous described fossilised wood samples, M10-2 shows a very altered and corroded fossilised wood piece. The wood-structure is still visible, but there is overprinting visible by quartz, calcite and micas (Fig. S25.E, F).

#### 2.4.10 M11

Sample M11 contains small ( $<0,1 - 0,2$  mm), angular, moderately-sorted grains in a cement. The grain composition is dominated by quartz, but oxide, micas and glauconite were observed as well. This sample contains more glauconite than the previous described samples from the mounds, probably because the sample was taken from the glauconite interval. There are some bands with darker cement visible, probably due to some alteration or micritisation (Fig. S26.A). The grains seem to be slightly elongated along these bands.

#### 2.4.11 M12

Two thin sections were made from M12: M12-1 and M12-2 (Fig. S24). Sample M12-1 contains the similar type of altered fossilised wood as observed in thin section M10-1. However, the wood structure within M12-1 is better preserved than in sample M10-2 (Fig. S26.B, C). Sample M12-2 was taken close by the glauconite interval and contains small ( $<0,1 - 0,3$  mm), poorly sorted, sub-rounded to angular, non-oriented grains in a brown-colored cement. The grain composition is dominated by quartz and glauconite (Fig. S26.D). There are also some quartz grains that are overprinted by glauconite. Some glauconite grains are altered by a yellow-colored clay at the grains edges (Fig. S26.E).

#### 2.4.12 K1

Sample K1 also originates from the glauconite interval and looks very similar to M12-2. The thin section comprises small ( $<0,1 - 0,3$  mm), poorly sorted, sub-rounded to angular, non-oriented grains in a brown-colored cement. The grain composition is dominated by quartz and glauconite. The thin section also contains a well preserved plant or wood fragment and a gastropod fossil (Fig. S26.F).



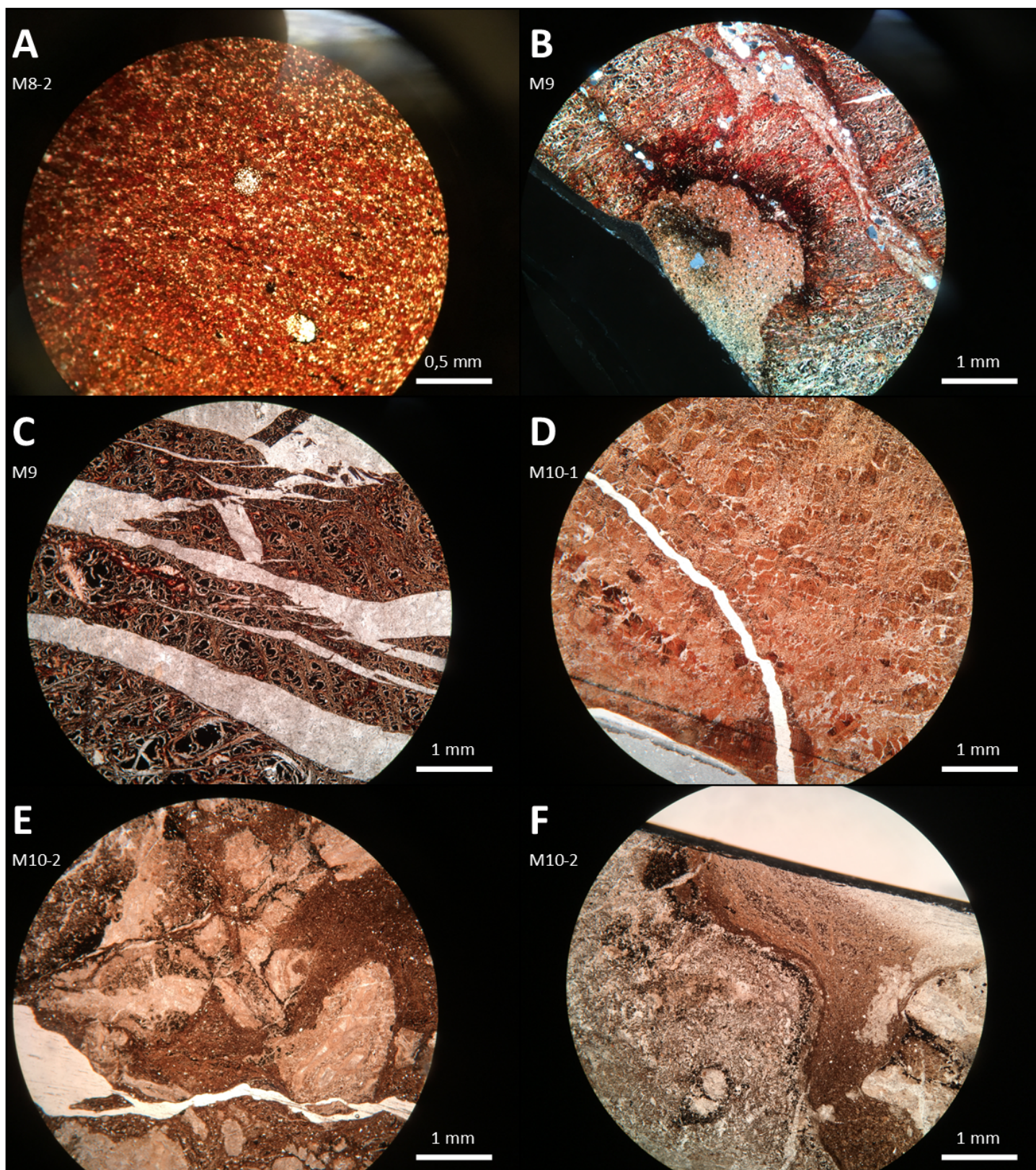


Figure S25: Pictures from samples M8, M9 and M10. (A): PPL picture of the vein structure found in sample M8-2; (B): XPL picture of the spot with muddy material and quartz grains in sample M9; (C): PPL picture of the fossilised wood of sample M9; (D): PPL picture of the well-preserved cell-structure within sample M10-1; (E): PPL picture of the altered fossilised wood of sample M10-2; (F): PL picture of the altered fossilised wood of sample M10-2.



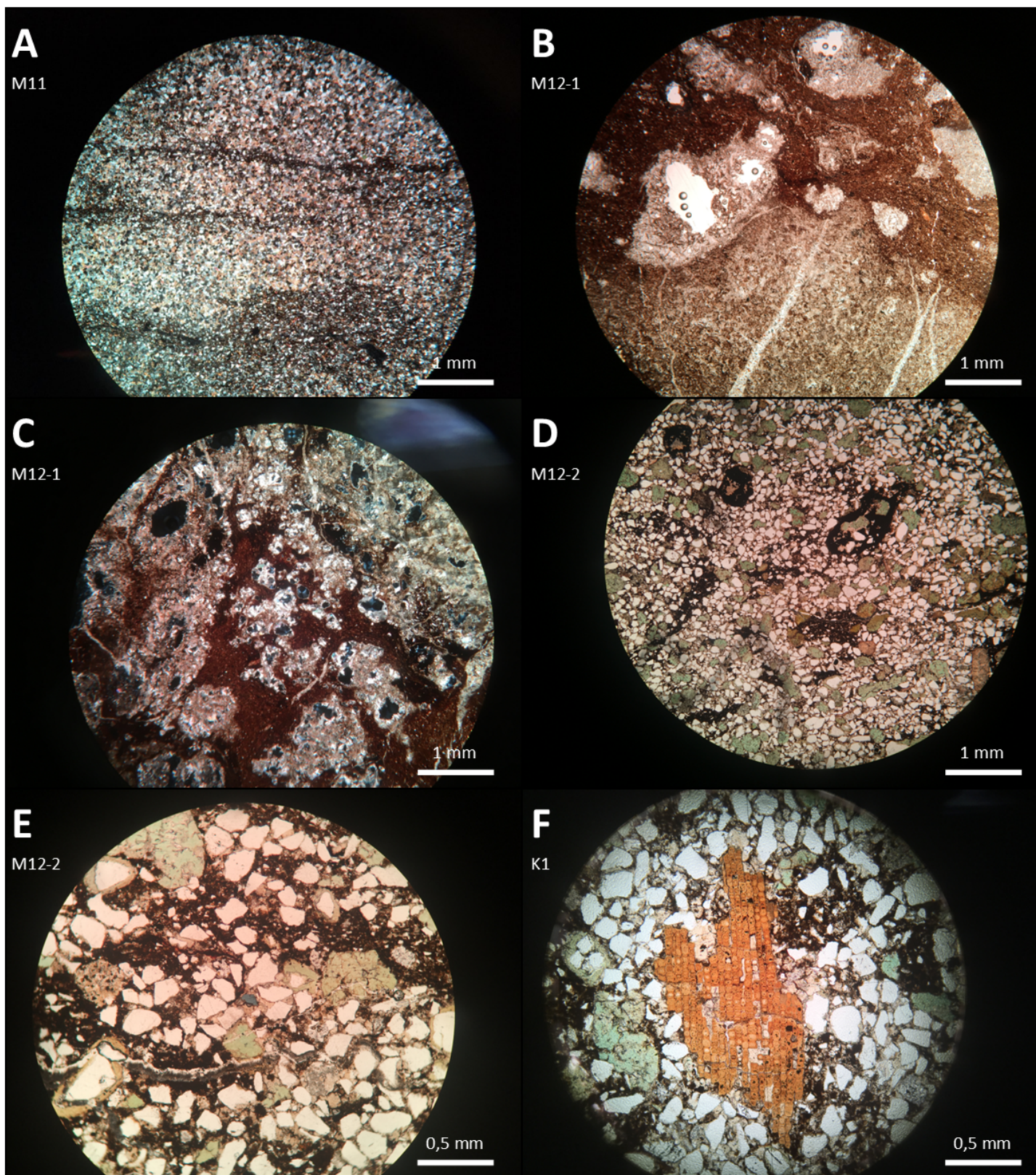


Figure S26: Pictures from samples M11, M12 and K1. (A): XPL picture of sample M11, showing an overview of the sample and the present darker bands; (B): PPL picture of the altered fossilised wood of sample M12-1; (C): XPL picture of the altered fossilised wood of sample M12-1; (D): PPL picture showing the interior of sample M12-2; (E): PPL picture, showing the glauconite overprinting quartz and yellow clay at the edges of the glauconite grains; (F): XPL picture of the cell-structure found in sample K1.



## 2.5 Lenses

Apart from the injectites and mud mounds, lenses containing the same material as the mud mounds, crop out at Micadalen. Therefore, some samples from the lenses were taken as well, described below.

### 2.5.1 L1

The thin section from sample L1 contains small ( $<0,1 - 0,1$  mm), subangular, moderately-sorted, non-oriented quartz grains in a cement. Furthermore, oxide dots were observed. There are bands with lighter colored material, comprising quartz grains and calcite crystals of around 0,1 mm. There are bands with lighter material: quartz grains and calcite crystals (Fig. S28.A). The sample contains one crack, filled with calcite.

### 2.5.2 L2

From sample L2, 3 thin sections were made: L2-1, L2-2 and L2-3 (Fig. ??). From the bottom to the top of the sample: L2-3, L2-2 and L2-1. Samples L2-1 and L2-2 contain a layer of shell fragments that lay in a groundmass as described for L1; small ( $<0,1 - 0,1$  mm), subangular, moderately-sorted, non-oriented quartz grains in a cement (Fig. S28.E). Also here, oxide dots were observed. The shells are probably ostracods, with three-layered shells (Fig. S28.B, C, D). The fossils have two types of infilling: the groundmass or calcite crystals (Fig. S28.D). The calcite crystals were probably formed after the groundmass, filling up pores formed by air bubbles.

### 2.5.3 L3

This thin section looks like L1 and L2-3; the sample contains small ( $<0,1 - 0,1$  mm), subangular, moderately-sorted, non-oriented quartz grains in a cement. There are calcite veins going through the whole thin section and the oxide dots, observed in L1 and L2 are also present in this thin section (Fig. S28.F). Also, shell fragments ( $<0,1$  mm) of three-layered shells are present.

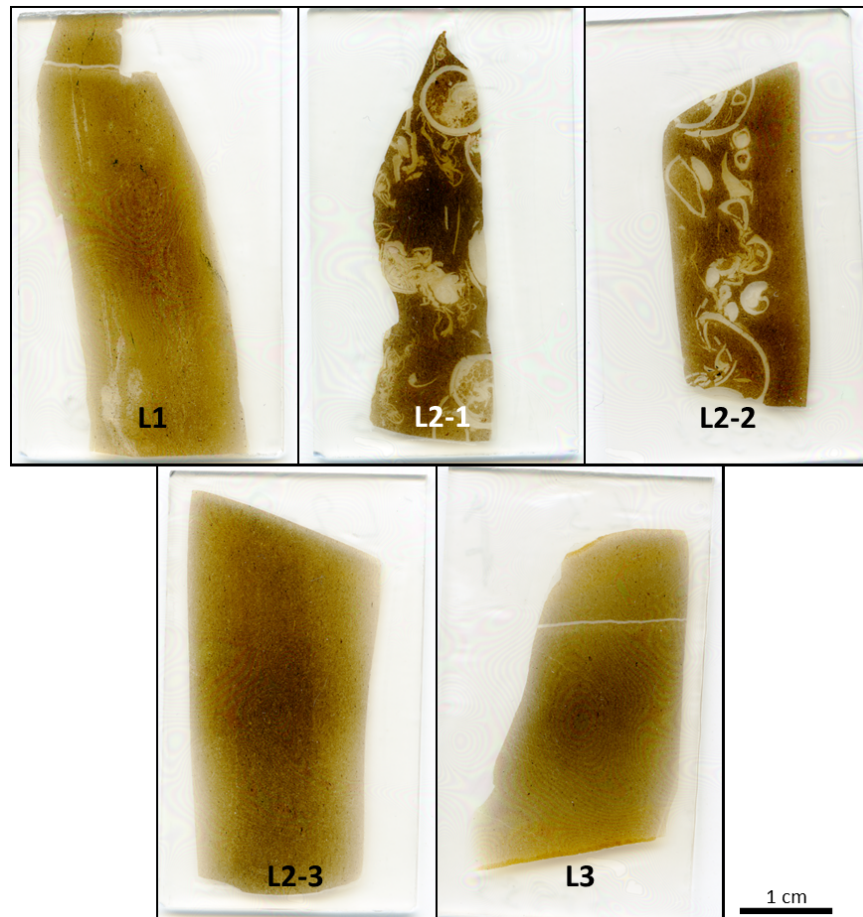


Figure S27: Scans from the thin sections of the samples from L1, L2 and L3. The thin sections are arranged in the order they will be described.



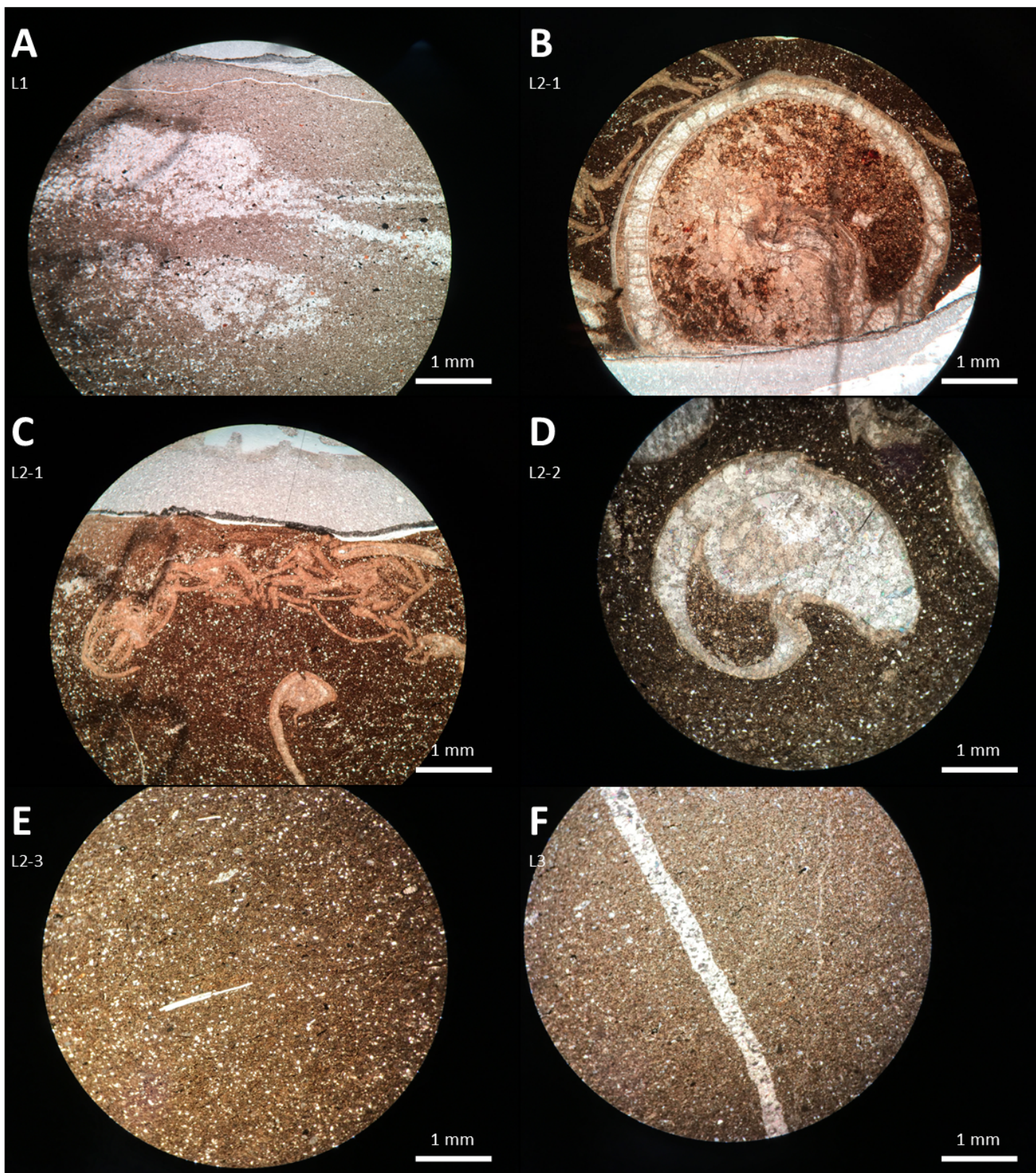


Figure S28: Pictures from samples L1, L2 and L3. (A): PPL picture of sample L1, showing the lighter bands; (B): PPL picture of an ostracod shell in sample L2-1; (C): PPL picture of the broken shell fossils in sample L2-1; (D): PPL picture of the different fillings of the ostracod fossils in sample L2-2; (E): PPL picture showing the interior of sample L2-3; (F): XPL picture of sample L3.



### 3 SEM-EDS

With SEM-EDS the interior of all studied injectites, two country rock samples and the non-oriented samples from the injectite material were studied. With SEM, detailed pictures of the thin sections have been made. EDS was used to study the samples geochemically, indicating the chemical differences between the cement present in samples and detecting differences and similarities between the injectites and host rock. For thin sections I1S2, I2S2, I3S1-1, I4S1, I5S1, I6S1-2, I7S2, M3-1, M6, M12-1, M13 and F8 a carbon coating was used to measure with SEM-EDS.

#### 3.1 Upper complex

##### 3.1.1 I1S2

Grains that were not well understood with the polarized microscope were studied with SEM-EDS. There is no carbonate-related cement present, all grains lay in a fine-grained matrix composed of the same material as the bigger grains. Most oxide grains are composed of rutile. Recognized feldspars are orthoclase and albite. Furthermore, alumino-silicates, muscovite, quartz and carbon were found. The recognized wood fragments are composed of carbon (spot F, Fig. S30.B). A quartz grain with an overgrowth to small to determine under the polarized microscope, has been analysed as well (spot B, Fig. S30.A & Fig. S5.A). SEM-EDS shows that the grain is composed of albite with illite inclusions or alteration.

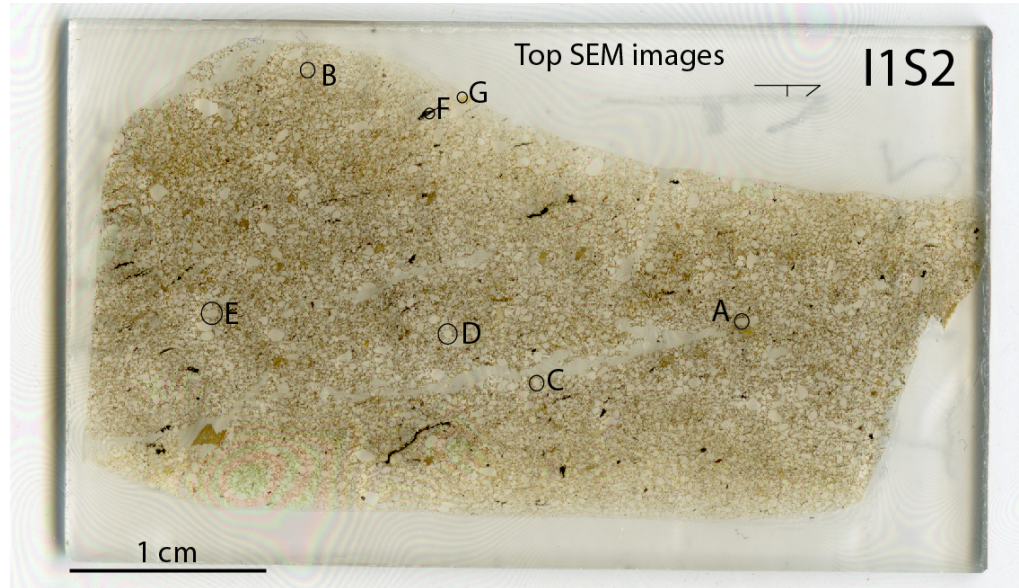


Figure S29: Scan of thin section I1S2, showing the locations analysed with SEM-EDS.

Line measurements along four well rounded quartz grains showed that the measured quartz grains are homogeneous. It also confirms the finding that the matrix has the same composition as the rest of the grains, being mostly composed of quartz and alumino-silicates.

I1S2		mass%									
Point	Comments	Al2O3	C	Cl	FeO	K2O	MgO	Na2O	SO3	SiO2	TiO2
A1	Orthoclase	11.94	31.65			9.68				46.73	
A2	Titanite/rutile	11.81	17.09		1.07	0.22				26.31	43.51
A3	Quartz		34.1							65.9	
A4	Quartz		34.94							65.06	
B1	Illite	23.68	29.02		1.48	8.53	2.08			35.2	
B2	Albite	14.79	29.75					7.85		47.62	
B3	Quartz		32.57					0.11		67.32	
B4	Muscovite?	14.1	32.46		12.27	4.17	9.51			26.27	1.22
B5		16.69	30.75		21.84		7.76			22.96	
C2		16.34	16.8			12.53				54.33	
E2		31.71	32.95							35.34	
F1	Carbon		94.66	5.34							
F2	Carbon		98.4						0.94	0.66	
F3	Quartz		38.54							61.46	
G1	Alumino-silicate	27.62	44.11							28.27	
G2	Quartz		38							62	

Table S2: EDS results of thin section I1S2. The points correspond with the letters of the analysed locations given in Fig. S29.



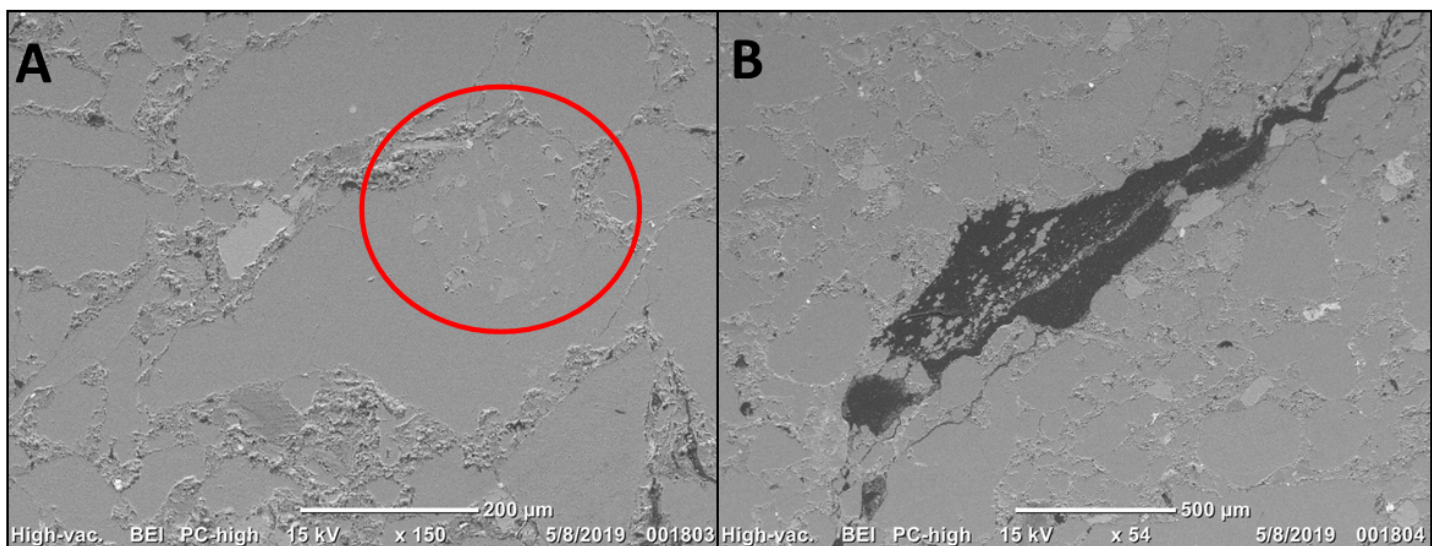


Figure S30: (A): Picture of location B, showing quartz grains and the albite with muscovite grain (red circle). (B): Picture of location F, showing a flake comprising 95% carbon.

### 3.1.2 I2S2

The measured grains comprise quartz, alumino-silicates, siderite, carbon, albite, sanidine, rutile and chalcopyrite. Similar to I1S2, this sample does not contain a cement. The matrix between the grains comprises the same material as found in the rest of the sample, mainly composed of  $\text{SiO}_2$  and  $\text{Al}_2\text{O}_3$ , suggesting it is mainly Al-rich clay minerals. The found feldspars, sanidine and albite are both alkali feldspars. Line measurements on three well-rounded quartz crystals show a homogeneous composition of the quartz grains and no remarkable structures around them. At point B4, a small % of phosphor was measured inside a siderite grain. The cracks inside the quartz grain at spot D are filled with a clay that contains a bit of Ca. The chalcopyrite crystals measured at spot I have a rim composed of carbon, suggesting the crystals may have an organic origin.



Figure S31: Scan of thin section I2S2, showing the locations analysed with SEM-EDS.



I2S2		mass%													
Point	Comments	Al <sub>2</sub> O <sub>3</sub>	C	CaO	Cl	CuO	FeO	K <sub>2</sub> O	MgO	N	Na <sub>2</sub> O	P <sub>2</sub> O <sub>5</sub>	SO <sub>3</sub>	SiO <sub>2</sub>	TiO <sub>2</sub>
A1	Sanidine	13.88	29.35					10.66			0.89			45.22	
A3	Quartz		32.25											67.75	
A4	Alumino-silicate	30.49	34.23											35.28	
B1			61.76							37.26			0.98		
B2			50.46		0.33		7.94			24.44		0.53	0.33	15.99	
B3	Alumino-silicate	24.2	35.94				1.53	4.53	1.11					32.68	
B4	Siderite with P?	3.11	31.45				50.38	0.38				1.89	3.16	9.63	
B5	Alumino-silicate	32.25	31.86											35.89	
D1	Albite?		6.75	6.09					5.29		16.71			65.16	
D5	Calcite?	19	26.11	16.8			5.44							32.66	
G1	Sanidine	13.46	28.76					12.04			0.5			45.24	
G2	Alumino-silicate	32.34	31.75											35.92	
G3	Quartz		29.09											70.91	
G5	Rutile		13.28											2.27	84.45
G6	Sanidine	26.51	31.82					7.73			0.39			32.38	1.18
H1	Carbon		96.3	1.66									1.34	0.69	
H2	Quartz		31.43											68.57	
I1	Chalcopyrite		18.7			21.84	21.18						37.82	0.46	
I2	?	1.47	52.73	2.43			2	0.44		36.22		1.28	0.54	2.89	
J1	Rutile	1.67	17.13											2.31	78.89
L3		22.29	30.98				2.92	8.01	1.41					34.38	

Table S3: EDS results of thin section I2S2. The points correspond with the letters of the analysed locations given in Fig. S31.

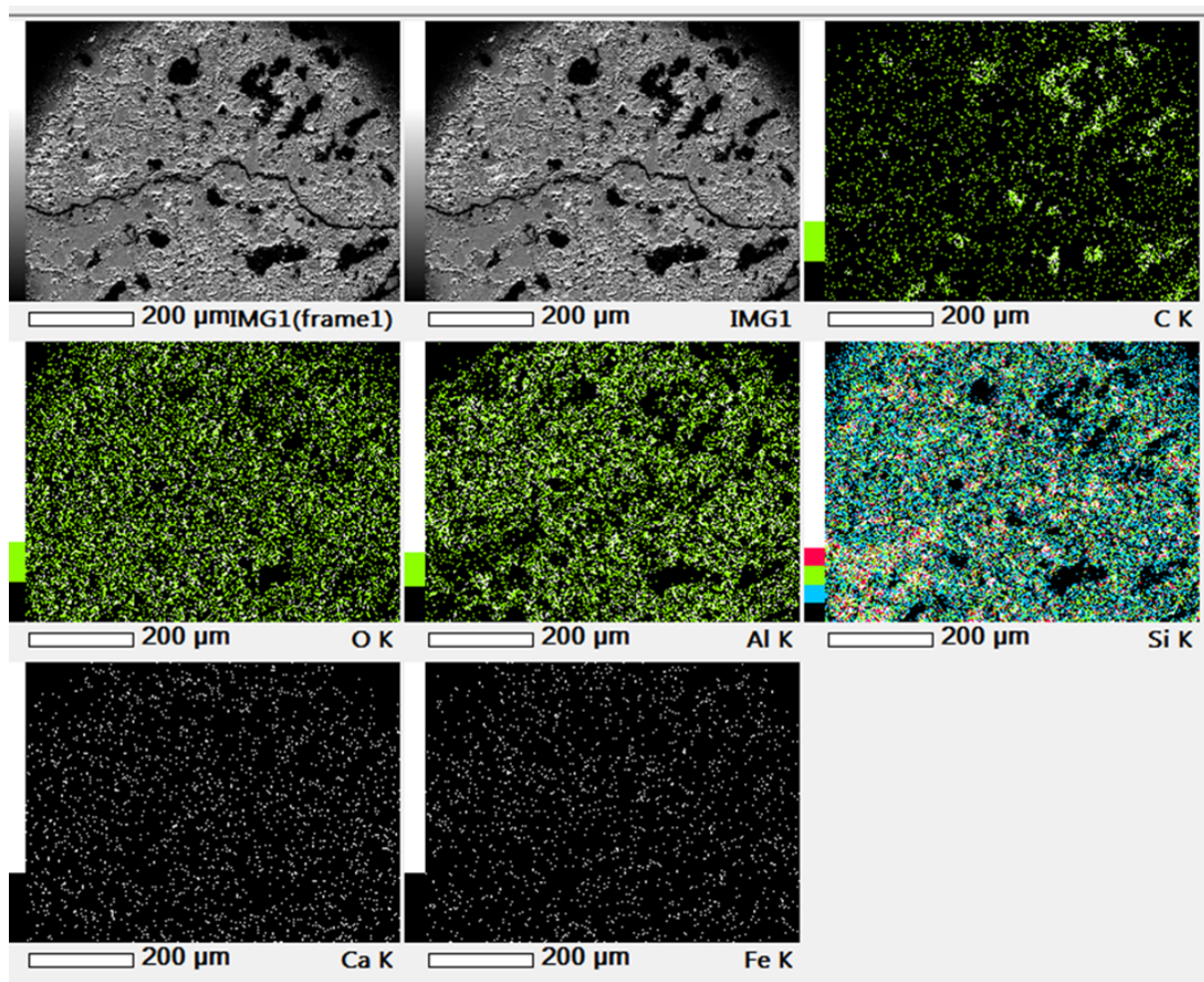


Figure S32: Element map of location G (Fig. S31), showing the matrix between the grains



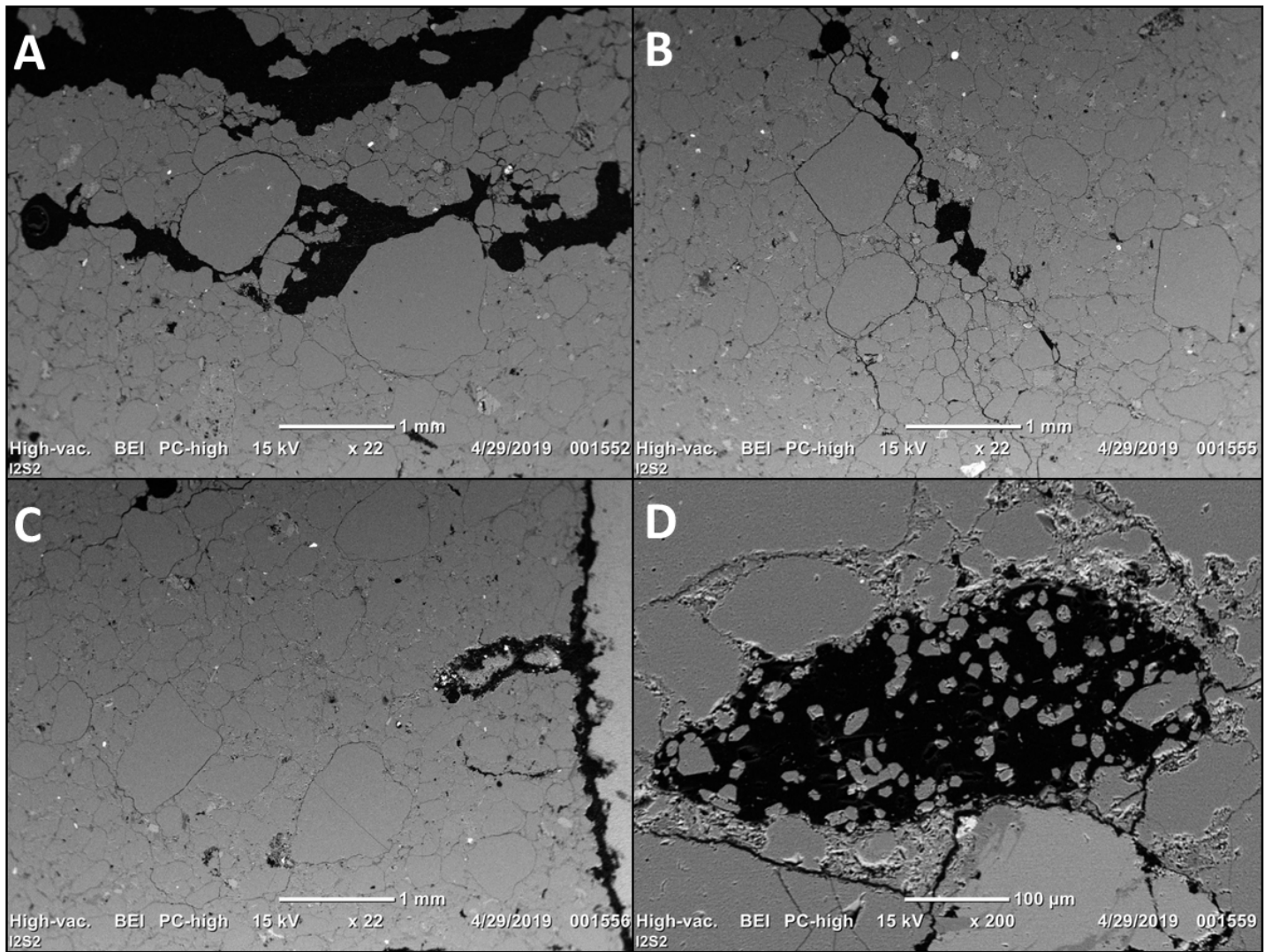


Figure S33: (A): Location C, showing mainly quartz grains. Cracks (black) are visible. (B): Location E, showing mainly quartz crystals. Cracks (black) are visible. (C): Location F, showing mainly quartz. Edge of thin section on the right side. (D): Location H, a grain comprising 95% carbon.



## 3.2 Lower complex

### 3.2.1 I3S1-1

The samples from Injectite 3 contain three zones: zone 1 (host rock), zone 2 (injectites margin) and zone 3 (injectites interior). Line analysis across quartz grains that were well rounded have been conducted in all three zones. This showed homogeneous quartz grains in all three zones and no different signatures between the zones (Fig. S35).

**Zone 1:** Analysed spots I, J and P are located in the host rock strata. During petrographic microscopy quartz, feldspar, plagioclase, mica, glauconite and oxide grains have been observed. SEM-EDS analysis shows that the grains lay in an ankerite cement. One sanidine grain was measured. Also, most oxide grains are composed of pyrite. The organic material is filled with pyrite or carbon (spot J). Most pellets are filled with pyrite (spot I).

**Zone 2:** Spots G, H, N and O are located in the transition zone, forming a boundary between the injected material and the host strata. At spot G oxide crystals next to a quartz grain were analysed, showing that these are barite crystals. Spot H shows a carbon flake. The grains in this zone are matrix-supported, laying in an ankerite cement. The cement is quite homogeneous, but line measurements show eroded holes filled with aluminosilicates. The fractures in the grains are filled with the same type of cement as the cemented ground mass.

**Zone 3:** In the injectite material spots A, B, C, D, E, F, K, L and M were analysed. During microscopic analysis quartz, chert, mudstone, mica, glauconite and plagioclase grains were observed. SEM-EDS analysis add siderite, rutile, zircon, aluminosilicate, carbon and pyrite. All grains lay in a mix of aluminosilicate and ankerite cement. Fractures in quartz grains are filled with the same type of ankerite cement as found around the grains. Spots A, B and M are analysing a big chert grain (0,5 mm) and adjacent reworked conglomerate. The fractures, filled with ankerite, going through the chert grain, continue in the reworked grain, but do not continue in the injectite material. The reworked grain consists of quartz, feldspar, zircon, rutile and siderite grains in an aluminosilicate matrix. Some iron-rich grains contain a carbon rim around them. Around the big chert grain a rim of ankerite cement is located where the neighbouring injectite material is located. This rim does not continue where the reworked grain is located, wherefore they seem attached to each other. This rim is not located around the reworked grain. A mudstone grain has been analysed at spot C, showing small pyrite, carbon and quartz grains in a carbon-rich matrix. The black grain analysed at spot D is a big pyrite grain (0,2 mm) with a surrounding ankerite rim.

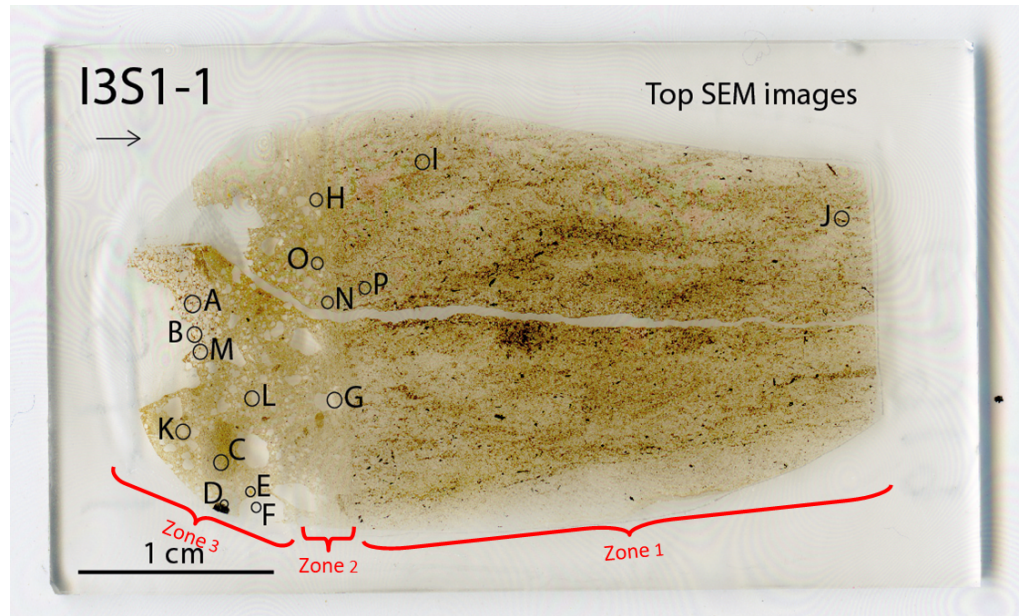


Figure S34: Scan of thin section I3S1-1, showing the locations analysed with SEM-EDS.

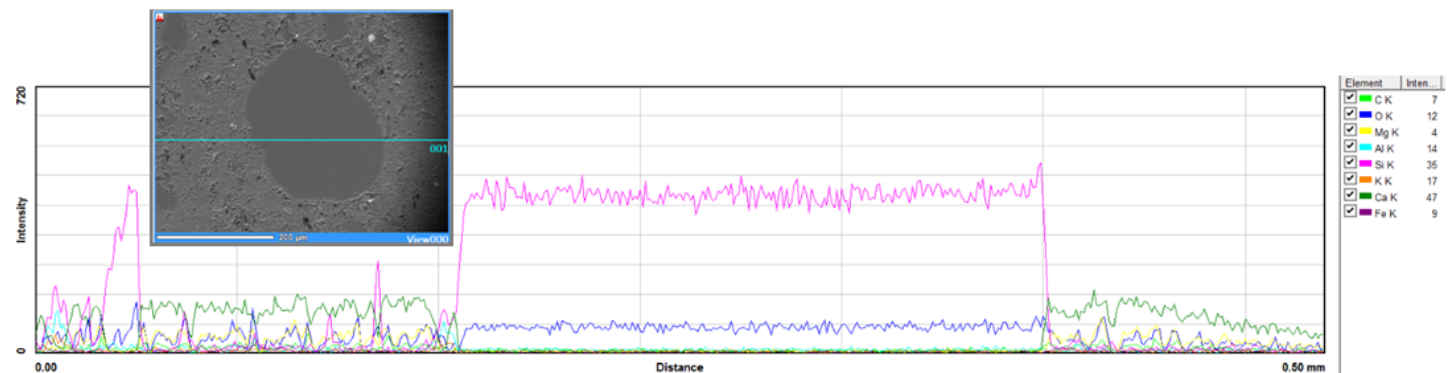


Figure S35: Line measurement at point O, zone 2.



I3S1-1		mass%																					
Point	Comments	Al2O3	BaO	C	CaO	CeO2	Cl	FeO	K2O	La2O3	MgO	N	Na2O	Nd2O3	P2O5	PbO	SO3	SiO2	ThO2	TiO2	U3O8	ZrO2	
A1	?			19.05	1.89	22.28				13.38				5.22	23.7			1.04	7.76		5.69		
A2	Carbon	1.21		76.96	9.97			3.69			4.15						2.69	1.31					
A3	Zircon			34.92														21.26			43.83		
A4	Rutile			13.9																86.1			
A5	Ankerite cement			35.77	38.93			3.92			21.38												
A6	Siderite							28.94									71.06						
A7	Alumino-silicate	45.34																54.66					
A8	Siderite			24.52				21.66									53.82						
A9	?	11.31		48.23	0.46		0.53		1.83									16.03		21.61			
B1	Ankerite cement			34.41	36.82			10.77			17.99												
B2	Alumino-silicate	31.29		34.52														34.19					
B3	Ankerite cement			35.36	37.62			11.08			15.94												
B4	Siderite			23.24				21.24									55.52						
C1	Pyrite			28.12	1.59			30.86			0.78						38.65						
C2	?			55.68			0.11					44.21											
C3	Ankerite cement	2.5		42.28	26.26			10.27			13.86							4.83					
D1	Pyrite	0.72		23.23				23.85									51.11	1.09					
D2	Ankerite cement			34	37.65			11.28			17.07												
D3	Ankerite cement	2.7		39.88	28.86			8.66			14.99							4.92					
D4	Ankerite cement	2.03		37.69	30.53			8.71			15.46							5.59					
D5	Ankerite cement	3.16		42.75	23.38			9.28	0.95		11.26							9.22					
D6	Ankerite cement			34.92	36.77			9.7			16.61							2					
D7	Ankerite cement			36.7	34.05			9.67			17							2.57					
D8	Siderite	1.38		32.59	1.83			53.62			1.3		1.01					8.26					
E1	Zircon			30.77								8.73						19.56				40.94	
E2	Quartz	3.23		29.88	5.68				1.01		2.36							57.84					
E3	Quartz			31.16	7.02			1.95			2.94							56.93					
F1	Carbon			78.42			0.89		0.93				0.65					19.1					
F2	Quartz			36.45			0.04						0.04					63.47					
F3	Quartz			35.05														64.95					
G1	Barite		36.81	21.56												11.13	20.74	0.51		9.25			
G2	Barite		38.49	20.85												10.8	19.95	0.7		9.2			
G3	Ankerite cement			38.48	35.3			2.76			23.46												
G4	Ankerite cement	1.4		34.9	37.39			4.98			18.43							2.9					
G5	Ankerite cement			30.99	39.26			8.37			21.38												
H1	Ankerite cement			33.85	40.22			3.35			22.59												
H2	?			60.7								38.55					0.75						
I1	Ankerite cement			33.88	34.59			10.56			18.64						1.38	0.95					
I2	Pyrite			24.29				22.09									53.63						
I3	Ankerite cement	1.26		33.65	37.27			6.43			18.1							3.29					
I4	Carbon			92.66	4.56						0.59						1.57	0.63					
J1	Ankerite cement	1.09		40.78	30.01			5.28			20.39							2.46					
J2	Pyrite			24.54				29.94									45.52						
J3	Carbon			98.58													1.42						
J4	Sanidine	14.56		26.34					11.56				0.4					47.15					

Table S4: EDS results of thin section I1S2. The points correspond with the letters of the analysed locations given in Fig. S34.

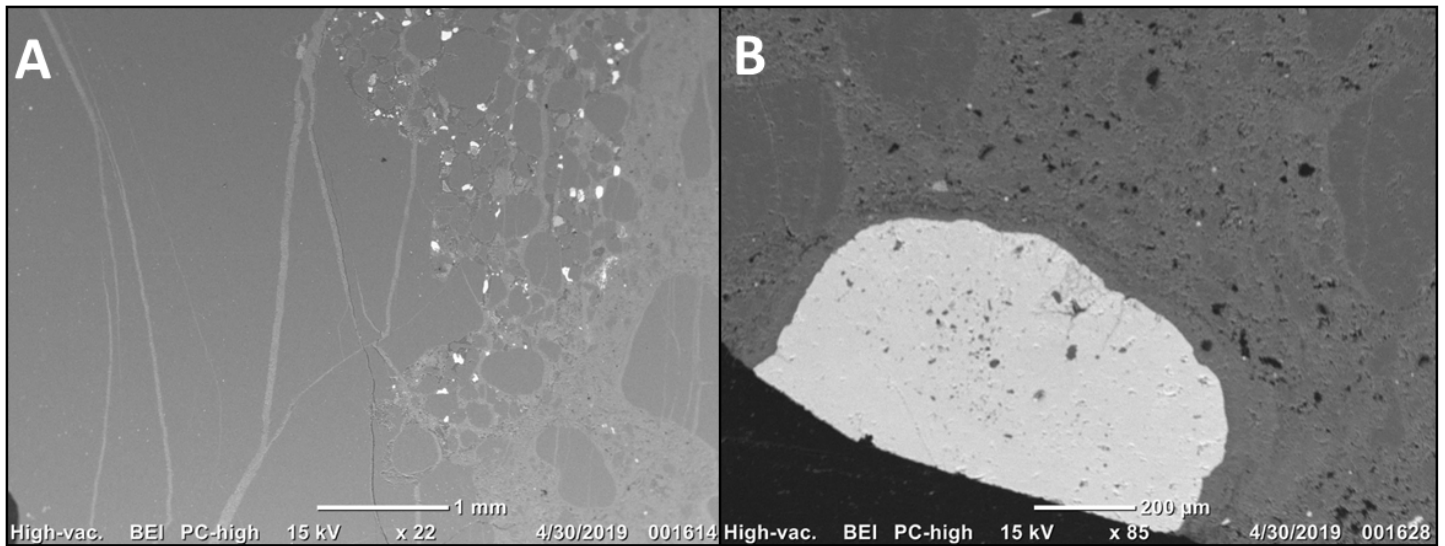


Figure S36: (A): Location A (zone 3), showing cracks in a quartz grain, filled with with similar material as the cement. (B): Location D (zone 3), showing a pyrite grain (white) in the injectites interior.



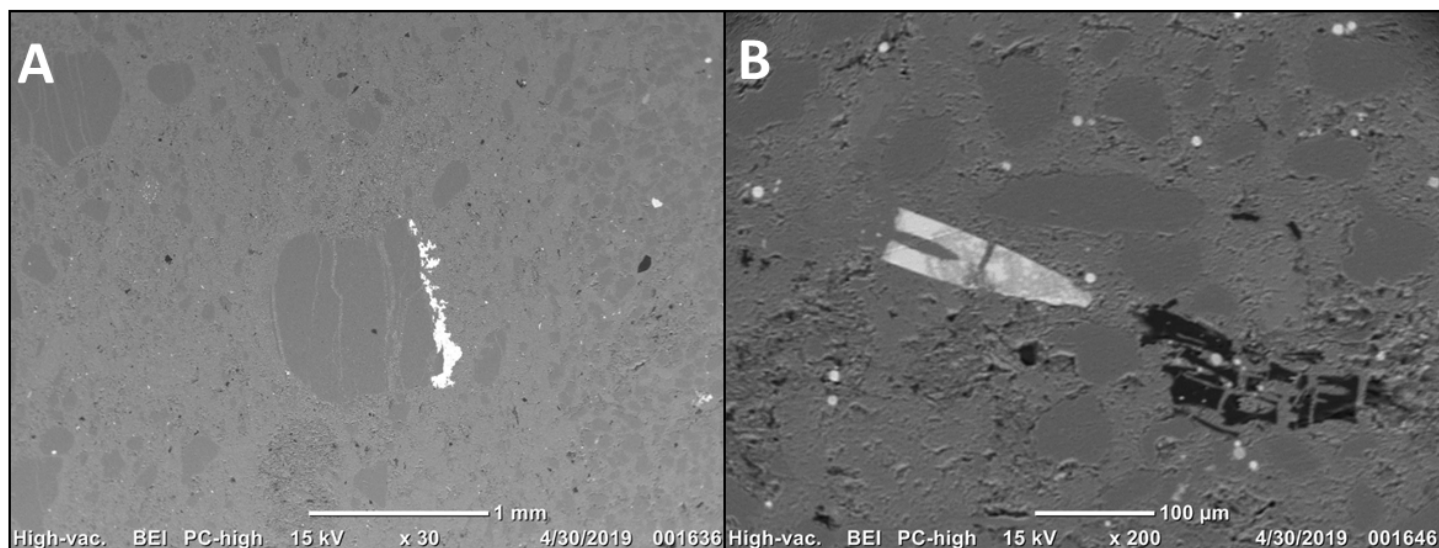


Figure S37: (A): Location G (zone 2), showing a quartz grain with barite on its right edge. (B): Location J (zone 1), showing fossil remnants filled by pyrite (white) and carbon (black). The white dots are framboidal pyrite structures.

### 3.2.2 I4S1

SEM-EDS analysis of Injectite 4, added alumino-silicate, carbon, pyrite, orthoclase, sanidine and barite grains to the list of observed grains with the polarized microscope (quartz, chert, plagioclase, mudstone and mica grains). All grains lay in an ankerite cement. The cement is overprinted by alumino-silicate clays at some point. Some dark grains, interpreted as wood fossils during microscopy, are composed of pyrite with feldspar and quartz grains (spot B). Around these grains a rim of carbon is present. These grains probably have a biological origin, but are converted to pyrite. The carbonate rim is a remnant of the biological origin. The mudstone clasts (spot A and G) comprise carbon, pyrite, feldspar and quartz grains in a muddy matrix composed of alumino-silicate. Barite has been found surrounding structures that seem to have an biologic origin (spot F). Line measurements have been conducted on well-rounded quartz grains and showed homogeneous quartz grains. Cracks inside the quartz grains are filled with alumino-silicate clays.

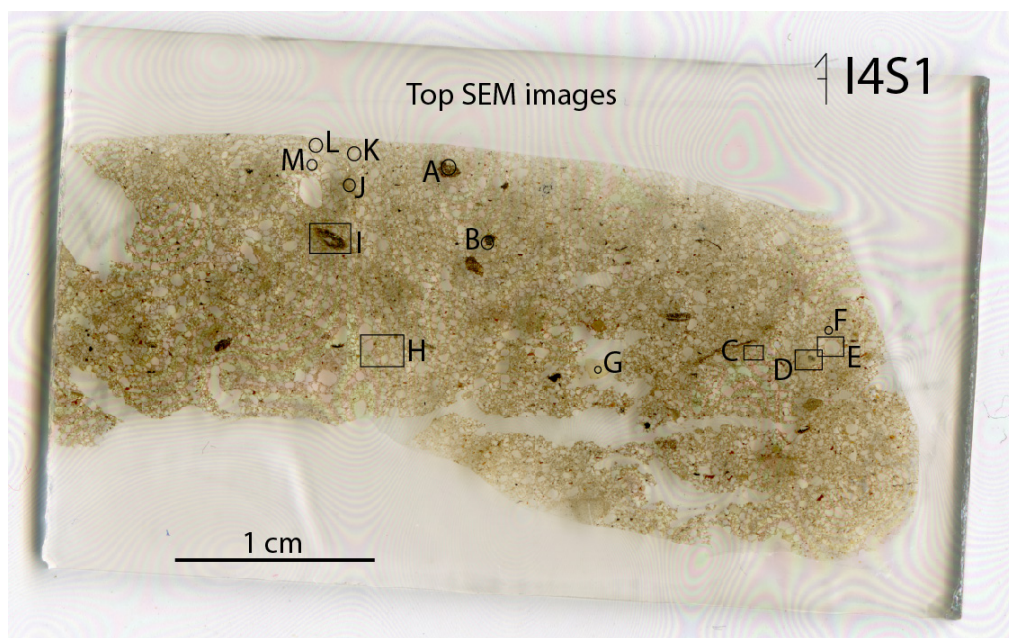


Figure S38: Scan of thin section I4S1, showing the locations analysed with SEM-EDS.



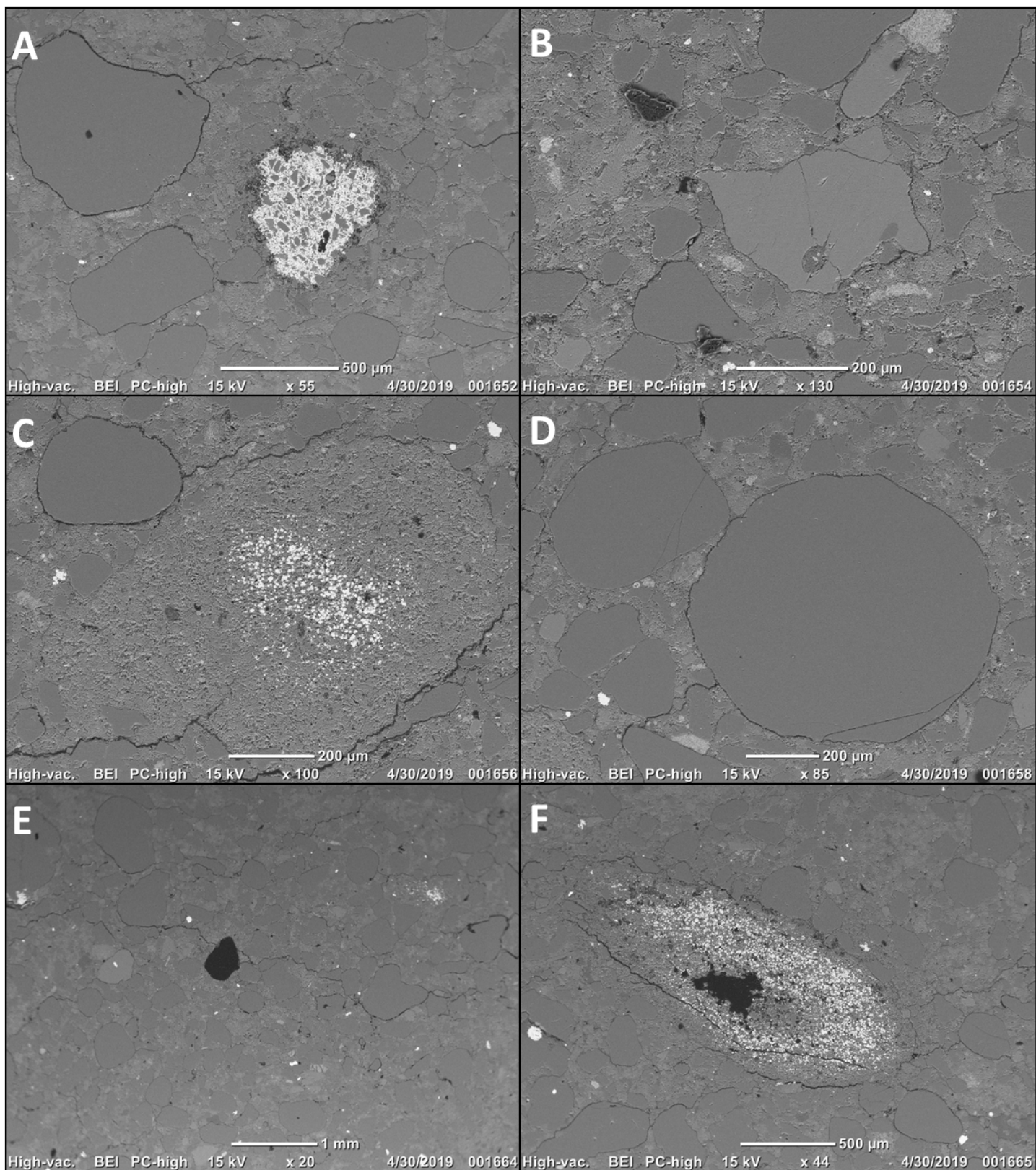


Figure S39: (A): Location B, showing a grain composed of quartz grain and framboidal pyrite (white grain), surrounded by a carbon (black material). (B): Location C, showing a bigger feldspar grain between quartz grains. (C): Location D, showing a space filled by cement with in the middle a cluster of framboidal pyrite structures (white dots). (D): Location E, showing a well-rounded grain. (E): Location H, showing cracks going through the sample. (F): Location I, showing clustered framboidal pyrite (white dots), with in the middle carbon (black).



I4S1		mass%													
Point	Comments	Al2O3	BaO	C	CaO	Cl	FeO	K2O	MgO	N	Na2O	PbO	SO3	SiO2	TiO2
A1	Alumino-silicate	14.97		51.13				2.77	1.06					30.07	
A2	Carbon			100											
A3	Pyrite			25.8			20.69						53.51		
A4	Alumino-silicate	30.42		31.08				0.75						37.75	
A6	Orthoclase?	13.44		30.69				11.29						44.58	
B1	Pyrite			21.86			22.17						55.97		
B2	Sanidine	19.3		25.9				2.81			4.94			47.06	
B3	?	0.58		54.83	0.68	0.3	1.31	0.29		40.71				1.3	
B4	Alumino-silicate	32.03		11.7	0.34	0.06	2.3	6.53		5.31				41.72	
B5	Alumino-silicate	53.66		29.86							0.49			15.99	
F1	Barite		35.99	18.74								12.34	22.02	0.58	10.33
F2	Alumino-silicate	27.86	27.36					3.97	1.29					39.52	
F4	Pyroxene?	20.2		27.51			22.46		8.34					21.49	
J1	Pyrite with Pb?			17.83			18.27					14.59	49.31		
J2	Orthoclase?	13.9		28.76				11.02						46.32	
J3	Ankerite cement			35.61	31.86		3.94		19.64						8.95
J4	Alumino-silicate	33.4		29.94										36.66	
M2	Ankerite cement			35.85	36.14		3.79		20.94					3.27	

Table S5: EDS results of thin section I4S1. The points correspond with the letters of the analysed locations given in Fig. S38.

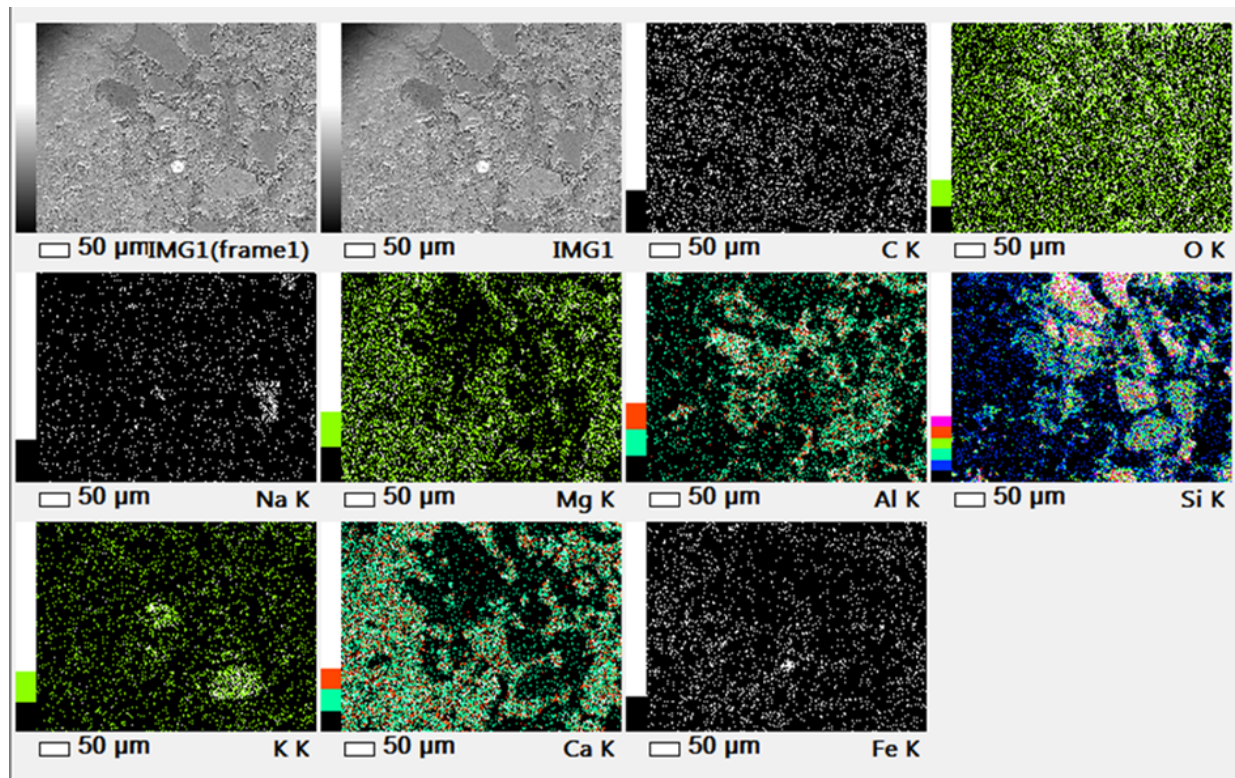


Figure S40: Element map of location J (Fig. S38), showing the matrix between the grains



3.2.3 M6

The interior of M6 looks similar to the injectite interiors. Therefore, the chemical composition of this sample was measured more in detail. Pyrite, siderite and orthoclase grains were analysed with SEM-EDS. All grains lay in an ankerite cement that is partly overprinted by alumino-silicate clays. Spot A shows that the interpret mudstone clasts are composed of ankerite cement. Line measurements of well-rounded quartz grains showed homogeneous quartz grains.

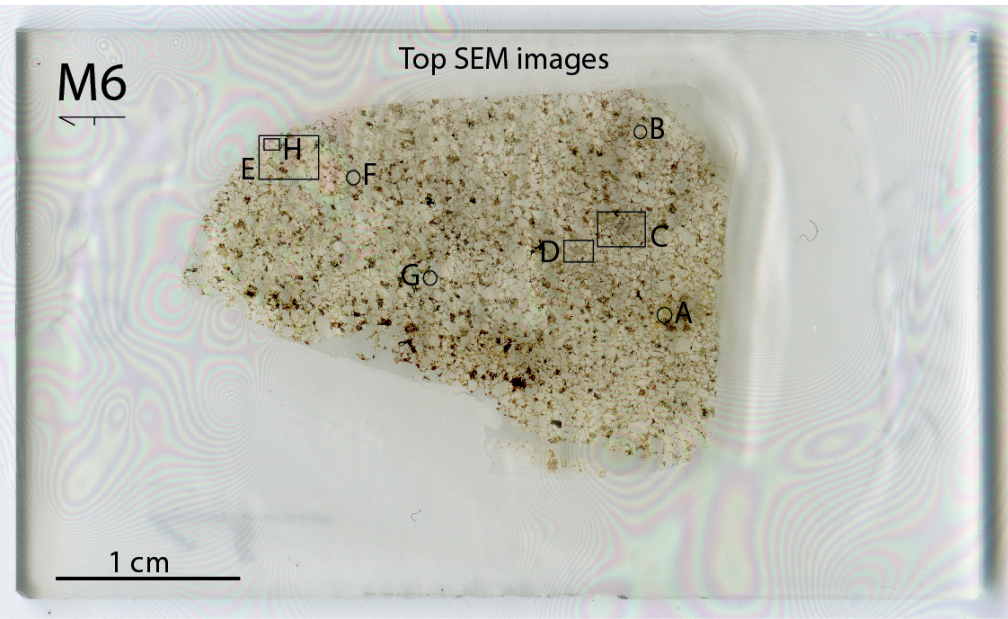


Figure S41: Scan of thin section M6, showing the locations analysed with SEM-EDS.

M6		mass%								
Point	Comments	Al2O3	C	CaO	Cl	FeO	K2O	MgO	SO3	SiO2
A1	Alumino-silicate	22.85	53.77		0.39					22.99
A2	Pyrite		21.87			22.63			55.5	
A3	Ankerite cement		35.03	34.26		9.85		20.05		0.81
A4	Siderite		33.63	5.32		49.29		11.22		0.53
B3	Ankerite cement		39.08	31		11.63		17.59		0.7
B4	Orthoclase	14.05	28.66				11.34			45.95
F2	Mg-calcite / Ankerite cement?	2.63	36.86	32.41		2.73		21.03		4.36
F3	Siderite		35.49	0.72		57.67		1.85		4.26
G2	Pyrite		22.14			22.51			55.35	

Table S6: EDS results of thin section I4S1. The points correspond with the letters of the analysed locations given in Fig. S41.

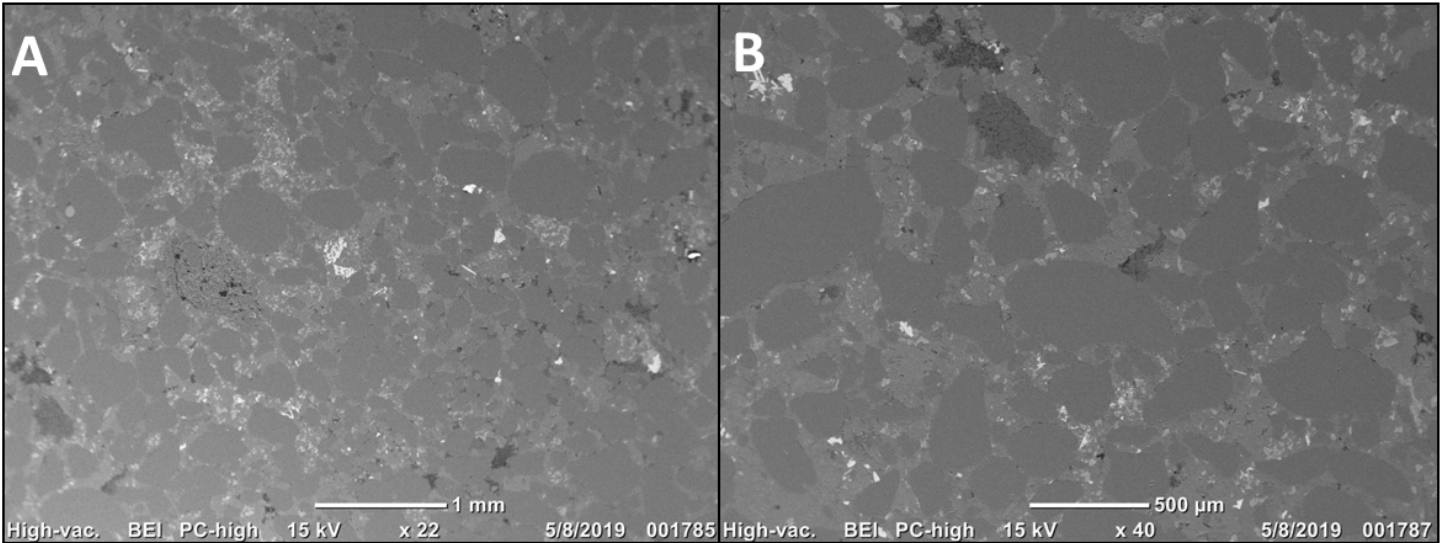


Figure S42: (A): Location C, giving an overview of the interior of M6. (B): Location D, showing the different types of grains: quartz, pyrite clusters, feldspars and alumino-silicate clays.



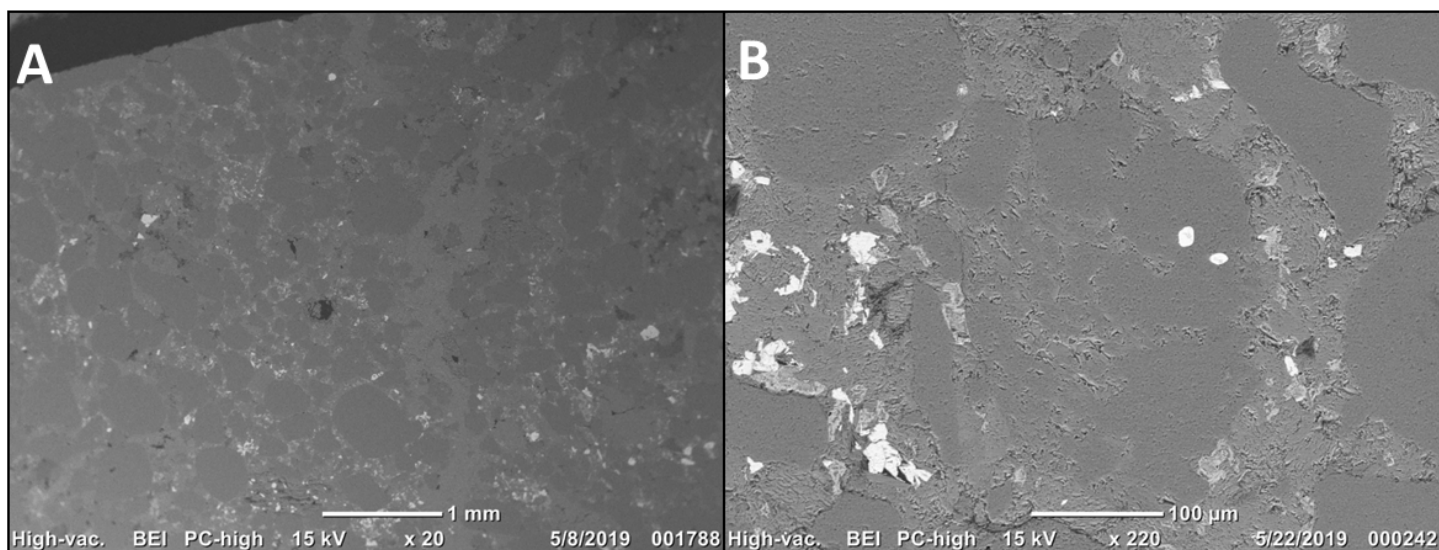


Figure S43: (A): Location E. (B): Location H, showing a silica grain (middle) that had a deviating extinction under the polarized microscope (stayed totally black under XPL).

### 3.2.4 I5S1

The sample of Injectite 5 comprises the injectite material and fabric of the mudstone clasts observed at the margins. Line measurements in both areas show only homogeneous quartz grains and no remarkable observations.

**Injectite interior:** The coarser grained material on shows the injected material. Analysed spots in this area are spots A, B, C, D, E, F, G, H, I, J, K, R, S and U. Rutile, siderite, pyrite, alumino-silicate, orthoclase, albite and biotite grains have been observed. With the polarized microscope quartz, plagioclase and colorless mica grains were already observed. Most clasts that were not well understood turn out the comprise the same material; pyrite and siderite crystals in an ankerite cement (spots B, C, D, E, G, H, J and K). This cement is in some cases partly overprinted with alumino-silicate clays and some of these clasts contain carbon in the cemented matrix. Therefore, different colors of these pyrite clasts are observed. Spot A shows a strange form of clast, comprising rutile and siderite bands. The pores between the bands are filled with ankerite cement. There are different types of lithic clasts analysed. Spot F shows a orthoclase grain with pyrite and albite inclusion. All grains lay in an ankerite cement that is partly overprinted with alumino-silicate clays, especially around the pyrite clasts. Some of these more altered pyrite clasts have

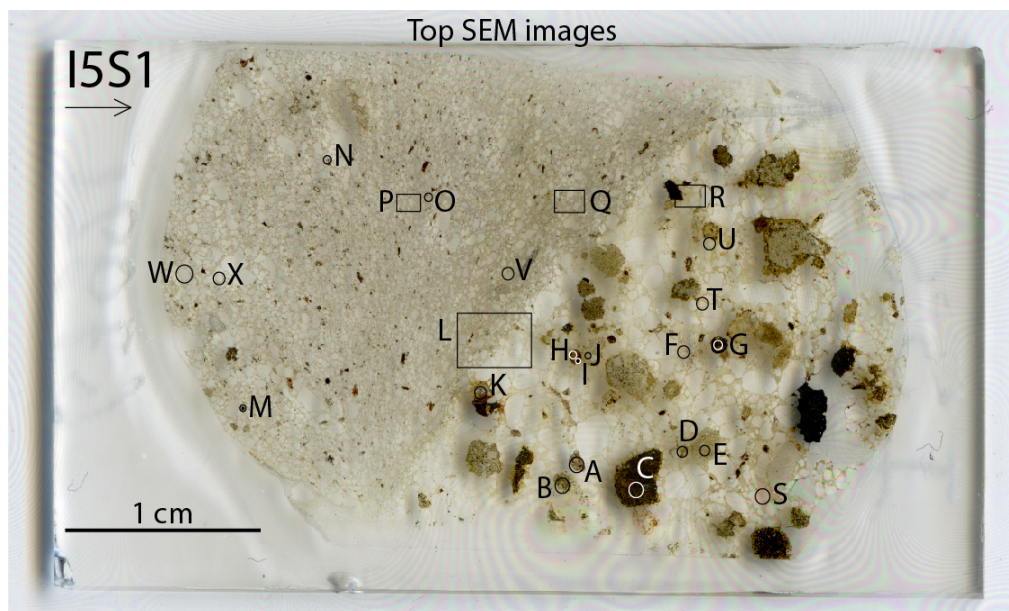


Figure S44: Scan of thin section I5S1, showing the locations analysed with SEM-EDS. On the right side of the thin section, the coarser grained material represents the injectites interior. On the left side, the finer grained material is part of a mudstone clasts, which is part of the injectite as well.

**Mudstone clast:** Spots L, M, N, O, P, Q, W and X were analysed in the mudstone clast section. Pyrite, rutile, zircon and siderite grains were analysed. The mudstone clast further comprises quartz, plagioclase, feldspar and mica grains, observed with petrographic microscopy. Spot N contains a grain similar to spot A; an strange clast filled up with rutile and cement in the pores. Different are the pyrite dots around the clast. All grains lay in an ankerite cement, partly overprinted by alumino-silicate clays.



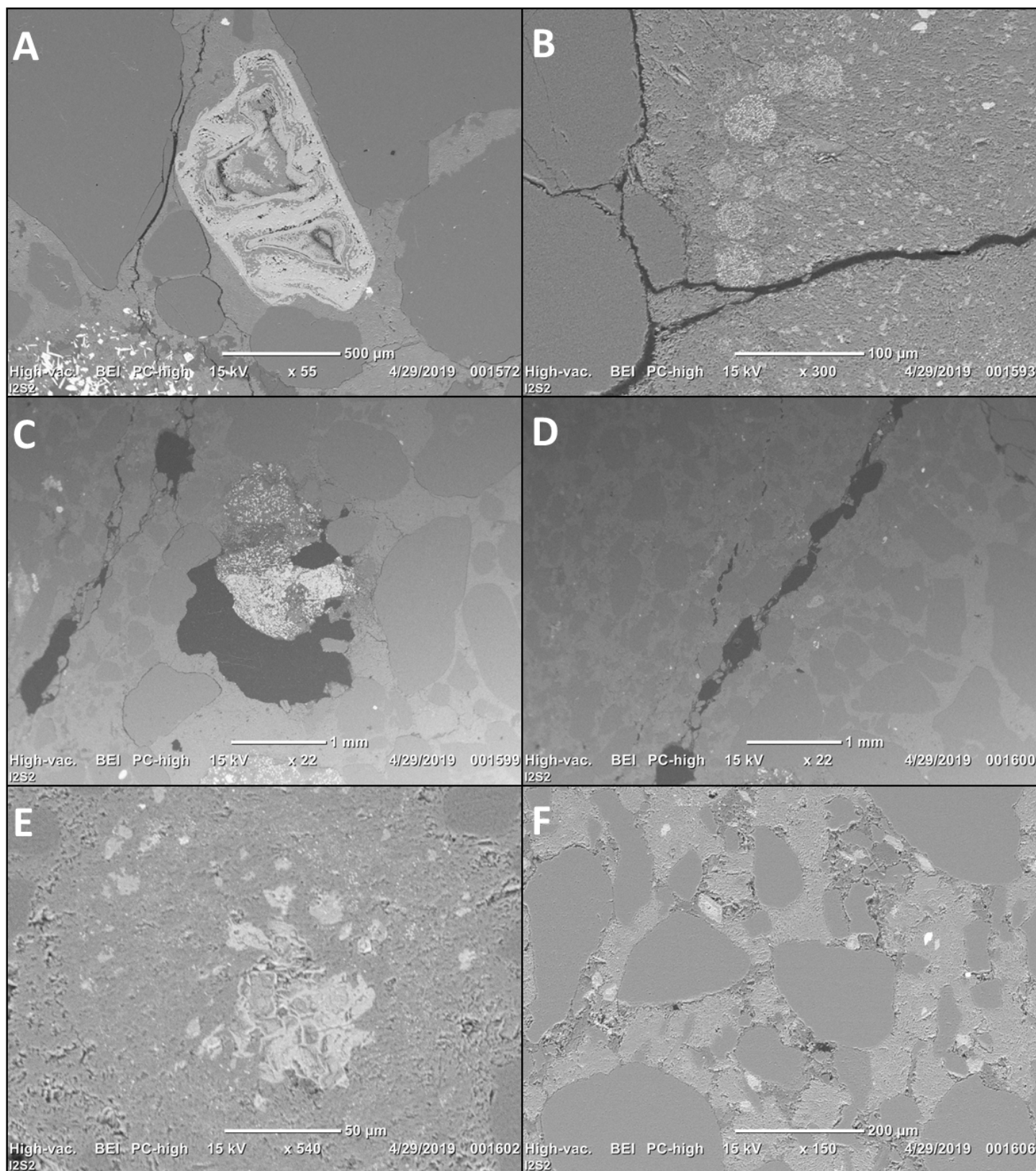


Figure S45: (A): Location A, showing a grain composed of rutile and siderite in the injectites interior. (B): Location H, showing framboidal pyrite structures within the injectite interior. (C): Location K, showing a cluster of pyrite crystals and framboidal pyrite, surrounded by carbon in the injectites interior. (D): Location L, showing the boundary between the injectite interior (right) and mudstone clast (left). (E): Location M, showing pyrite with a strange pyrite structure in the mudstone clast. (F): Location P.



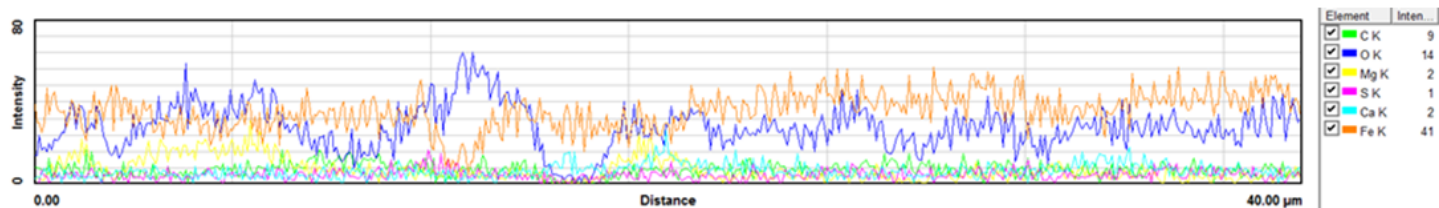


Figure S46: Line measurement through the pyrite grain shown at location M (Fig. S45.E).

I5S1		mass%													
Point	Comments	Al2O3	C	CaO	Cl	FeO	K2O	MgO	N	Na2O	PbO	SO3	SiO2	TiO2	ZrO2
A1	Rutile		12.11											87.89	
A2	Siderite		38.89	3.08		40.77		17.27							
A3	Rutile	1.59	16.67			2.42							2.52	76.79	
A4	Rutile	0.7	73.82			1.57						1.18	1.01	21.71	
A5	Ankerite cement		34.53	33.93		12.56		18.98							
A6	Rutile		24.28											75.72	
A7	Ankerite cement		29.46	39.23		11.78		19.54							
A8	Quartz												100		
A9	Rutile		39.73								6.58	9.45		44.24	
B1	Pyrite		21.53			22.16						56.31			
B2	Ankerite cement		32.65	37.19		8.61		21.55							
B3	Alumino-silicate	30.6	37.26										32.13		
C1	Pyrite		18.95			18.63					15.89	46.52			
C2	Orthoclase	29.72	36.62				1.22						32.44		
C3	Carbon	2.47	93.88										3.66		
D1	Pyrite		27.14	0.5		20.78						51.58			
D2	Quartz												100		
D3	Carbon		96.32		3.68										
D4	Alumino-silicate	31.83	36.62										31.55		
D5	Siderite		29.39			70.61									
E1	Pyrite		22.7			22						55.3			
E2	Ankerite cement		33.48	34.81		10.93		20.78							
F1	Sanidine/Orthoclase	14.44	27.3				11.49			0.47			46.3		
F2	Albite	14.35	29.3							8.86			47.49		
F3	Pyrite					36.99						63.01			
G1	Ankerite cement		32.46	39.31		11.73		16.51							
G2	Siderite		35.27	1.4		56.32		3.8					3.21		
G3	Alumino-silicate	29.12	28.82			1.62	3.98						36.46		
H1	Ankerite cement		39.66	13.18		30.05		9.01				8.09			
H2	Siderite/pyrite?		27.38	4.19		37.11		1.88			8.62	19.82	0.99		
H3	Ankerite cement		34.29	36.24		11.93		17.55							
H4	Ankerite cement		33.03	37.46		15.51		14							
J1	Alumino-silicate	31.5	38.58										29.93		
J2	Pyrite		19.49			18.66					15.17	46.68			
K1	Pyrite		20.09			19.19					13.64	47.08			
K2	Biotite	32.5	10.36			10.48	5.05						41.61		
N1	Rutile		15.45										1.22	83.32	
N2	Rutile	1.42		1.11		1.02							1.38	95.06	
N3	Pyrite					28.68						71.32			
N4	Ankerite cement		35.72	34.96		12.54		16.78							
O1	Zircon		30.83						8.43				19.61		41.13
O2	Ankerite cement	0.9	40.33	29.71		8.42		19.22					1.42		
O3	Siderite		36.41	3.64		53.13		6.82							
X1				10.59		2.67		4.58					82.16		

Table S7: EDS results of thin section I4S1. The points correspond with the letters of the analysed locations given in Fig. S44.



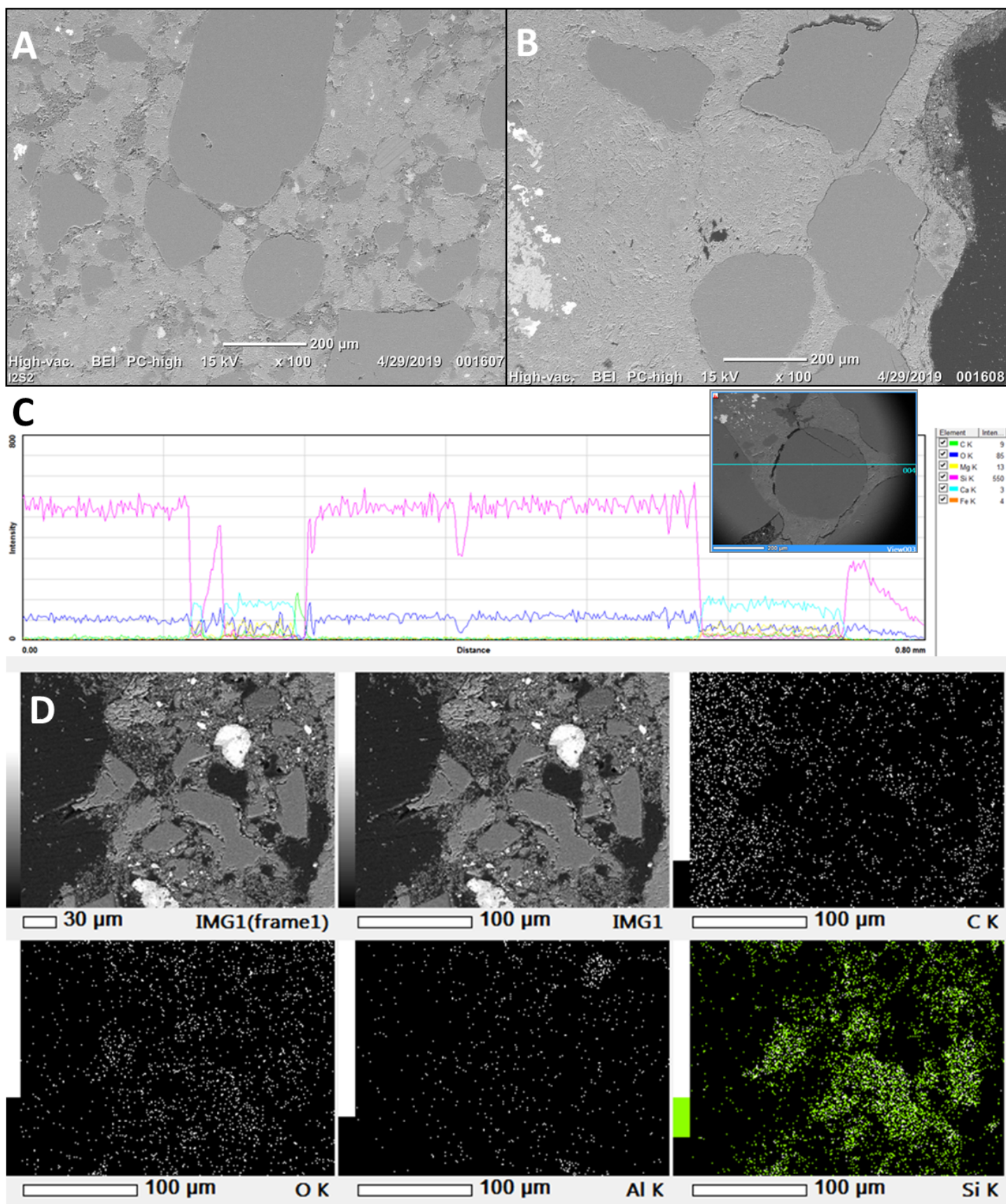


Figure S47: (A): Location Q, showing the interior of the mudstone clast. (B): Location R, showing the injectites interior. (C): Line measurement of a quartz grain at location T (injectite interior). (D) Element map of location D (injectite interior, Fig. S44).



3.2.5 I6S1-2

Analysed grains with SEM-EDS comprise carbon, barite, orthoclase, pyrite and zircon. Adding them to the list already observed with polarized microscope (quartz, feldspar, plagioclase, mica). All grains lay in an ankerite cement that is partly overprinted by aluminosilicate clays. Spot B contains an aluminium-chromite, probably from the spinel-group, inside a barite grain. The grain is almost totally converted to barite. Spots D and E show clusters of pyrite crystals between quartz grains inside the ankerite cement. Spot F comprises a clast composed of pyrite in an ankerite cement that is partly overprinted with aluminosilicate clays.

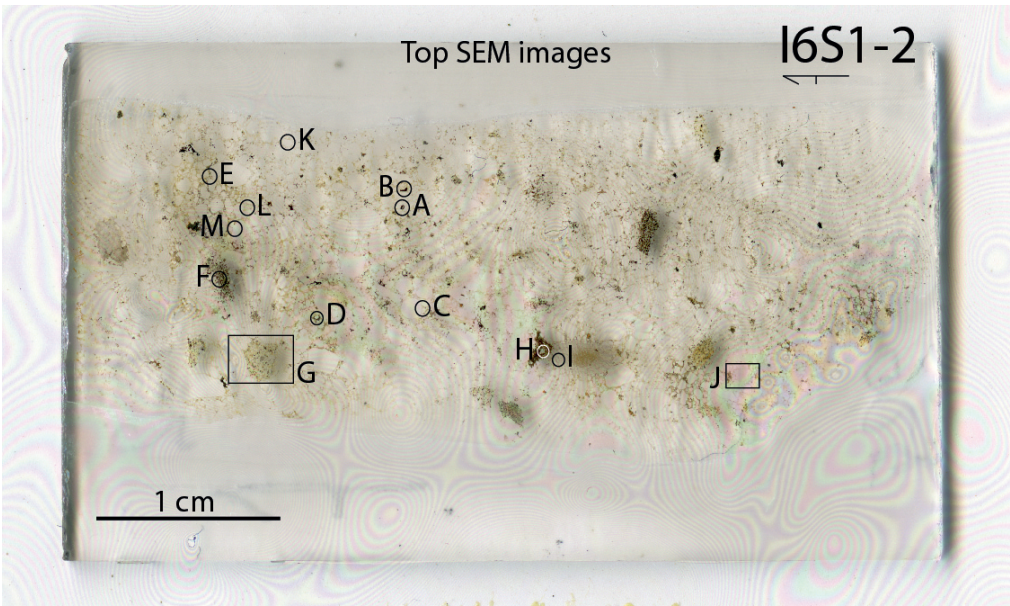


Figure S48: Scan of thin section I6S1-2, showing the locations analysed with SEM-EDS.

I6S1-2		mass%																				
Point	Comments	Al2O3	As2O3	BaO	C	CaO	CeO2	Cl	Cr2O3	FeO	K2O	La2O3	MgO	N	Na2O	P2O5	PbO	SO3	SiO2	ThO2	TiO2	ZrO2
A1	?				21.7	1.2	24.19					12.02				22.34			2.05	9.56		6.95
A2	?				24.99		27.48					13.27				20.48				6.7		7.08
A3	Carbon	2.51			88.18						0.47							3.99	4.38		0.48	
A4	Carbon	1.6			88.25											0.82		5.63	3.7			
B1	Aluminium-chromite (spinel)	17			20.34				35.44	12.57			14.64									
B2	Orthoclase	13.78			29.01						11.81								45.4			
B3	Orthoclase	14.01			27.55						11.81				0.56				46.06			
B4	Carbon	1.96			51.34	0.39				1.23	1.15			36.61					7.31			
B5	Pyrite				19.07	0.81				20.66	0.59						14.99	42.02	1.87			
B6	Barite	1.76		43.16	8.86					1.33			0.72				10.75	16.26	2.05	15.11		
C2	Ankerite cement				44.32	29.13				5.6			20.3						0.64			
C3	Ankerite cement				43.1	28.38				6.69			21.59						0.24			
C4	Ankerite cement				23.04	46.66				12.22			18.08									
C5	Zircon				31.1														21.85			47.05
D1	Pyrite				24.07					22.5								53.43				
D2	Ankerite cement				36.64	35.71				5.94			21.71									
E2	Ankerite cement				37.23	33.43				5.69			23.18					0.04	0.43			
E3	Pyrite				24.12					21.49								54.39				
F1	Ankerite cement				26.75	42.82				9.56			20.87									
F2	Pyrite				13.84					40.93								44.51	0.73			
F3	Orthoclase	14.66			66.9		0.52				0.48								17.43			
I3	Ankerite cement				37.83	35.29				6.51			20.38									
I5	Ankerite cement	1.47			37.56	28.95				5.48			23.61						2.93			
K2	Ankerite cement		2.85		37.54	32.28				9.05			18.28									
L3	Ankerite cement				31.33	40.1				8.43			20.15									

Table S8: EDS results of thin section I6S1-2. The points correspond with the letters of the analysed locations given in Fig. S48.



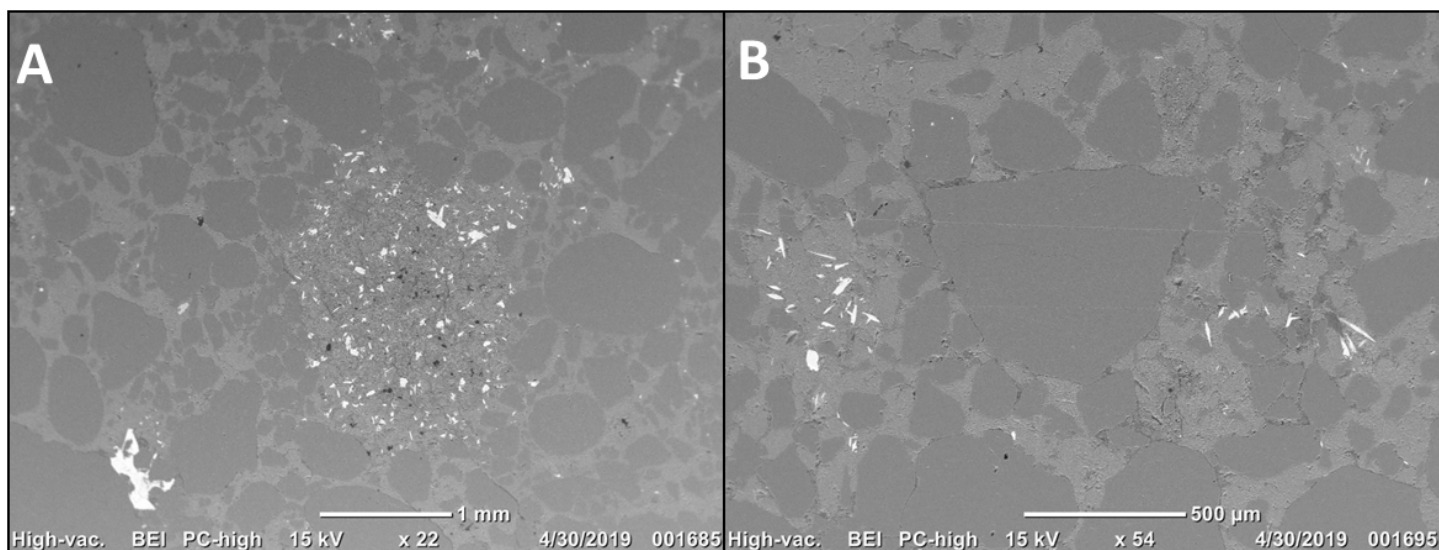


Figure S49: (A): Location G, showing a cluster of pyrite (white flakes) and carbon (black flakes), surrounded by cement. (B): Location J, showing a quartz grain (middle grain) that stays black under the petrographic microscope with a XPL filter.

### 3.2.6 I7S1

The two measured spots of sample I7S1 comprises the only two type of lithic clasts observed in this thin section. Furthermore quartz, plagioclase, colorless mica and zircon grains have been observed with the polarized microscope. Spot A comprises a part of the dark round grain. This grain is composed of small quartz grains ; 0,1 mm (quartz, feldspar, framboidal pyrite) in a matrix of ankerite cement and carbon flakes. Spot B has analysed the composition of the brown colored grains. These spots also contain small quartz grains ; 0,1 mm in an ankerite cement. This cement also contains some carbon, but less than spot A. All grains lay in an ankerite cement.

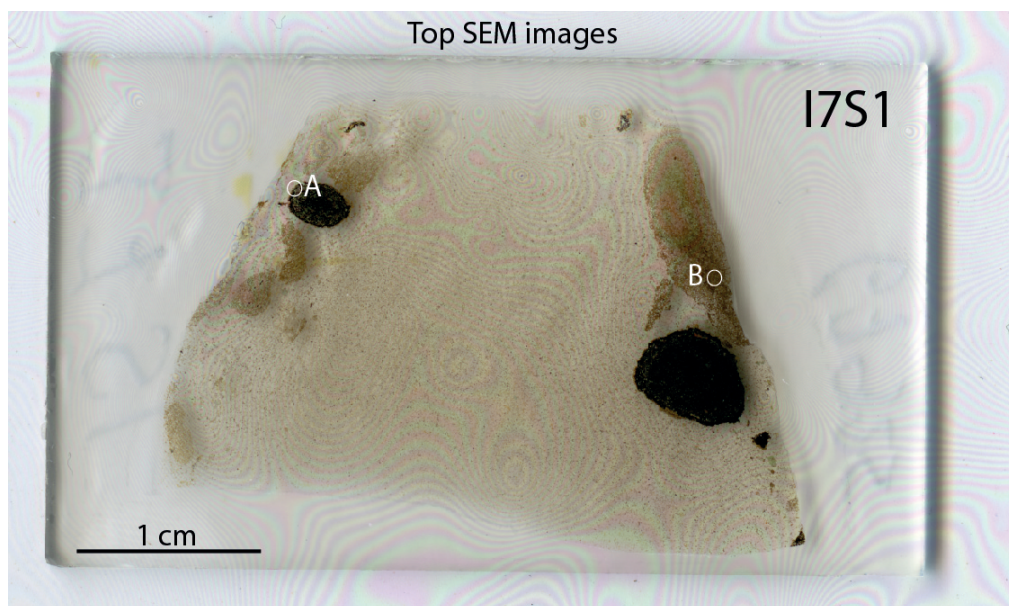


Figure S50: Scan of thin section I7S1, showing the locations analysed with SEM-EDS.

I7S1		mass%						
Point	Comments	Al <sub>2</sub> O <sub>3</sub>	C	CaO	FeO	N	SO <sub>3</sub>	SiO <sub>2</sub>
A1	Ankerite cement		38.79	28.92	4.52		0.55	3.78
A2	Quartz		25.5	1.61	0.94		0.43	70.65
A3	?		59.72	0.8	0.62	36.05	0.52	1.85
A4	Quartz		14.58	0.92				84.5
B5	Ankerite cement	2.67	35.04	28.59	4.93			10.37
B6	Quartz		13.44	1.28				84.56

Table S9: EDS results of thin section I6S1-2. The points correspond with the letters of the analysed locations given in Fig. S50.



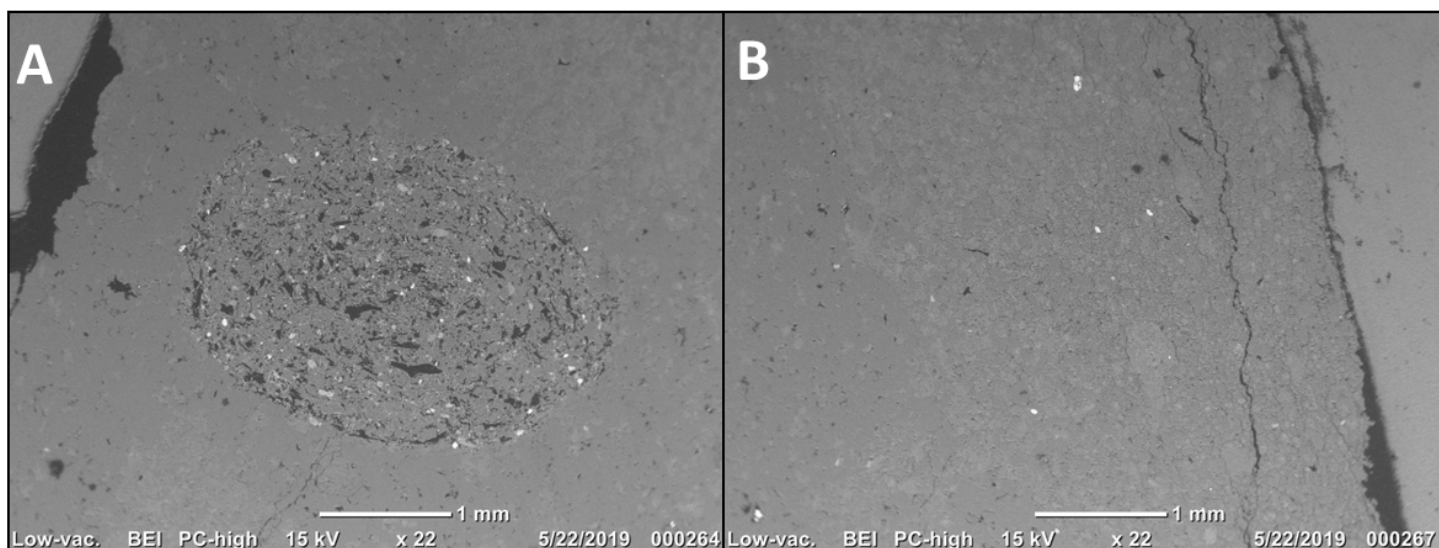


Figure S51: (A): Location A, showing one of the big black grain as seen in Fig. S50. (B): Location B, showing one of the brown grains as seen in Fig. S50.

### 3.2.7 I7S2

Sample I7S2 comprises quartz, plagioclase, feldspar and colorless mica grains observed with the polarized microscope and alumino-silicate, carbon, pyrite, zircon, rutile, barite and orthoclase grains were analysed with SEM-EDS. All grains lay in an ankerite cement that has been partly overprinted by alumino-silicate clays. At some spots the cement gives the SEM a darker color, caused by enrichment in sulphur and titanium. Some dark spots on the thin section contain a high carbon content. Spots F comprises the same type of pyrite clasts as in I5S1 (clustered pyrite crystals in an ankerite cement). Also, a quartz grain with pyrite inclusions was analysed. Spot I contains barite crystals surrounded by rutile grains, a pyrite crystals and ankerite cement.

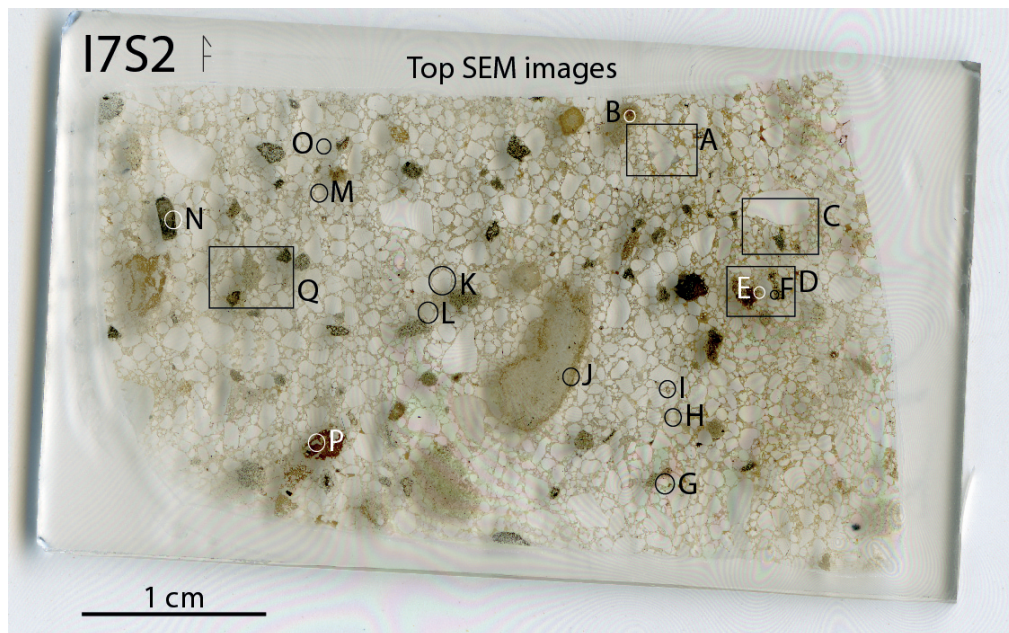


Figure S52: Scan of thin section I7S2, showing the locations analysed with SEM-EDS.



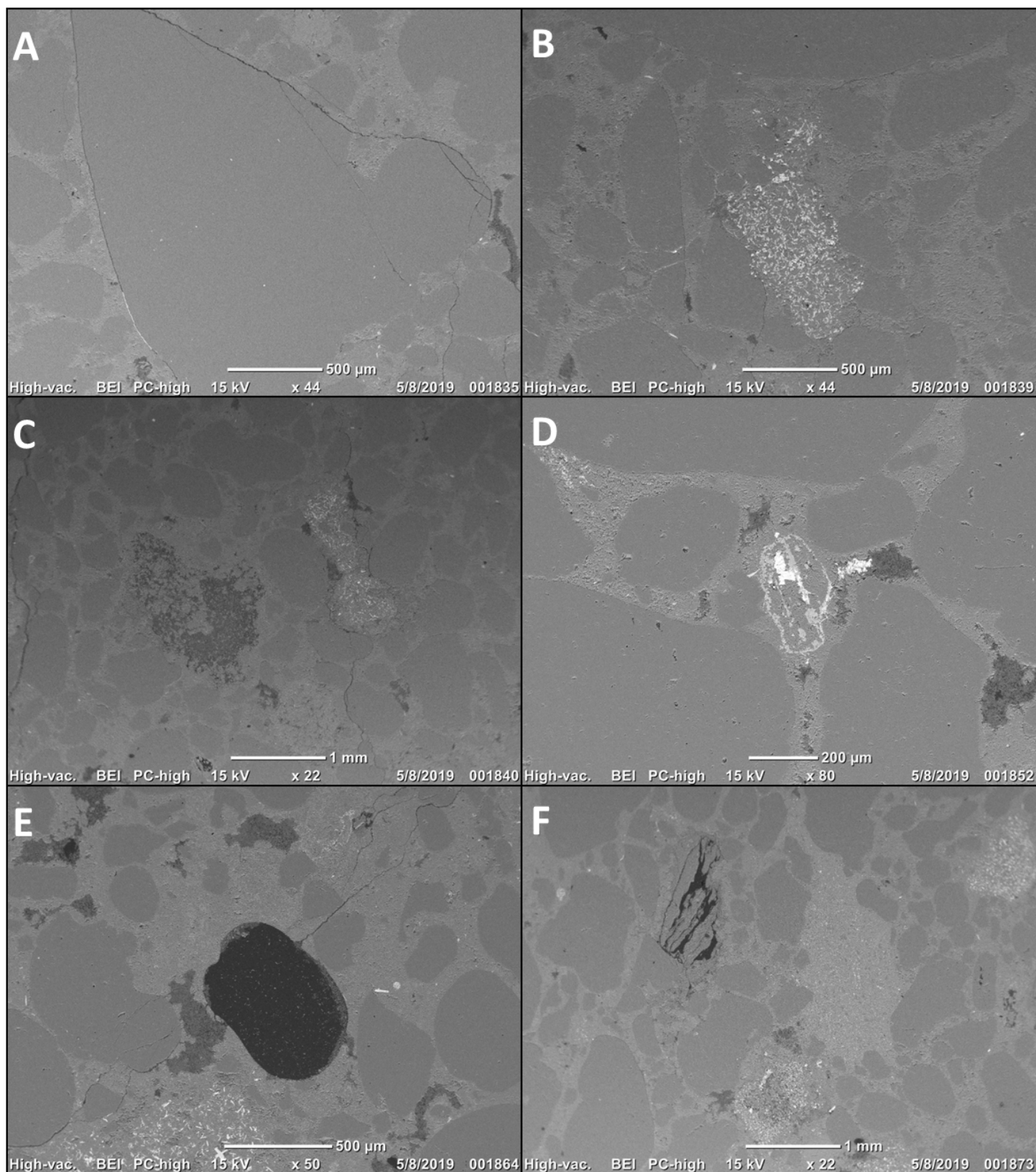


Figure S53: (A): Location A, showing a chalcedony grain, homogeneously composed of silica. (B): Location C, showing a cluster of pyrite crystals. (C): Location D, showing a grain mainly composed of carbon flakes (left, darker grain) and a cluster of pyrite crystals (white flakes). (D): Location I, showing a structure composed of rutile (light gray material) and barite (white material) in cement. The dark grey material are alumino silicate clays, filling up pores in the cement. (E): Location L, showing a black grain composed of 95% carbon and 5% chlorine. (F): Location Q, showing some pyrite clusters (white flakes) and a grain with non-filled cracks (grain with black stripes).



I7S2		mass%																	
Point	Comments	Al2O3	As2O3	BaO	C	CaO	Cl	FeO	K2O	MgO	Na2O	P2O5	SO3	SiO2	TiO2	ZrO2			
B1	Ankerite cement	25.95	3.22	35.26	32.14	23.82		7.64		16.13		1.85	9.28	0.89	10.11				
B2	Alumino-silicate				46.18	0.28													27.59
B3	Ankerite cement				35.46	31.45		3.73									20.27		7.25
E1	Ankerite cement or Mg-calcite	46.2			24.35	2.32		25.03		2.1									
E2	Carbon	14.03			67.25	1.44	1.06			9.14	3.97	3.12							
E3	Mg-calcite				67.02								32.98						
F1	Pyrite				25.45	0.39							26.38		47.78				
F2	Ankerite cement				31.61	21.23		5.63		15.14		0.72	25.67						
F3	Alumino-silicate	22.53			30.97	0.44	0.25	1	2.67	2.82		39.55							
F4	Alumino-silicate	30.21			37.05									0.21	32.27				
G1	Zircon		32.28			21.54							46.07						
G2	Ankerite cement	23	32.55	37.97	6.36		19.89												
G3	Alumino-silicate		54.68	0.31							0.2			21.81					
H4	Ankerite cement		24.46												49.49	7.68	15.91	2.28	
I1	Rutile	13.98	35.26						86.02										
I2	Barite	23.82								30.44	10.49								
I3	Ankerite cement	37.68		31.62						5.14		25.57							
I4	Pyrite		25.4		27.96		46.64	1.82											
J1	Ankerite cement	1.76	39.22	30.68	2.75	0.54	23.77		30.53	2.37									
J2	Orthoclase	29.48	37.09																
J3	Carbon		98.77		1.23														
J4	Pyrite		33.72	1.52		30.15				33.57	1.04								
L1	Carbon		94.92		5.08		5.26	22.99											
L2	Ankerite cement		40.25	31.5									6.55	22.81	55.45	0.77	100		
M2	Ankerite cement		34.24	36.39								20.15							
N2	Pyrite		23.63																
N3	Quartz																		
N4	Ankerite cement				37.87	32.59		10.96		18.58	0.43			47.76	100				
O1	Orthoclase	14.58	24.11	0.1			13.01												
O2	Quartz																		
O3	Alumino-silicate	31.88			35	0.65								32.48	6.35				
P1	Alumino-silicate	23.82			46.29	2.18							21.37						
P2	Ankerite cement				39.75	31.72		13.07		15.46									
P3	Ankerite cement				26.58	46.17		7.59		19.66									

Table S10: EDS results of thin section I6S1-2. The points correspond with the letters of the analysed locations given in Fig. S52.

### 3.2.8 M13

M13 is the interpret mud volcano of the lower injectite complex. Siderite, pyrite, carbon and quartz grains have been observed. All grains lay in an ankerite cement, partly overprinted by alumino-silicate clays. The dark grain at spot B turns out the be totally composed of siderite. The ooid grain, observed at spot F, has a composition of quartz. The orange colored grain at spot G is composed of alumino-silicate clays, containing some small pyrite and quartz grains (<0,1 mm). This same type of grain is observed at spot H. Spot J and K show a grain composed of alumino-silicate clay and carbon, surrounded by ankerite cement dots, alumino-silicate clays (causing the orange coloring), quartz and pyrite crystals and carbon flakes. The ankerite cement seems to bind the clay particles. The strange grain observed with the polarized microscope at spot L is composed of quartz only and is surrounded by ankerite cement and some pyrite crystals. Line measurements on well-rounded quartz grains shows a homogeneous composition.

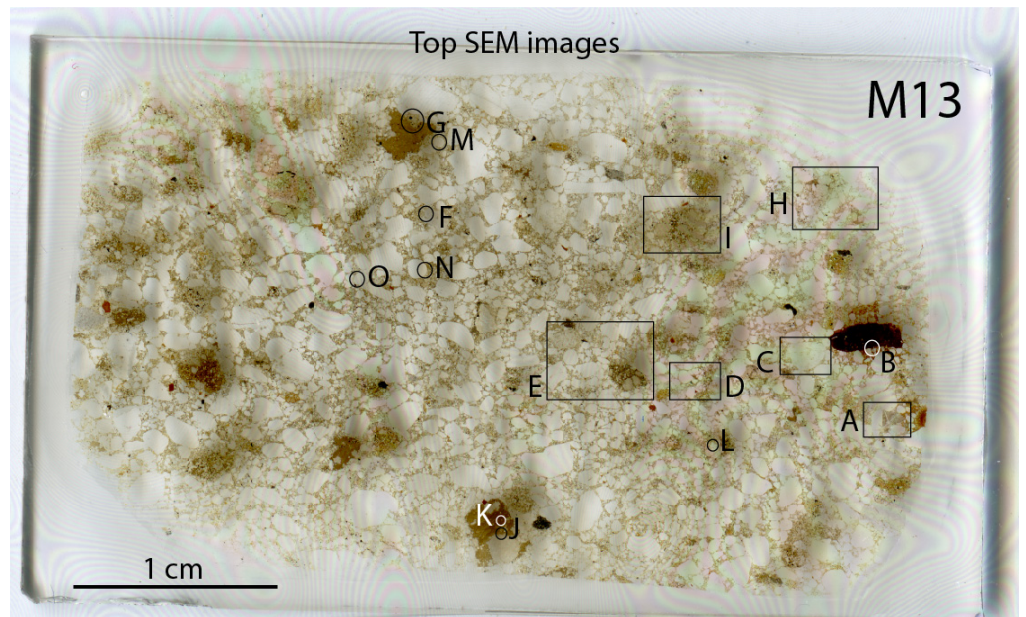


Figure S54: Scan of thin section M13, showing the locations analysed with SEM-EDS.



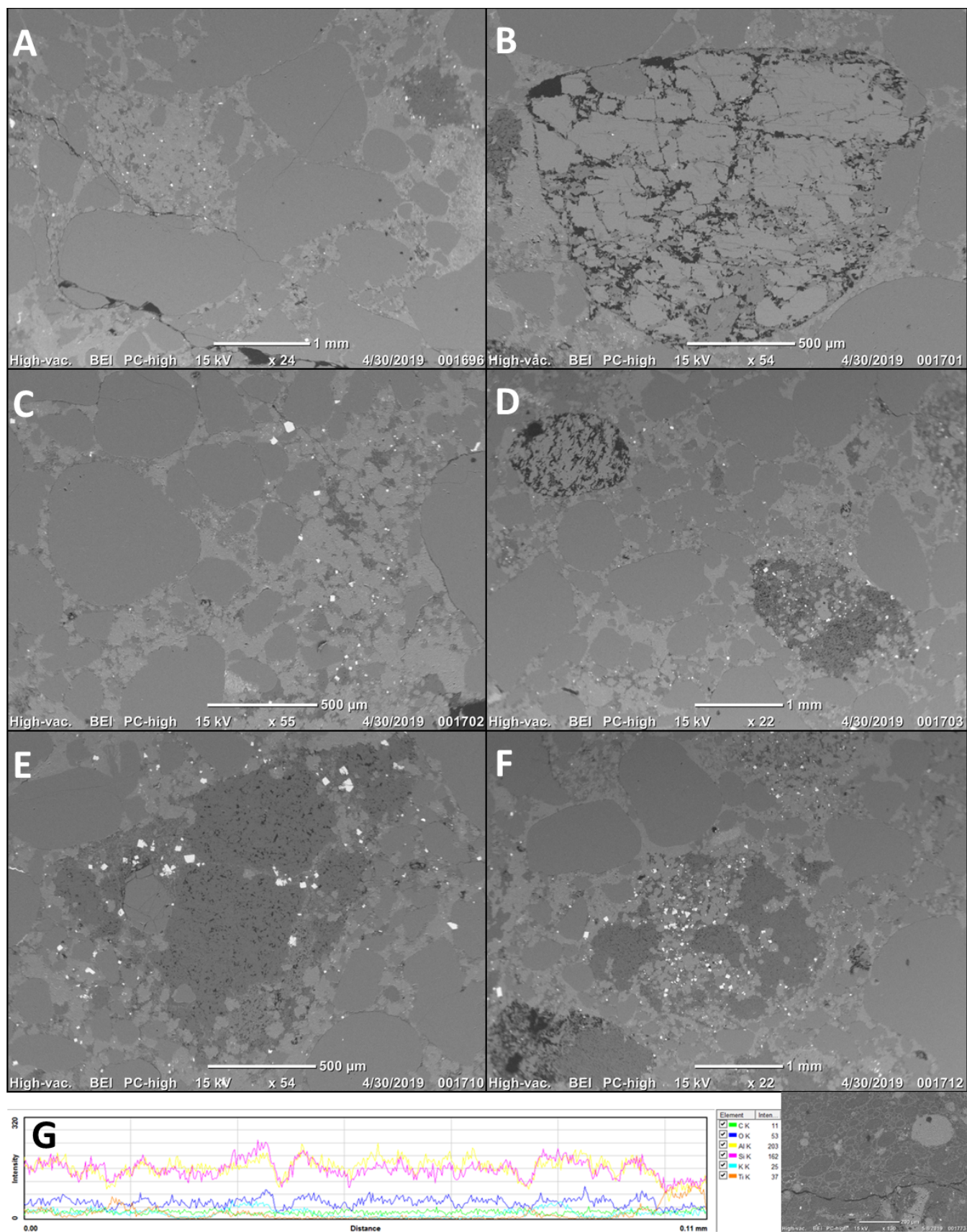


Figure S55: (A): Location A, showing quartz, pyrite, cement and aluminosilicate clays. (B): Location C, showing a reworked grain, composed of quartz, feldspar and carbon. (C): Location D, showing quartz, pyrite, cement and aluminosilicate clays. (D): Location E, showing quartz grains, a reworked grain (upper left) and a clay cluster (lower right). (E): Location H, showing a cluster of clay and pyrite crystals. (F): Location I, showing a cluster of aluminosilicate clays. (G): Line measurement through spot K (Fig. S54).



M13		mass%													
Point	Comments	Al2O3	C	CaO	Cl	CuO	FeO	K2O	La2O3	MgO	N	P2O5	SO3	SiO2	TiO2
B1	Siderite	1.34	38.36	7.49			40.27			7.17				5.37	
B2	Siderite	0.47	36.49	1.52			52.84			3.16				5.53	
B3	Alumino-silicate	24.39	30.41	0.4			0.77	1.52						35.83	6.67
F1	Quartz		30.91											69.09	
F2	Ankerite cement		38.12	32.1			9.66			20.12					
F3	Alumino-silicate	31.47	33.97											34.57	
F4	Pyrite		24.26				20.79						54.94		
G1	Alumino-silicate	31.08	34.19											34.73	
G2	Pyrite		23.83				21.05						55.13		
G3	Mg-calcite / Ankerite cement?		36.42	33.42			9.8			19.09				1.27	
G4	Alumino-silicate	27.04	41.56											31.4	
H1	Alumino-silicate	31.04	34.66											34.3	
J1	Alumino-silicate	26.47	43.98	0.27	0.27									29.01	
J2	Ankerite cement		34.56	34.51			11.27			19.65					
J3	Alumino-silicate	31.2	34.53											34.26	
J4	Mg-calcite / Ankerite cement?		35.41	35.12			9.1			20.37					
J5	Quartz		30.16											69.84	
J6	Pyrite		25.14				22.97						51.9		
J7	Carbon		99.45		0.55										
K1	Alumino-silicate	28.97	36.61		0.15									34.26	
K2	Rutile?	18.89	33.59				2.08	3.51						25.01	16.91
K3	Alumino-silicate	25.45	33.61	1.76				3.59						35.58	
K4	Ankerite cement		39.81	30.13			13.89			16.17					
K5	Alumino-silicate	22.17	41.67	3.95	0.25			2.3				2.63		27.02	
K6	Alumino-silicate	21.79	42.4		0.2						12.95			22.65	
K7	Alumino-silicate	20.25	45.97					1.6						25.75	6.43
L1	Alumino-silicate	32.02	32.86											35.12	
L2	Ankerite cement		33.45	36.18			13.42			16.96					
L3	Pyrite		24.67				21.37						53.96		
O2	Quartz								100						
O3	Alumino-silicate	31.88	35	0.65					32.48						
P1	Alumino-silicate	23.82	46.29	2.18					21.37	6.35					
P2	Ankerite cement		39.75	31.72	13.07	15.46									
P3	Ankerite cement		26.58	46.17	7.59	19.66									

Table S11: EDS results of thin section M13. The points correspond with the letters of the analysed locations given in Fig. S54.



### 3.3 Formations

#### 3.3.1 F6 - Carolinefjellet Formation

The grains of this sample lay in a microsparite matrix. The visible cement grains are composed of ankerite. Observed feldspar grains are albite and orthoclase.

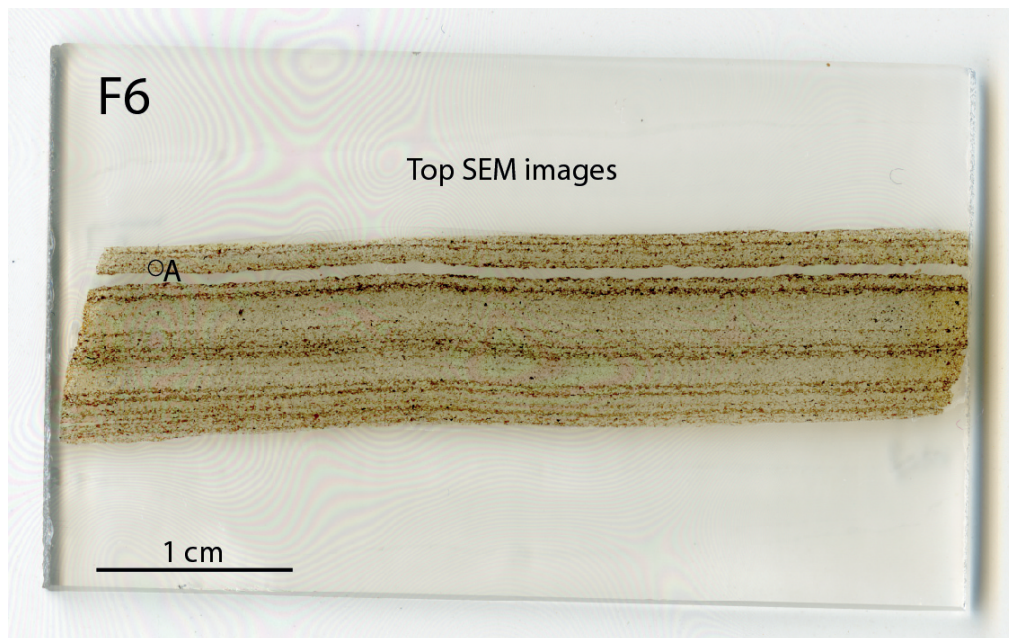


Figure S56: Scan of thin section F6, showing the locations analysed with SEM-EDS.

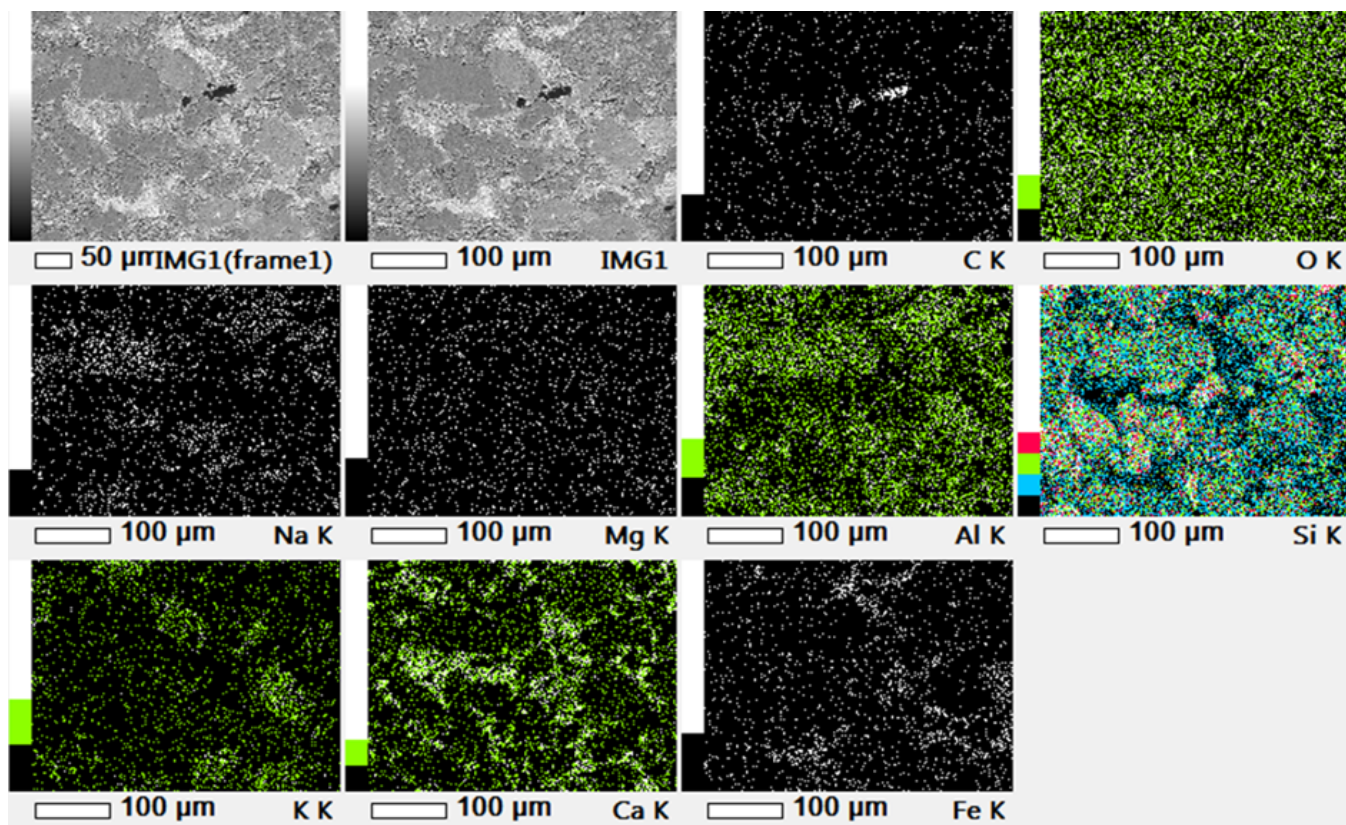


Figure S57: Element map of location A (Fig. S56).



### 3.3.2 F8 - Brentskardhaugen Bed

One of the first observations is the different color of the infilling between the grains. There are two darker spots (measurements A, C, D, E, H, M and N) between the lighter cement (measurements B, F, G, J, K and L). EDS measurements show that the composition between the two cements is different. The light colored cement is composed of ankerite. The magnesium-iron proportion changes slightly throughout the thin section. The darker colored cement spots consist of carbonate-fluorapatite, also known as Francolite. Between the Francolite cement, crystals of ankerite and calcite have been identified, showing that the Francolite has been a later phase of cementation.

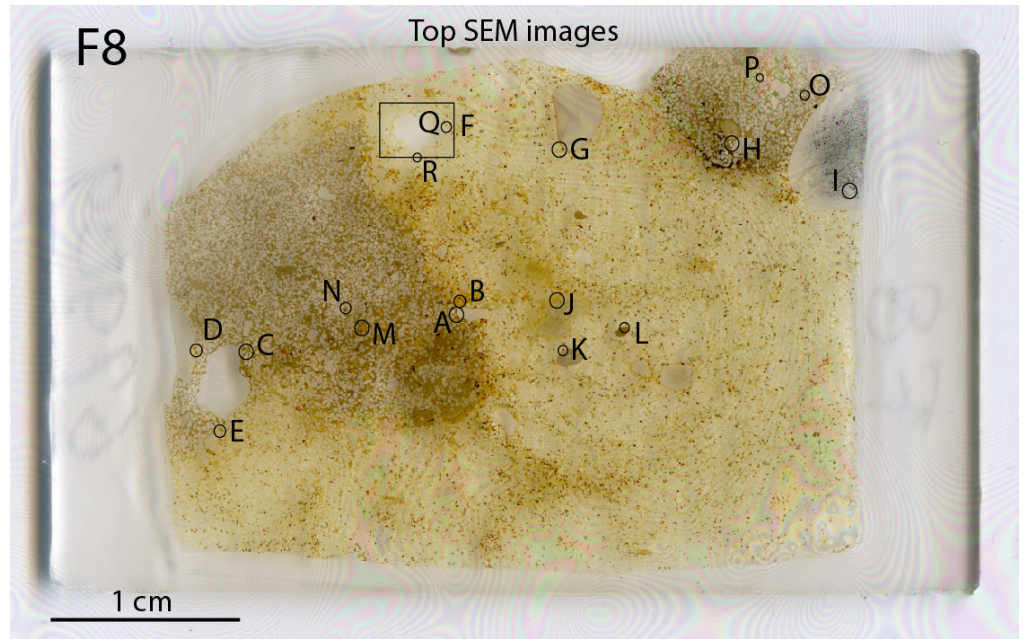


Figure S58: Scan of thin section F8, showing the locations analysed with SEM-EDS.

Except for the recognized grains with the polarized microscope, recognized grains with the SEM-EDS add siderite, pyrite, alumino-silicates, muscovite, orthoclase, albite, apatite and carbon. The foraminifera recognized with the polarized microscope consist of siderite.

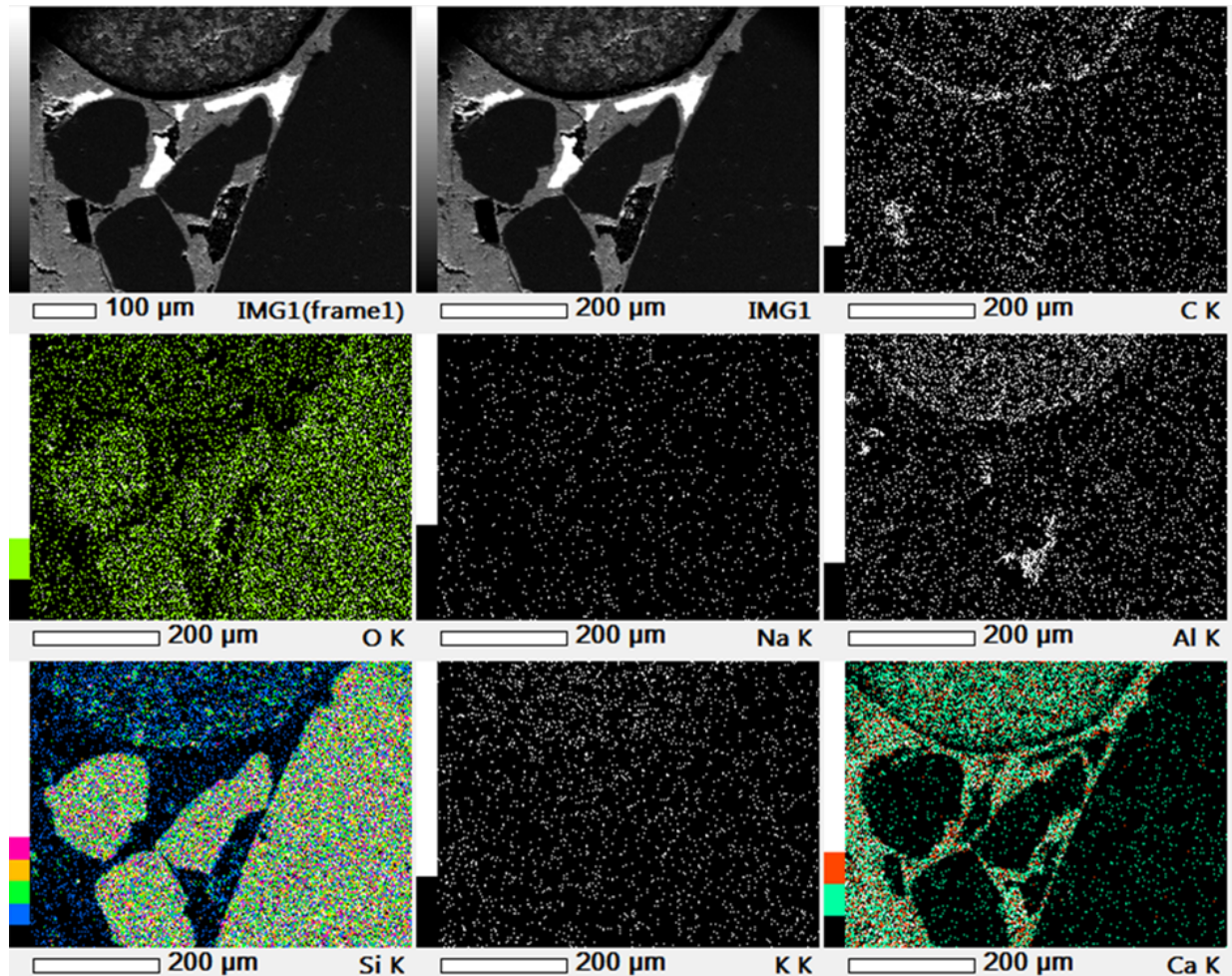


Figure S59: Element map of location H (Fig. S58).



F8		mass%															
Point	Comments	Al2O3	C	CaO	Cl	F	FeO	K2O	MgO	N	Na2O	NiO	P2O5	SO3	SiO2	ZnO	ZrO2
A1	Quartz		33.24												66.76		
A2	Carbonate-fluorapatite cement	1.68	36.73	28.94		5.47							24.11		3.07		
A3	Ankerite cement		30.55	42.26			23.55		2.26						1.38		
A4	Ankerite cement		11.27	59.12			20.7		8.22						0.69		
A5	Alumino-silicate	27.11	42.54												30.35		
B1	Ankerite cement		36.73	37.67			7.16		17.65						0.79		
B2	Siderite		36.87				59.15								3.98		
B3	Quartz		31.5												68.5		
C1	Pyrite		24.2				23.24							52.57			
C2	Quartz		34.13												65.87		
C3	Alumino-silicate	30.37	35.12												34.51		
C4	Carbonate-fluorapatite cement		24.6	39.31		6.46							29.64				
C5	Alumino-silicate	31.35	34.21												34.44		
C6	Pyrite	0.3	26.62	0.44			29.2							42.69	0.74		
C7	White mica	22	33.04				1.88	7.71	2.01						33.36		
C8	K-feldspar	16.38	27.41				12.52	8.03	0.92						34.74		
C9	Calcite		12.47	87.53													
D1	Alumino-silicate	24.55	46.79				0.61	0.21							27.85		
D2		10.17	43.58	23.78			10.61		0.72						11.14		
D3	Quartz		32.49												67.51		
D4	Carbonate-fluorapatite cement	0.36	40.22	20.71						17.94			18.26		2.5		
D5	Carbonate-fluorapatite cement	0.43	17.56	45.77		2.15							31.89		2.2		
E1	Quartz		34.62												65.38		
E2	Ankerite cement		31.74	36.42			13.77		10.51						7.55		
E3	Pyrite		28.19				15.23							37.02	19.56		
E4	Alumino-silicate	22.14	47.12				0.85	1.49							28.41		
E5	Alumino-silicate	3.39	48.37	0.2				0.84			0.47				46.73		
G1	Quartz		30.18												69.82		
G2	Siderite		31.68	0.77			61.01		2.47						4.07		
G3	Ankerite cement		34.07	41.73			8.33		15.15						0.73		
G4	Siderite		32.56	0.7	0.31		61.5		1.15						3.78		
G5	Albite	14.32	32.76	0.28				0.57			7.05				45.01		
H1	Carbonate-fluorapatite cement	4.69	26.43	33.36			0.77	1.43					25.16		8.18		
H2	Quartz		32.48	0.05				0.02							67.45		
H3	Carbonate-fluorapatite cement	7.19	38.43	18.19				1.53					14.05		20.61		
H4	Carbon	5.73	68.81	6.25	1.12			1.29					4.33		12.47		
H5	Carbon	0.4	95.17	0.45	2.81			0.01					0.4		0.76		
H6	Carbonate-fluorapatite cement	5.64	25.47	26.12	0.08			2.15					17.59		22.95		
H7			58.37	0.57	0.18					39.82					1.06		
H8	Pyrite		23.48				23.86							52.65			
H9	Alumino-silicate	21.78	53.73		0.27			0.46			0.28				23.49		
H10	Alumino-silicate	29.82	36.78		0.27			0.33			0.28				32.51		
I1	?		46.41	0.29	0.46				0.19	33.34	0.54			0.62	18.16		
I2	Carbonate-fluorapatite cement	9.46	25.94	29.81									24.39		10.39		
I3	Pyrite?	0.37	26.02				18.97							41.84	12.81		
I4	Quartz		31.41				0.05								68.54		
J1	Quartz		31.8												68.2		
J2	Orthoclase	18.98	41.45				2.97	5.04							31.56		
J3	Carbonate-fluorapatite cement		27.66	23.27			8.33				1.01		17.22	19.26			3.25
J4	Ankerite cement		33.19	40.09			12.78		13.94								
J5		4.88	45.99	1.66						34.46			1.07		11.94		
J6	Carbonate-fluorapatite cement		21.5	38.38						7.96			32.09		0.07		
K1	Quartz		30.86												69.14		
K2	Quartz		30.86												69.14		
K3	Ankerite cement		32.97	38.86			8.43		18.72						1.02		
K4	Siderite		31.92	0.81			61.71		1.98						3.59		
K5	?		26.15											19.69	31.21	22.95	
K6	Siderite		32.98	0.94			60.41		2.03						3.64		
L1	Apatite group mineral?		23.29	42.8									33.91				
L2	Alumino-silicate	18.06	56.94	1.72			1.56								21.72		
L3	Ankerite cement		35.32	40.25			8.77		15.67								
L4	Apatite group mineral?		23.88	35.14		6.69							32.57		1.72		
M1	Alumino-silicate	23	52.71												24.29		
M2	Carbonate-fluorapatite cement		23.23	41.33									33.51		1.93		
M3	Calcite		24.54	73.12					2.34								
M4	Ankerite cement		34.68	40.3			13.84		11.18								
M5	Quartz		31.92												68.08		
M6	Carbonate-fluorapatite cement		25.94	39.83		3.57							29.74		0.91		
M7	Carbonate-fluorapatite cement		23.18	39.78		4.37							32.67				
M8	Mica?	11.89	34.36				25.64	3.22	1.45						23.44		
N1	Siderite/pyrite		25.86				24.49							49.01	0.64		
N2	Cement with siderite?	15.32	33.35	10.51			4.34	3.79	1.06				5.64		26		
N3	Siderite	6.08	29.63	0.72			50.06	1.1	0.92				0.97	1.21	9.31		
N4	Carbonate-fluorapatite cement		23.55	40.23		3.88							32.33				

Table S12: EDS results of thin section M13. The points correspond with the letters of the analysed locations given in Fig. S58.



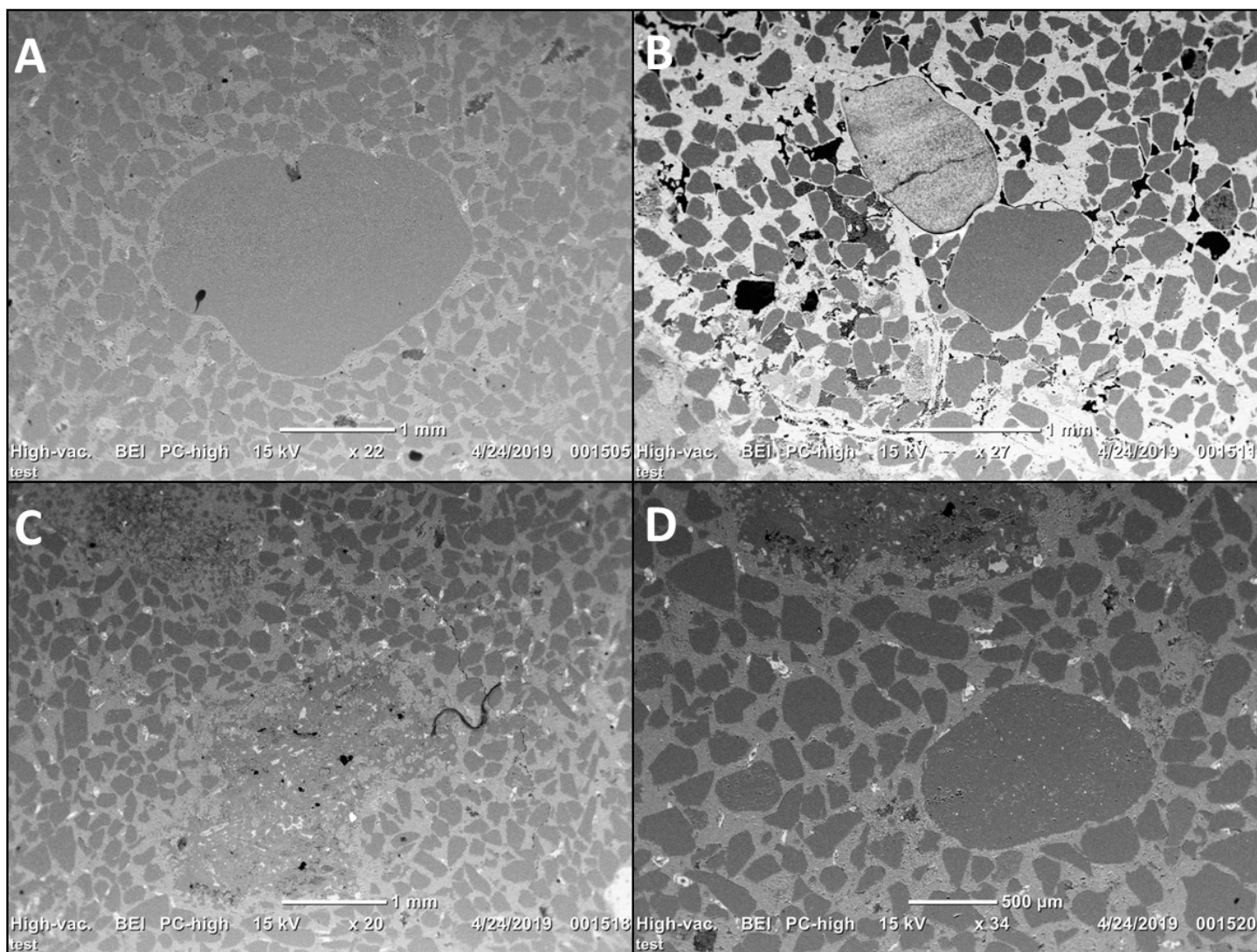


Figure S60: (A): Location F, with a big quartz grain in the middle of the picture. (B): Location H, the white material between the grains is carbonate-fluorapatite. (C): Location J. (D): Location K, the white dots are foraminifera comprising siderite.



### 3.4 Mounds

#### 3.4.1 M3-1

The big grain on the upper right side of M3-1 has been analysed with SEM-EDS. It turns out the ooid grains are all composed of  $\text{SiO}_2$  and the oxide grains on the sides, observed at spot A, are pyrite crystals. Spot B still contains an carbon grain, probably some sort of biologically remnant. Around this carbonate grain, a rim of aluminosilicate clays enriched in carbon and pyrite crystals can be observed.

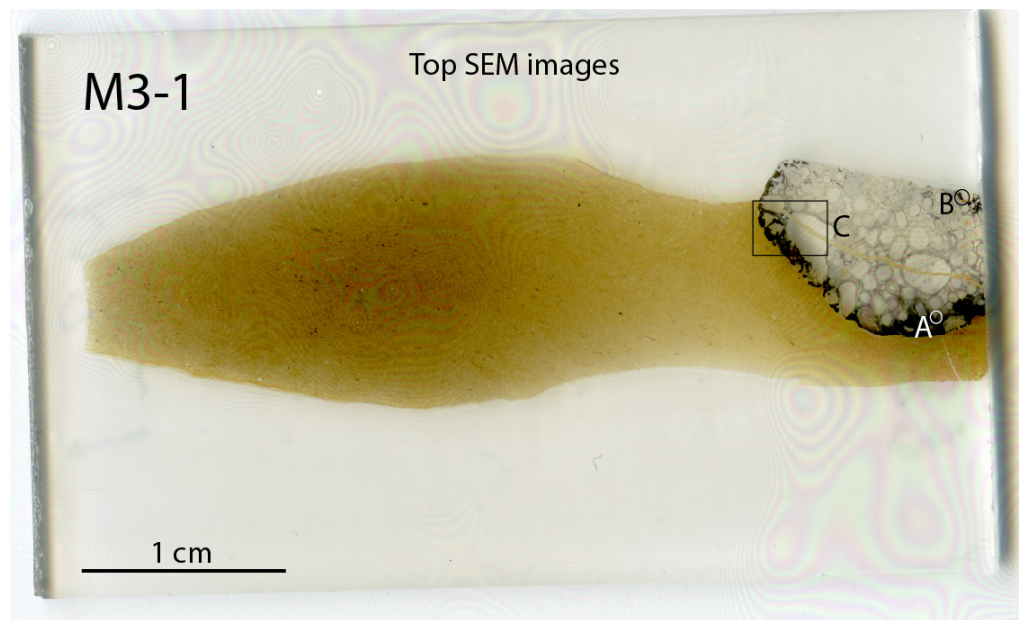


Figure S61: Scan of thin section M3-1, showing the locations analysed with SEM-EDS.

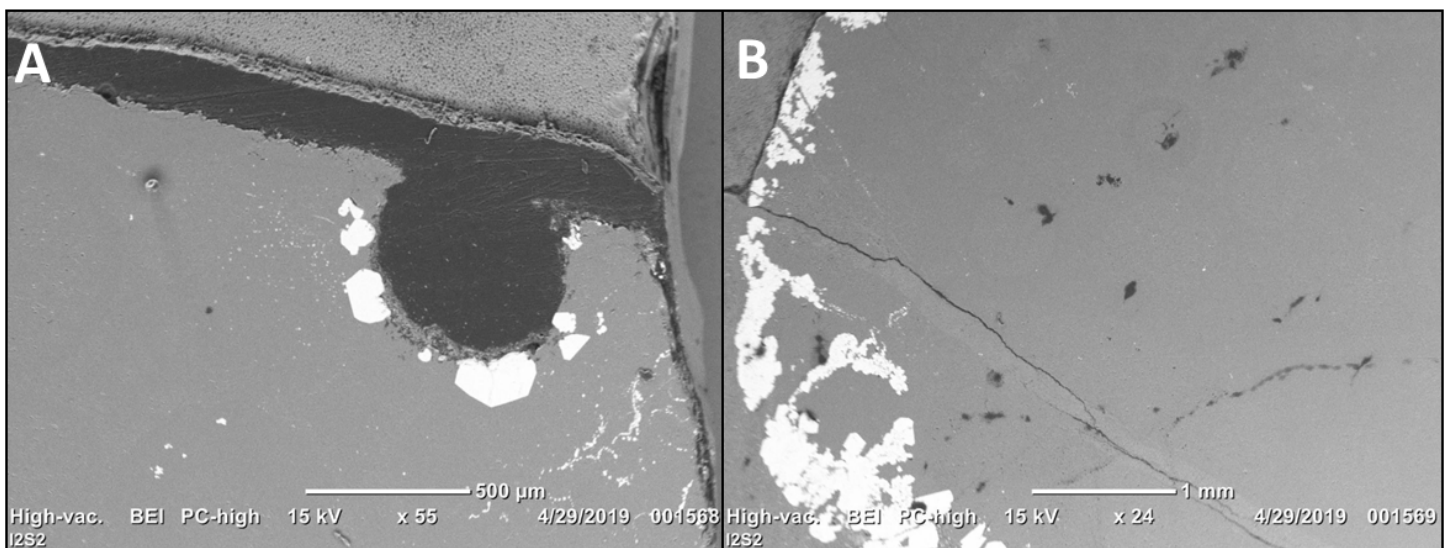


Figure S62: (A): Location B, showing the observed carbon grain, surrounded by pyrite crystals (white). (B): Location C, showing that the ooid structures all are composed of  $\text{SiO}_2$ . The white flakes are pyrite crystals.



### 3.4.2 M4

The measured big quartz grain at spot A contains an ankerite cement rim. The fractures crossing the grain are filled with ankerite as well. The observed cement of the rest of the sample also contains ankerite.

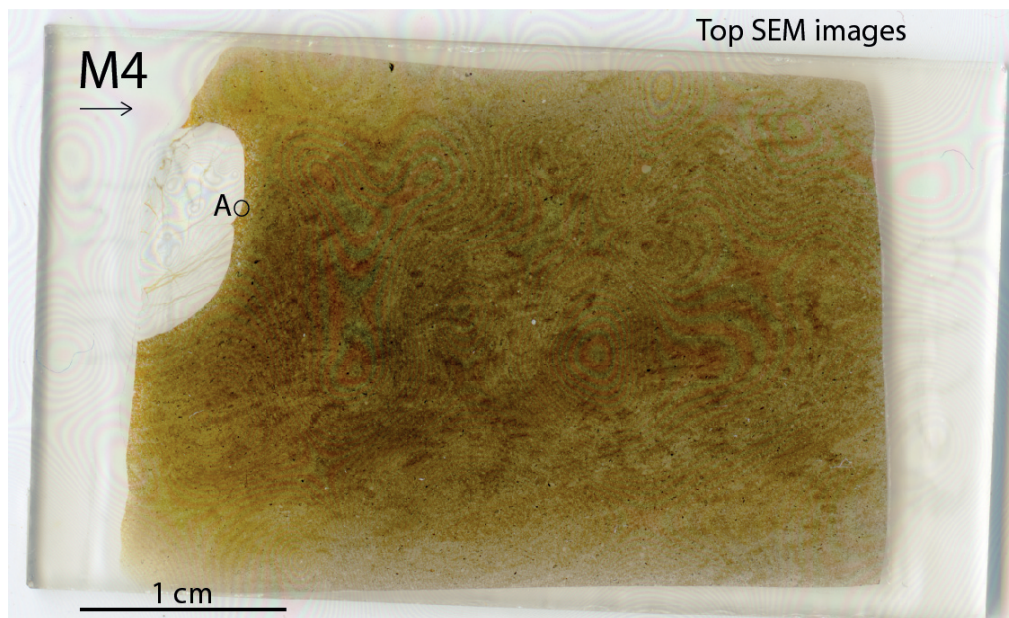


Figure S63: Scan of thin section M4, showing the locations analysed with SEM-EDS.

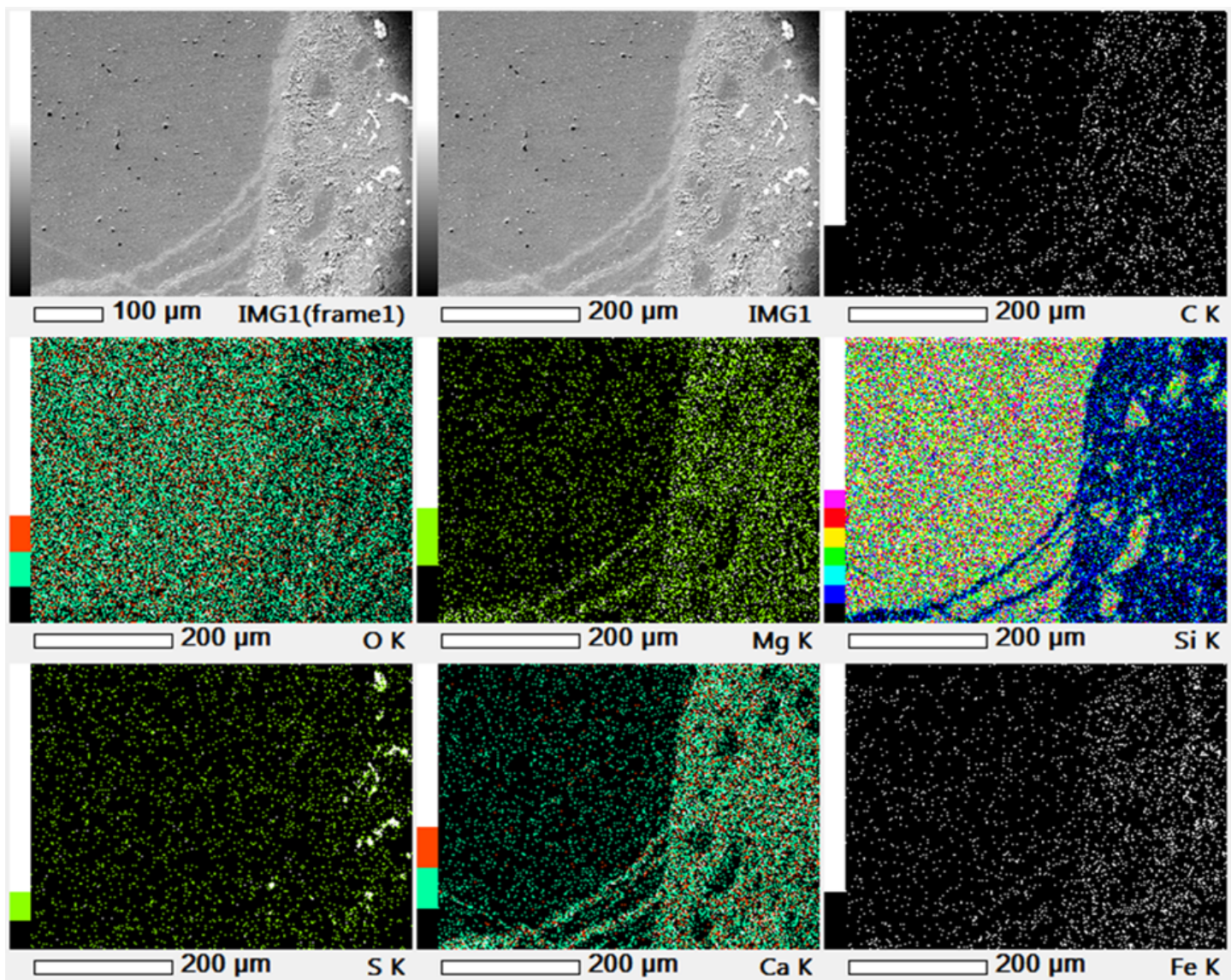


Figure S64: Element map of location A (Fig. S63).



### 3.4.3 M8-2

M8-2 shows a sample of the fossilised wood found on top of some mud mounds. It turns out that between the carbon wood structures, ankerite cement, pyrite and alumino-silicate clays are present (spot B), but also a carbonate-fluorapatite crystal has been measured. The orange colored material contains siderite and pyrite grains in an ankerite cement.

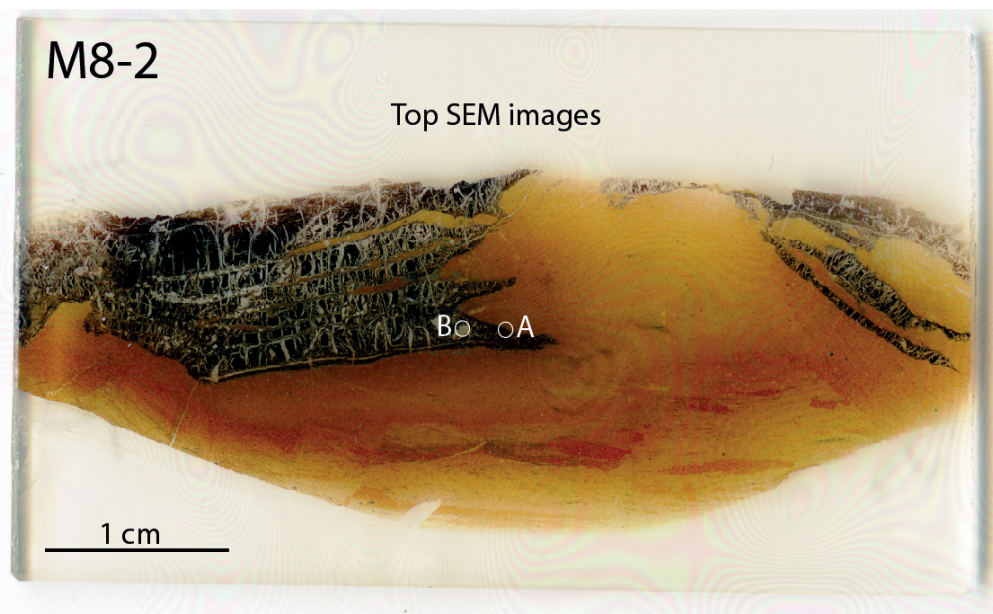


Figure S65: Scan of thin section M8-2, showing the locations analysed with SEM-EDS.

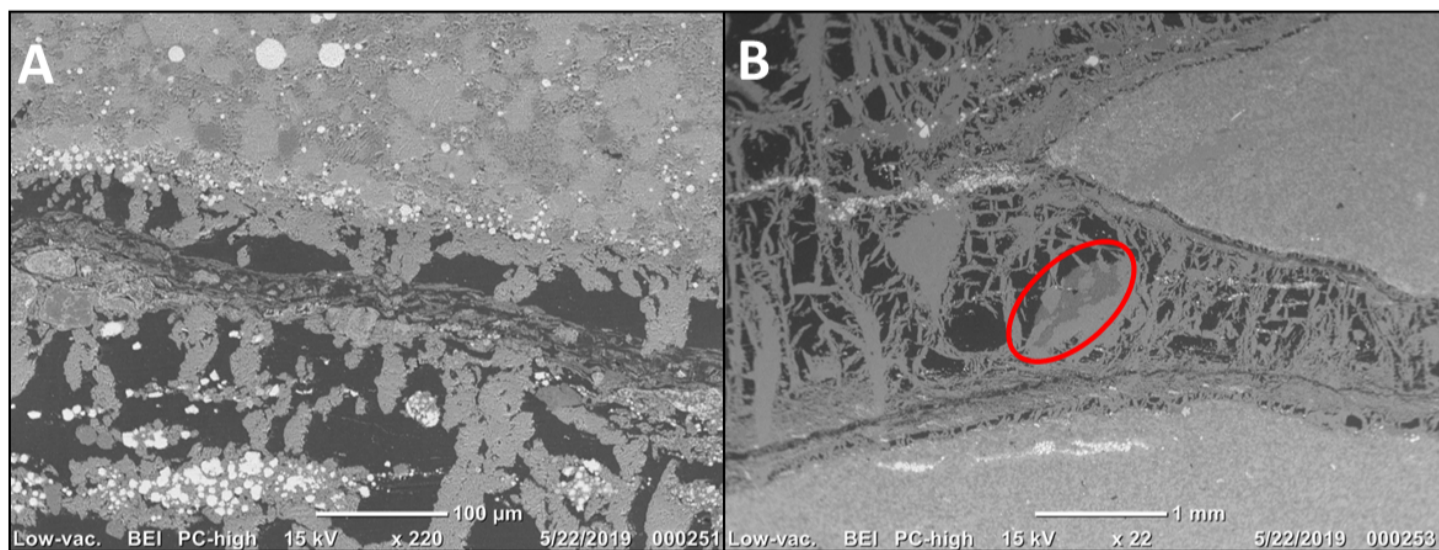


Figure S66: (A): Location A, showing carbon (black), framboidal pyrite (white) and cement. (B): Location B, showing the spot with ankerite cement (darker grey material in the red circle).



### 3.4.4 M12-1

From this sample only ankerite cement crystals have been measured, as well as one pyrite crystal (present at spot B). It turns out that at the darker spots, more carbon is present in the cement.

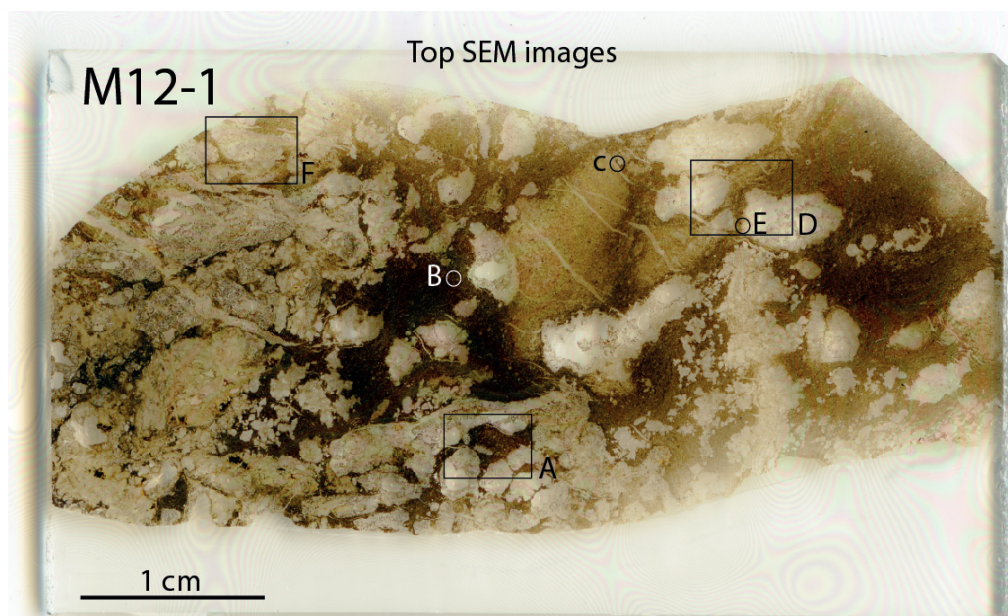


Figure S67: Scan of thin section M12-1, showing the locations analysed with SEM-EDS.

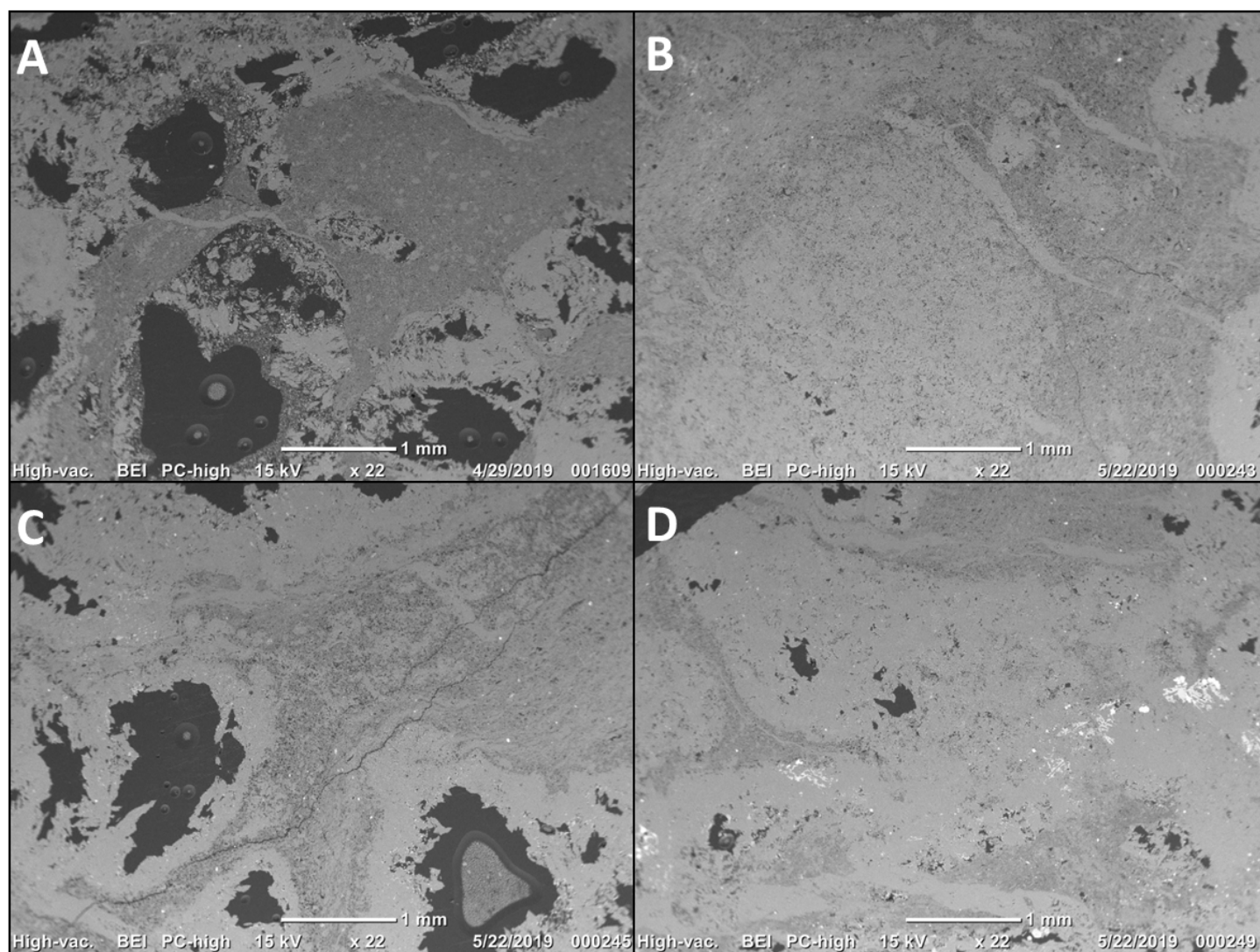


Figure S68: (A): Location A, showing the texture of sample M12-1. The black spots are pores. (B): Location C. (C): Location D, the black spots are pores. (D): Location F, the white material comprises pyrite.



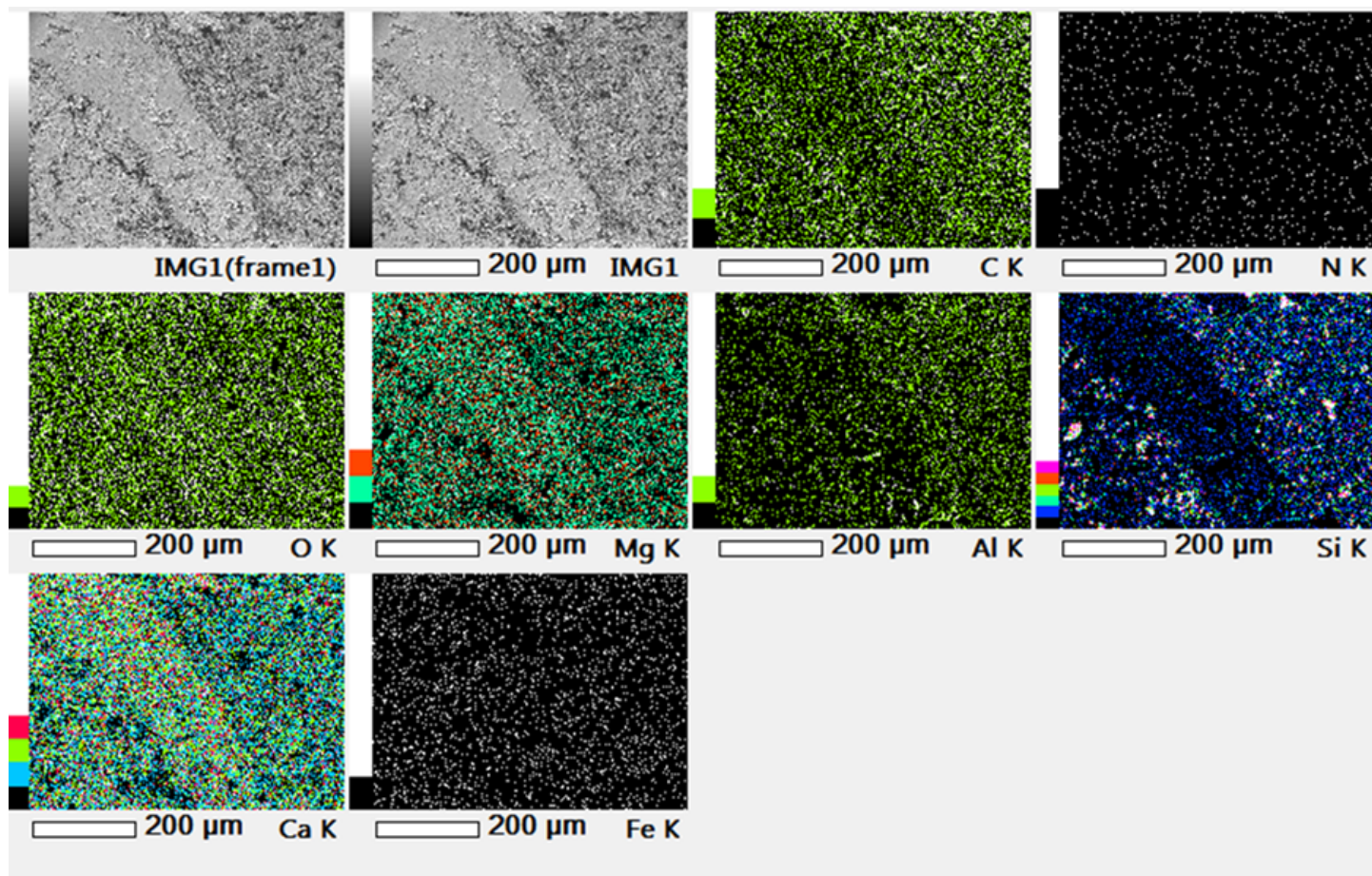


Figure S69: *Element map of location C (Fig. S67).*



### 3.4.5 K1

The organic remnant observed at spot A is composed of carbonate-fluorapatite and the pores of the fossil are filled with ankerite cement and siderite crystals. Also an gastropod fossil was analysed at spot B. The shell is composed of quartz and the pores filled with pyrite. The grains lay in an ankerite cement, partly overprinted with aluminosilicate clays.

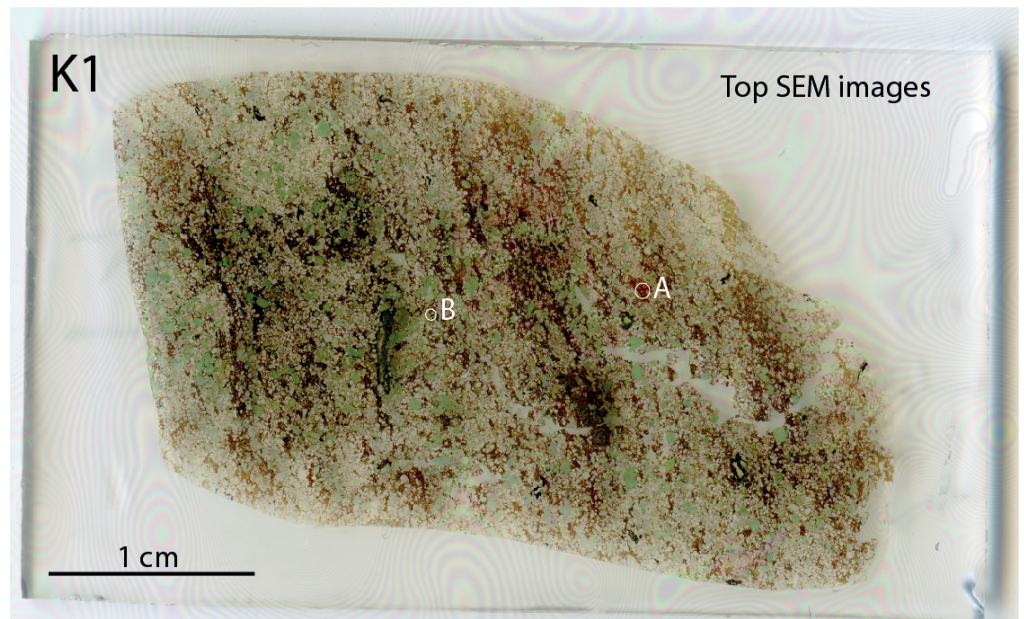


Figure S70: Scan of thin section K1, showing the locations analysed with SEM-EDS.

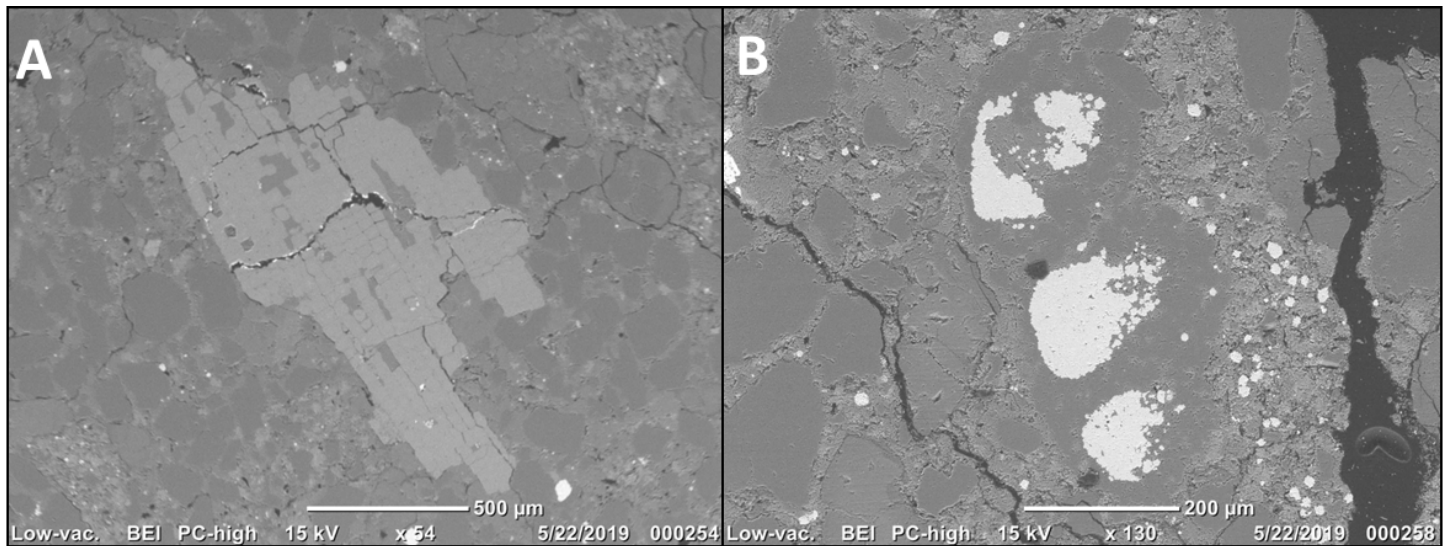


Figure S71: (A): Location A, showing a organic remnant will cell-structures, composed of carbonate fluorapatite (light grey material). (B): Location B, showing a gastropod fossil, filled with pyrite (white material).



3.5 Lenses

3.5.1 L2-2

The shells of the observed shell fossils are composed of the same type of ankerite cement as observed in the host strata.

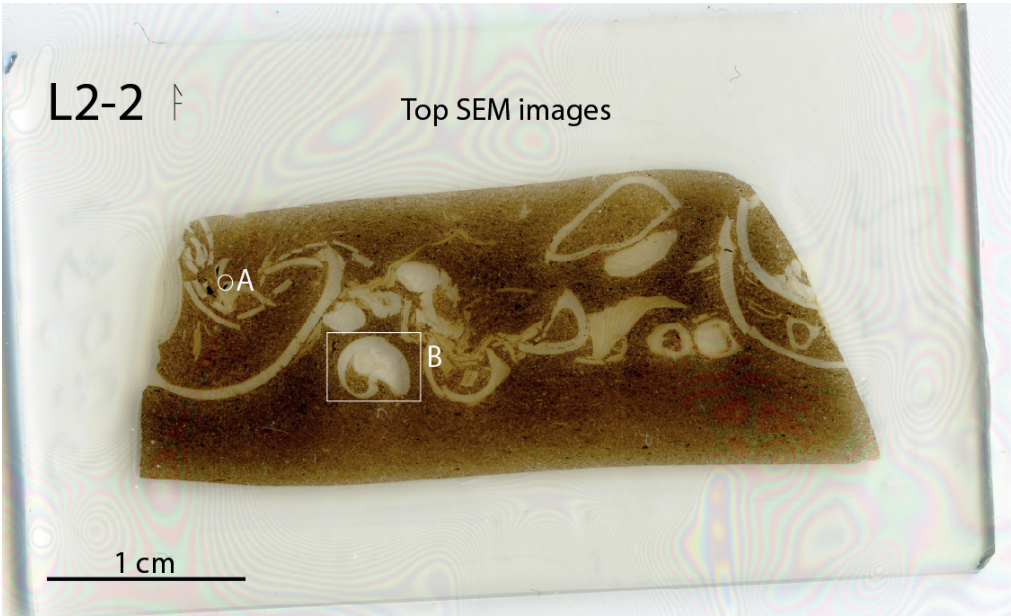


Figure S72: Scan of thin section L2-2, showing the locations analysed with SEM-EDS.

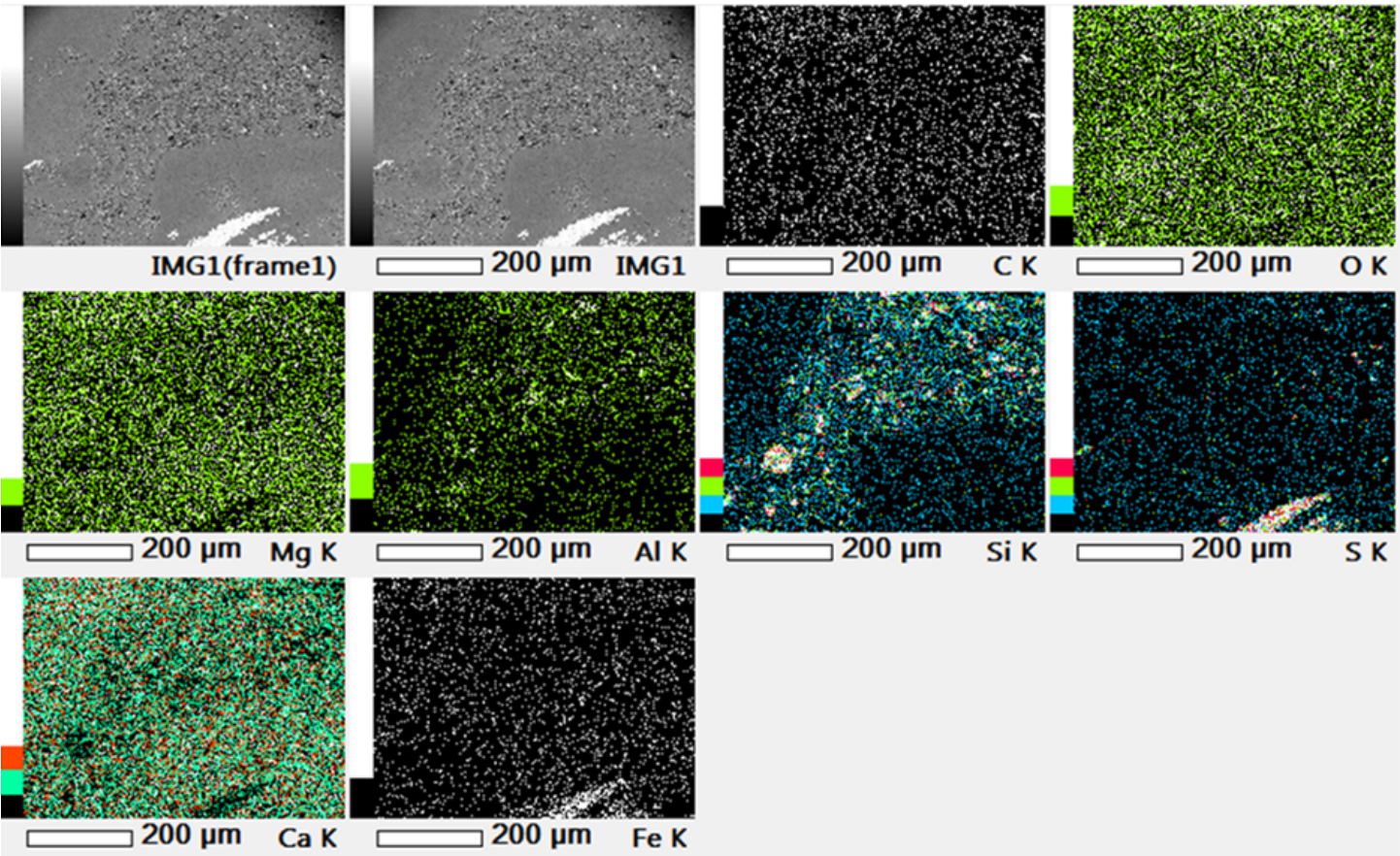


Figure S73: Element map of location A (Fig. S72).



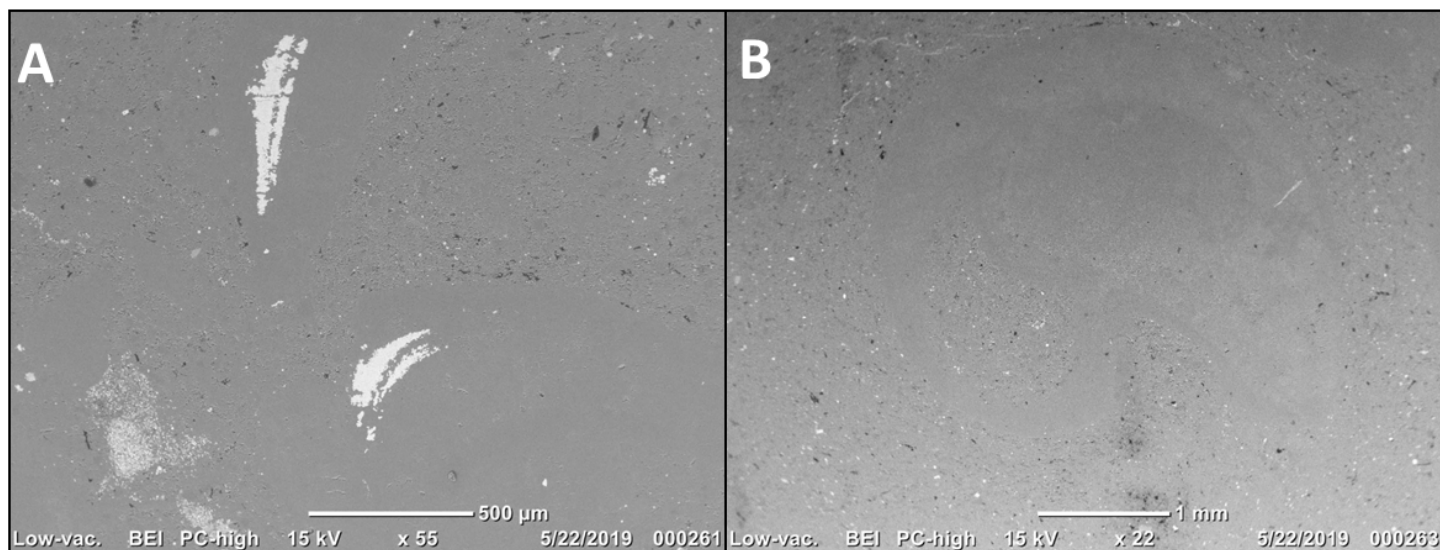


Figure S74: (A): Location A, showing pyrite (white material). (B): Location B.

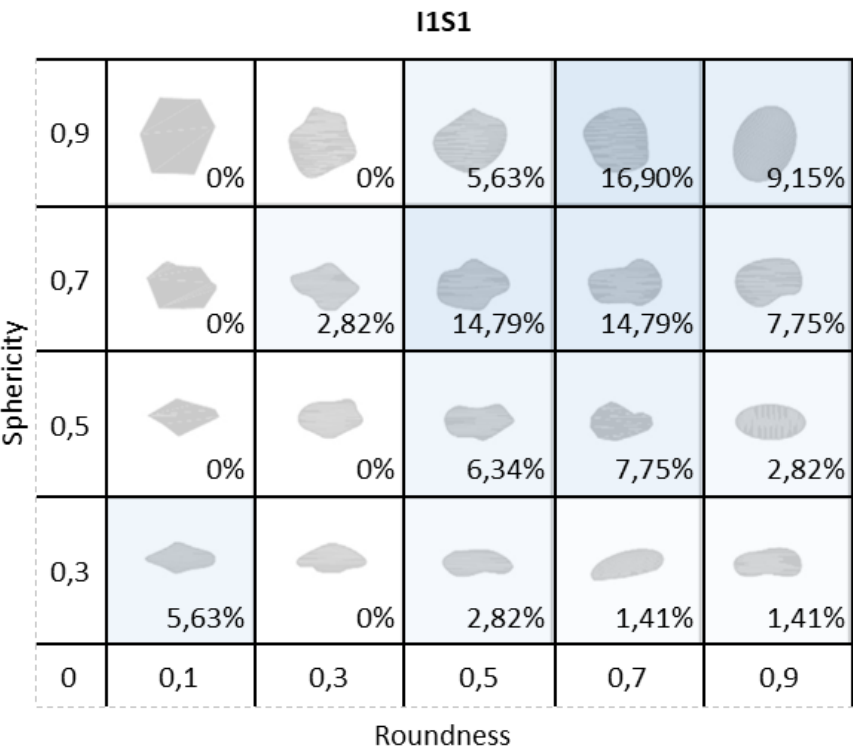


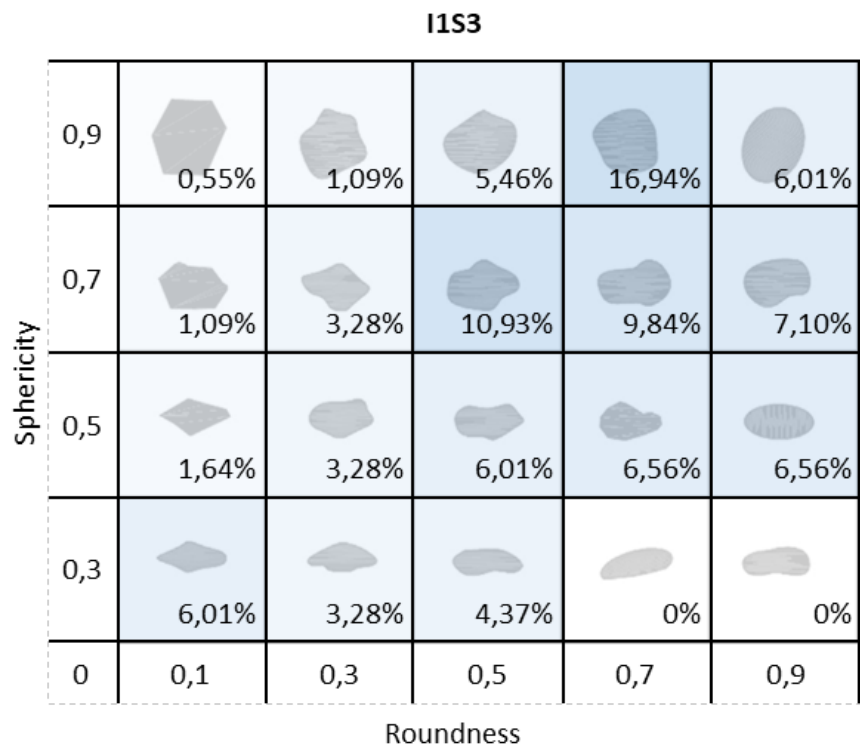
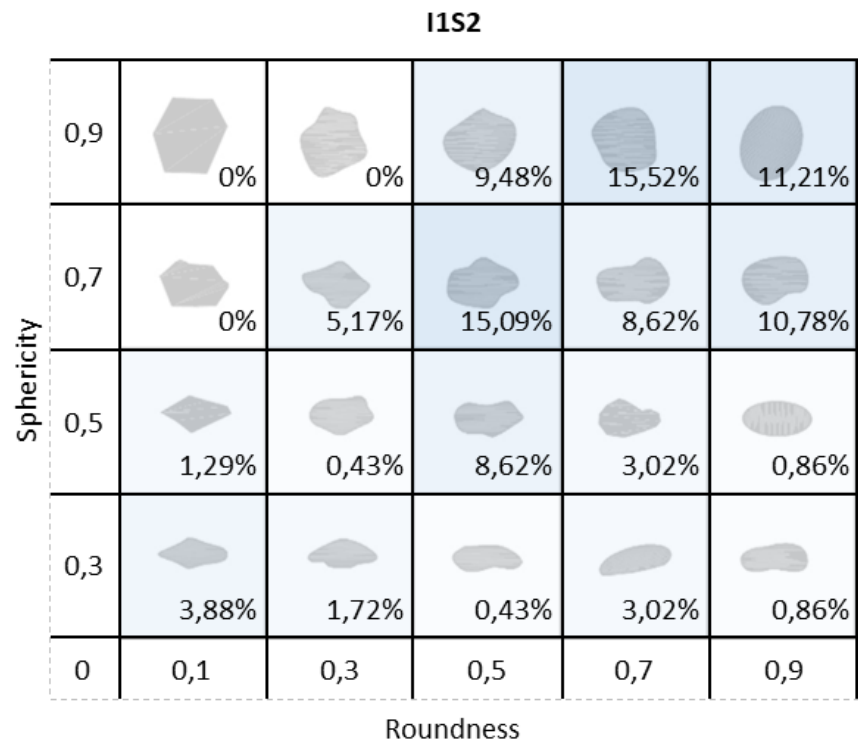
# 4 Micromorphology

To obtain the bulk sample composition, mineralogy, size, sphericity and roundness of over 100 random grains were studied. The results regarding the bulk sample composition, mineralogy and size are given in section 2: Optical Microscopy. Here, the tables regarding the roundness and sphericity study are given. To increase the readability of the tables, a blue color was added. The blue color becomes brighter with increasing percentages. This study was done only the thin sections coming from the injectites, M6, M13 and the samples from the Brentskardhaugen Bed and Carolinefjellet Formation.

## 4.1 Upper Complex

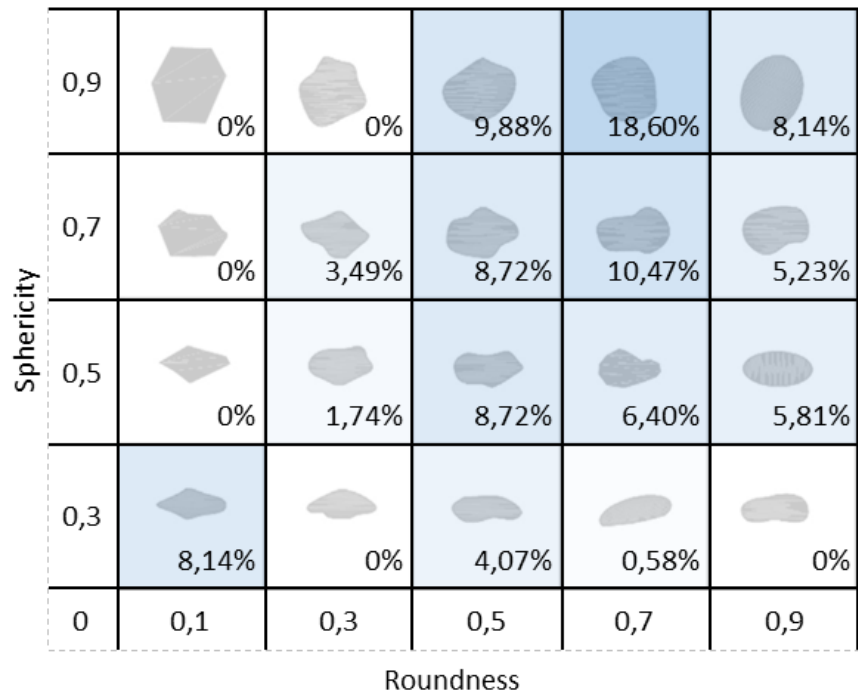
### 4.1.1 Injectite 1



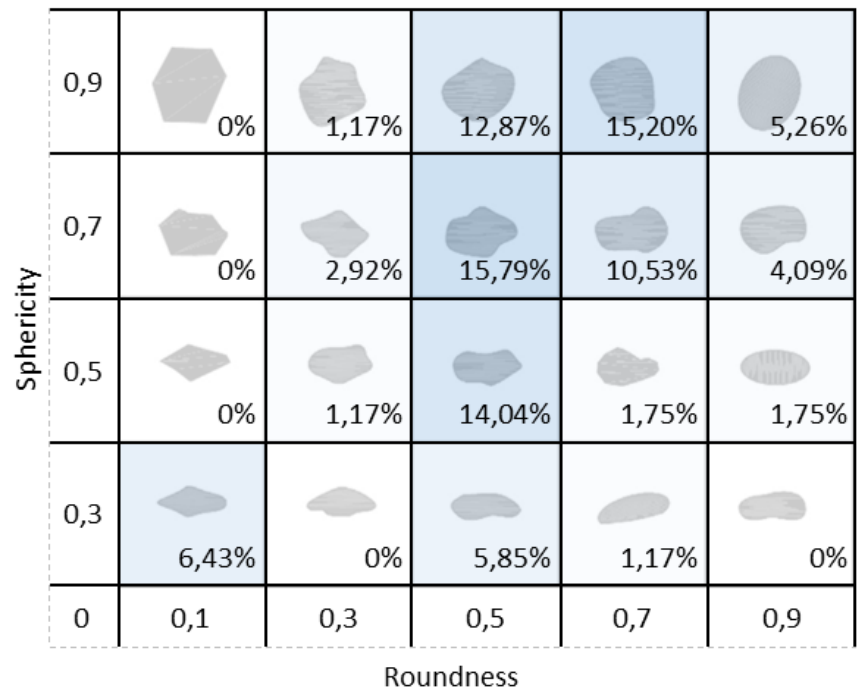




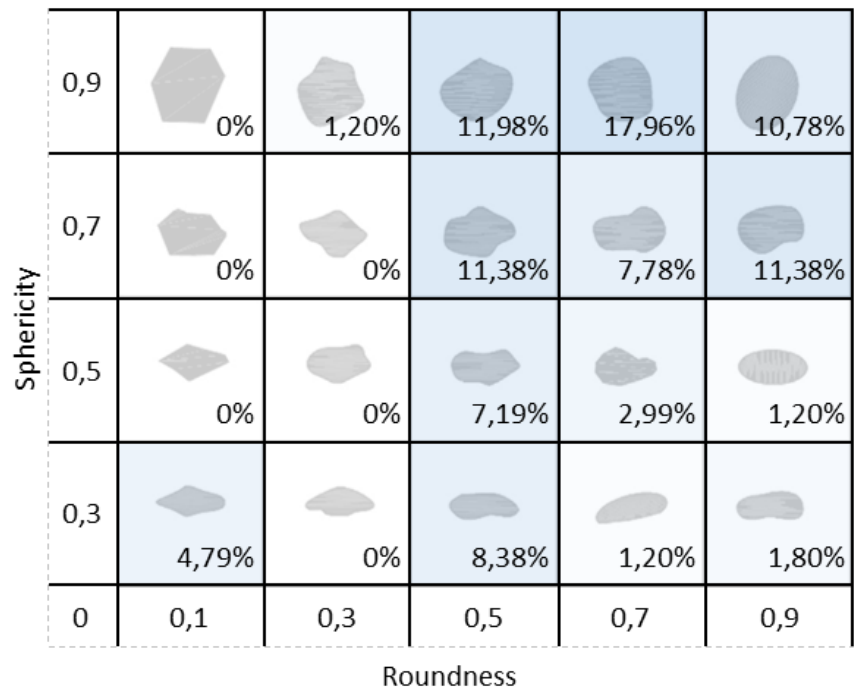
IIS4



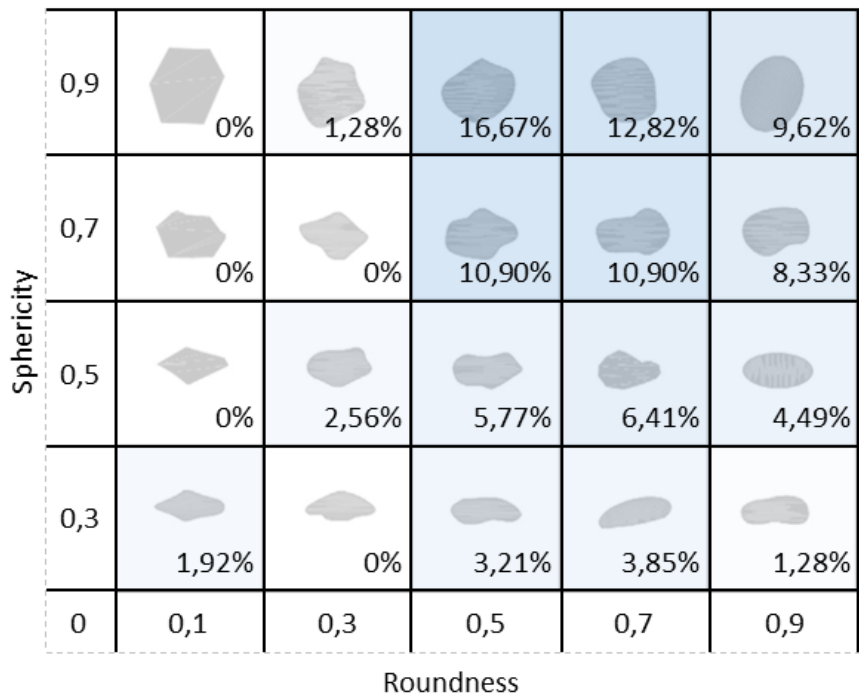
IIS5



### IIS6

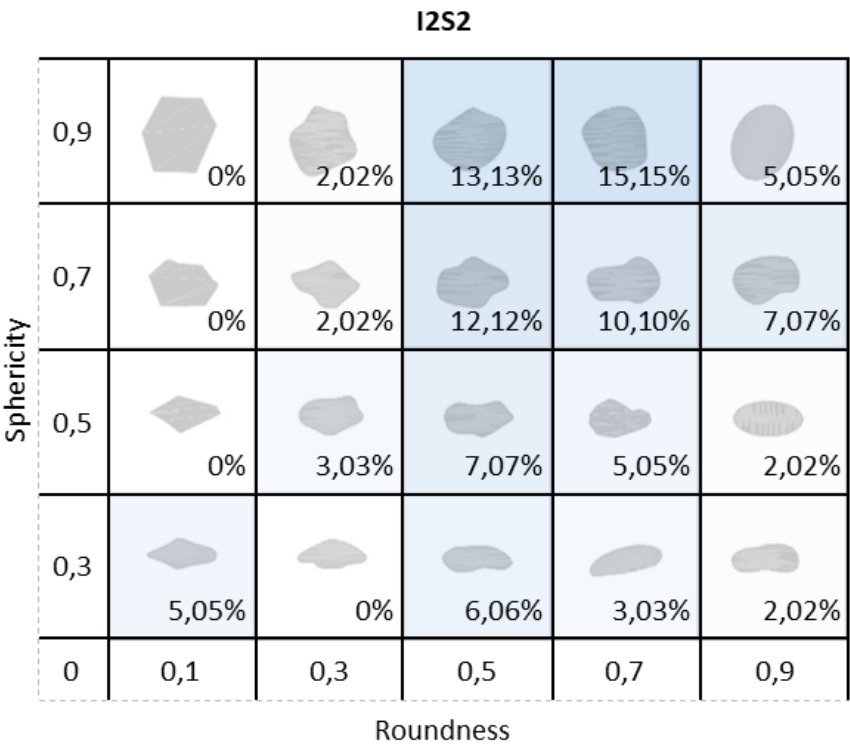
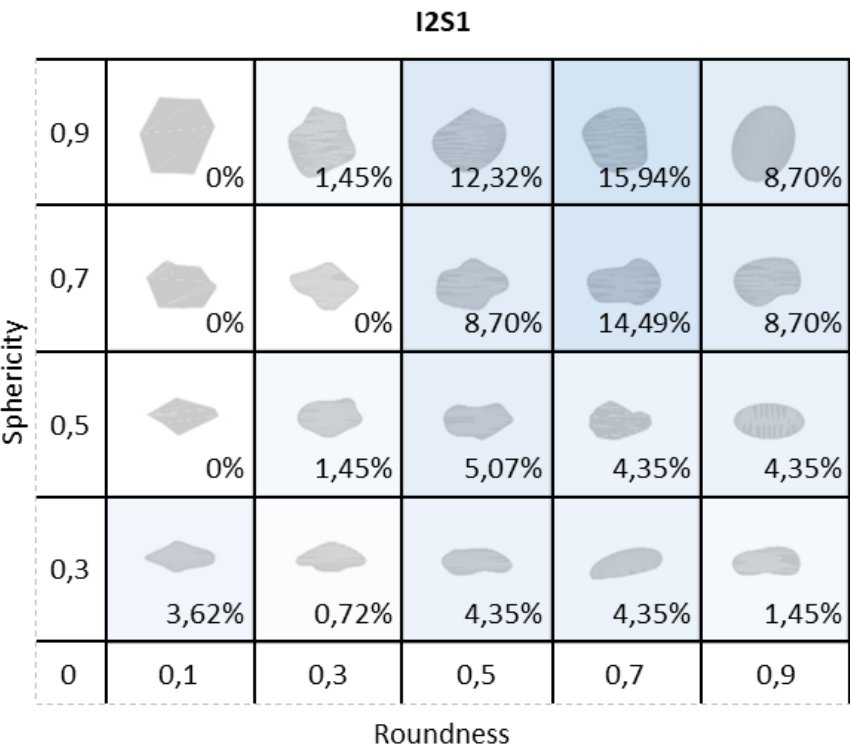


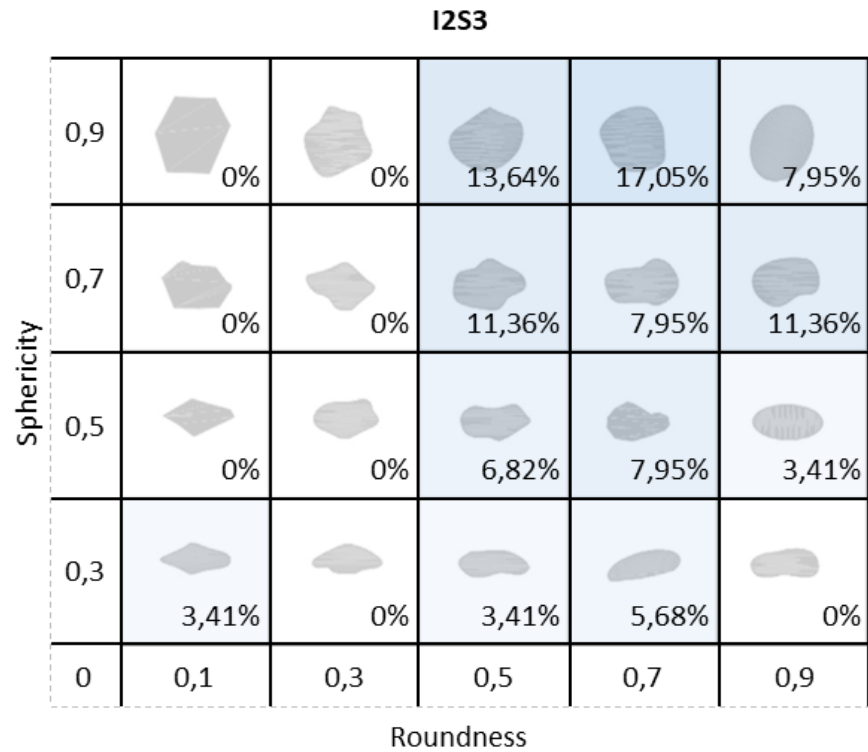
### IIS8





4.1.2 Injectite 2

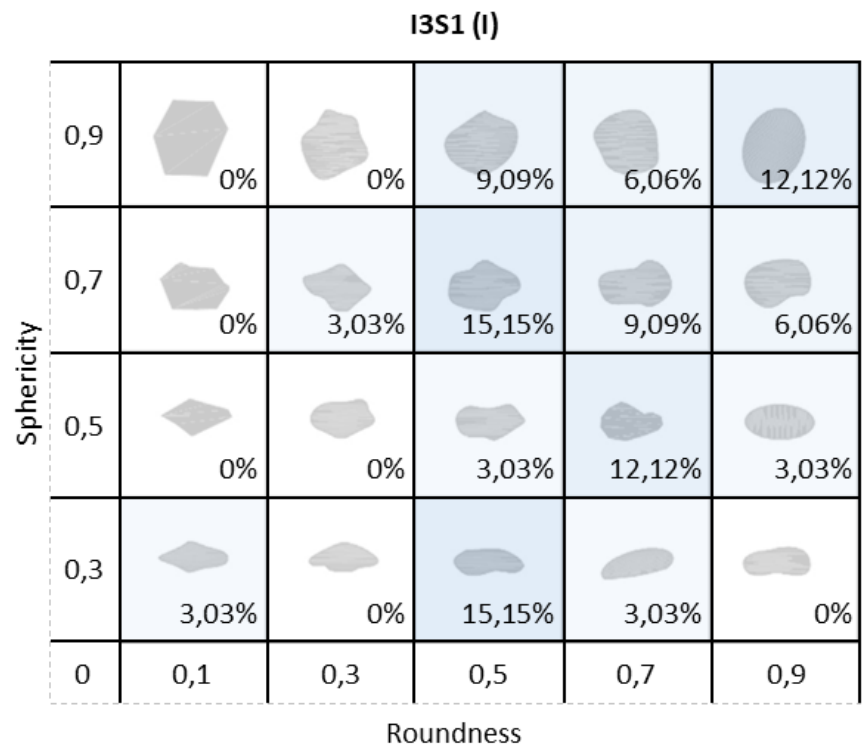




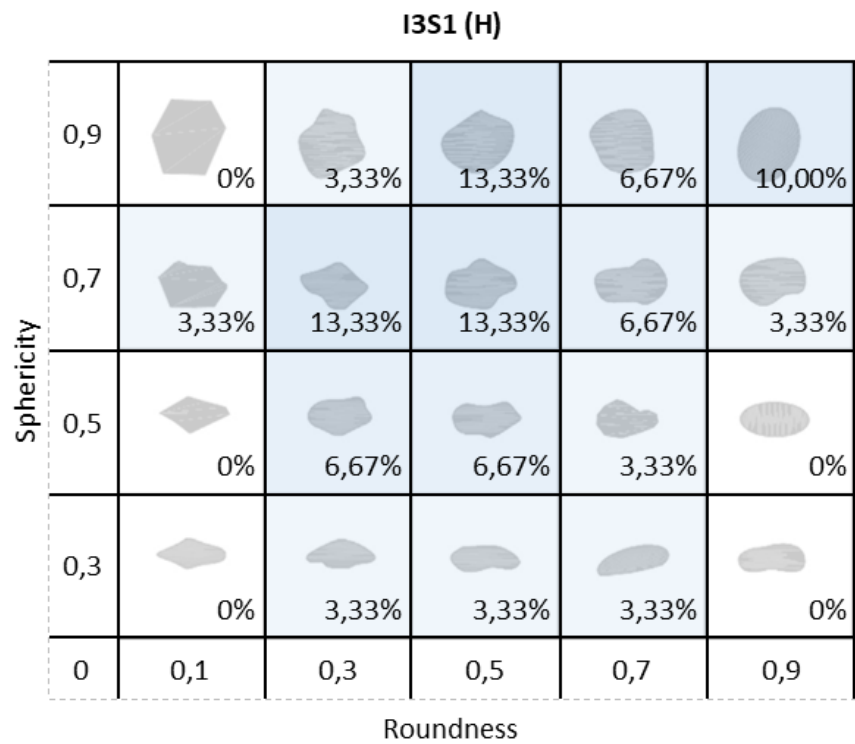
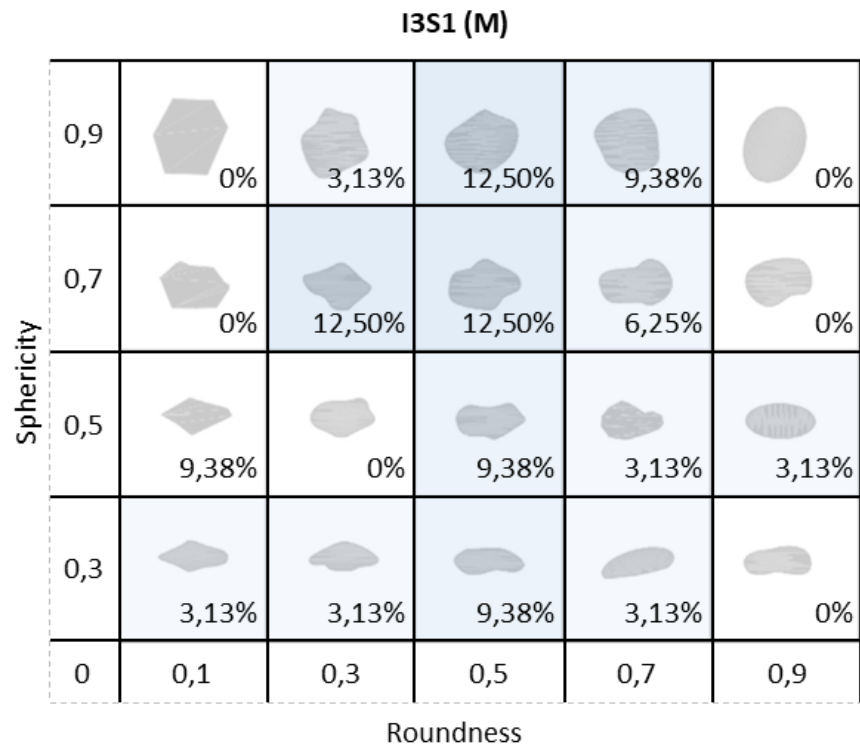
## 4.2 Lower Complex

### 4.2.1 Injectite 3

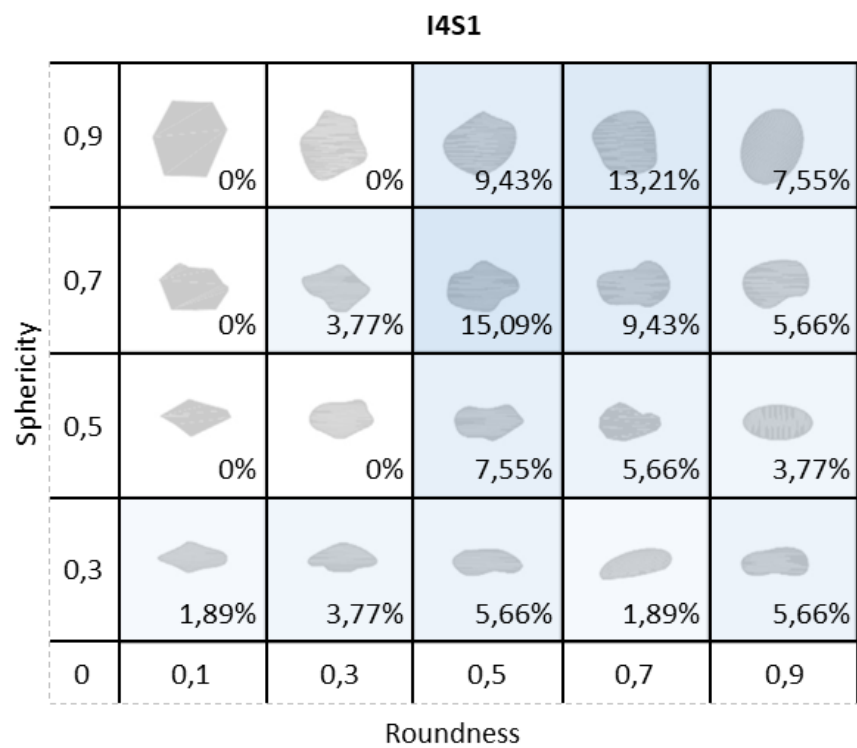
Here, the injectites interior (I), injectite margin (M) and host rock (H) were studied.



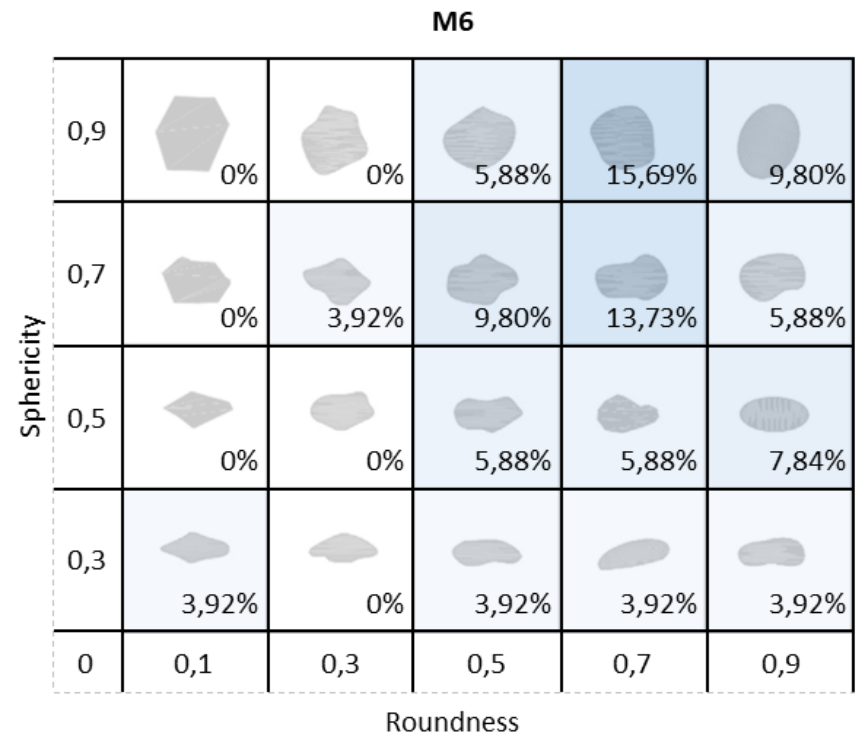




4.2.2 Injectite 4



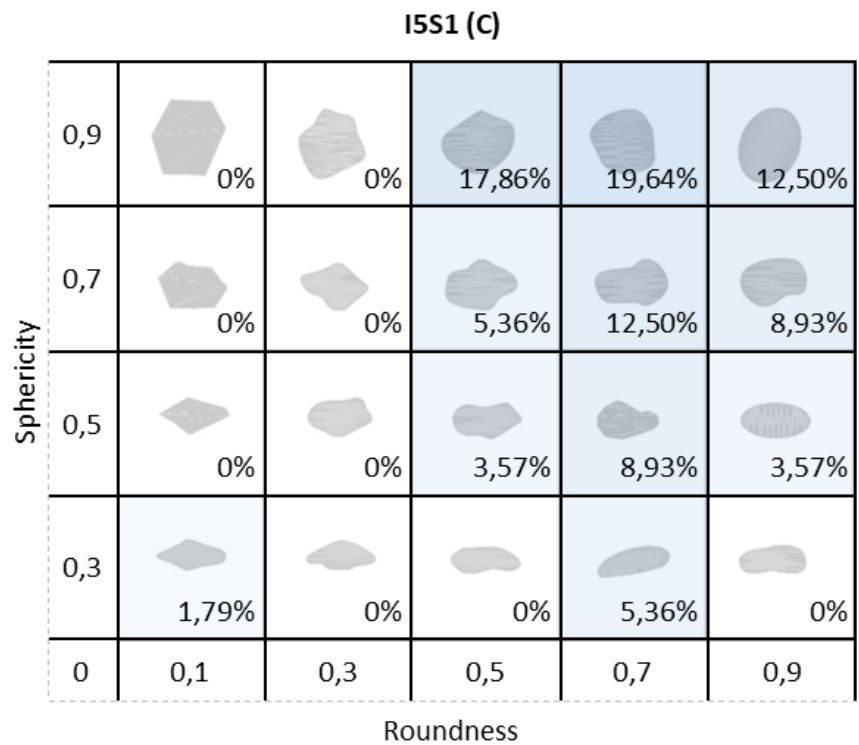
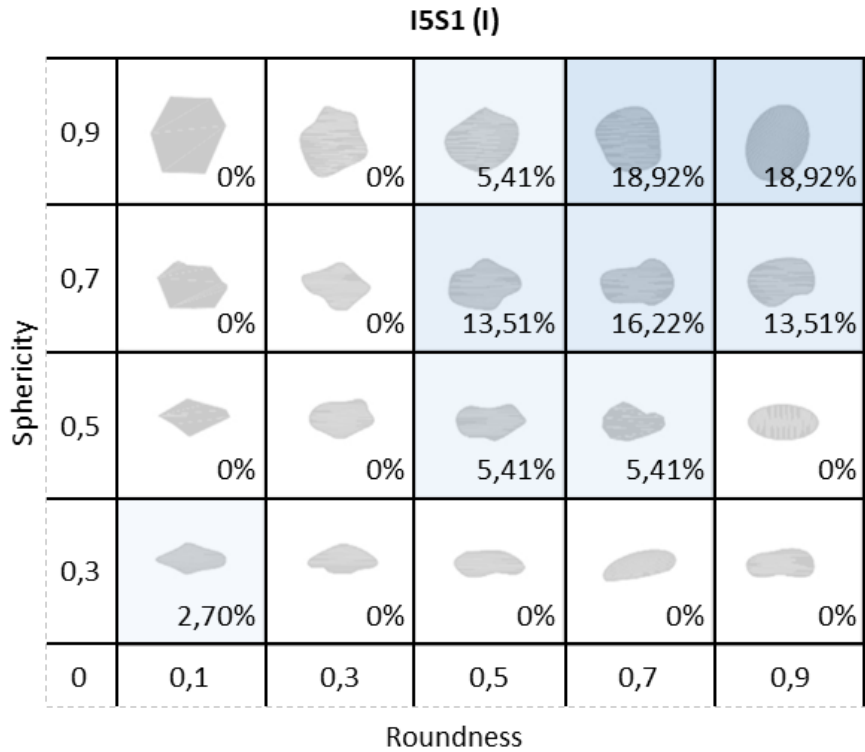
4.2.3 M6

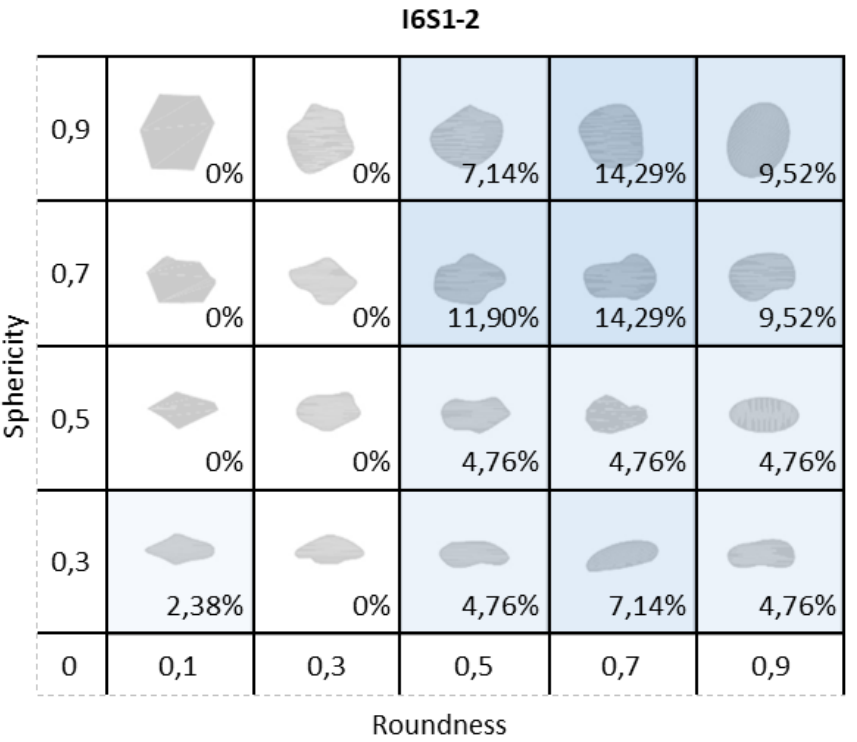
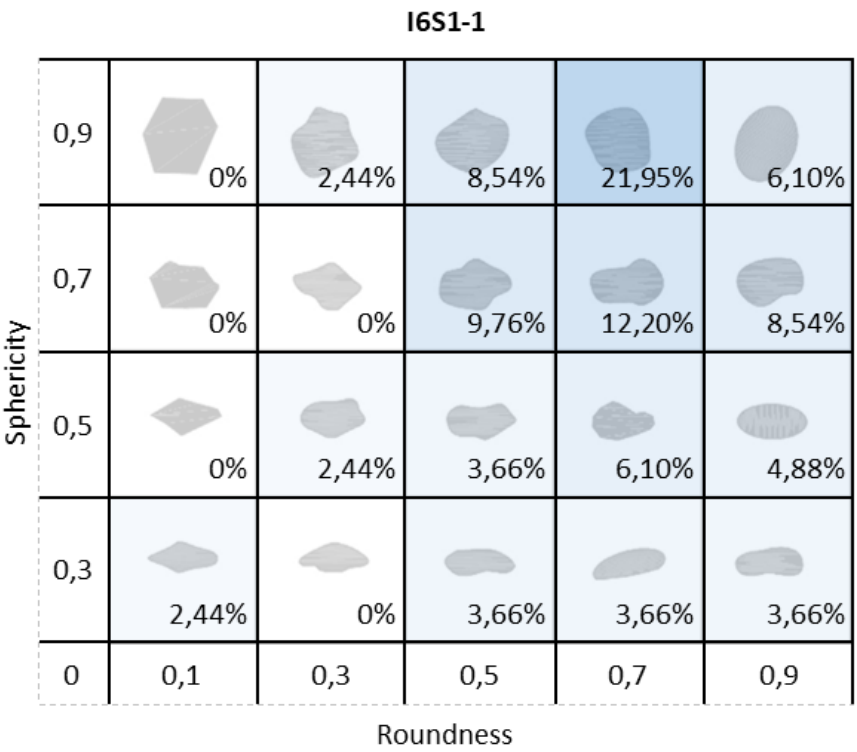




4.2.4 Injectite 5

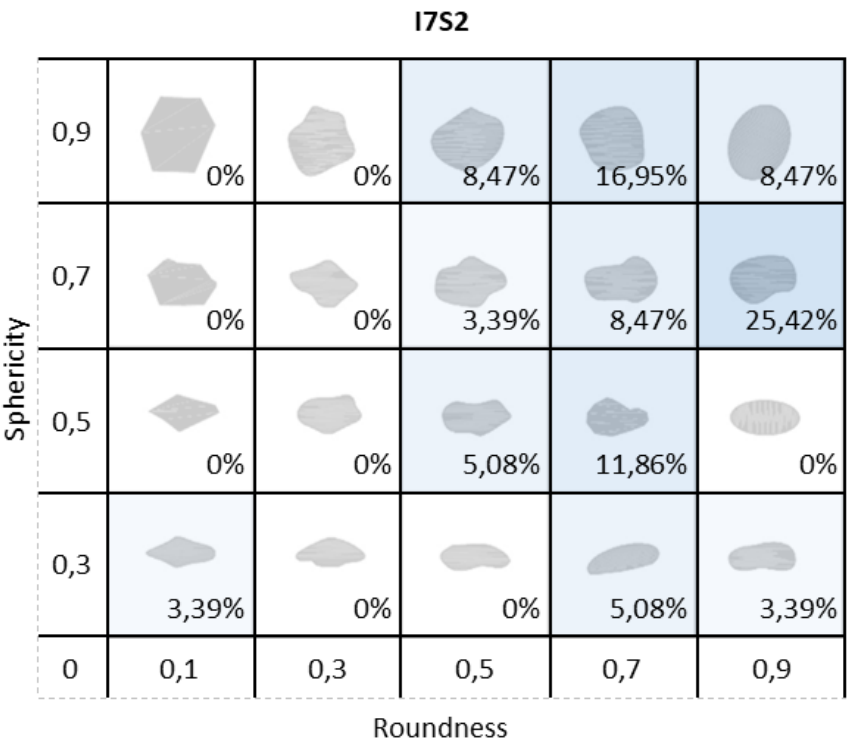
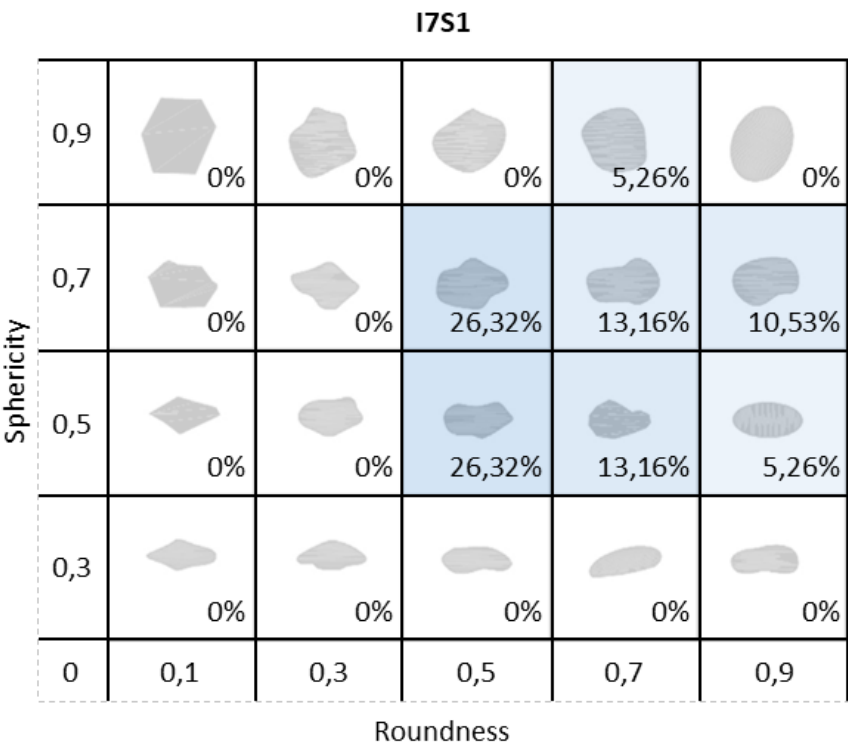
Here, the injectites interior (I) and mudclast (C) were studied.

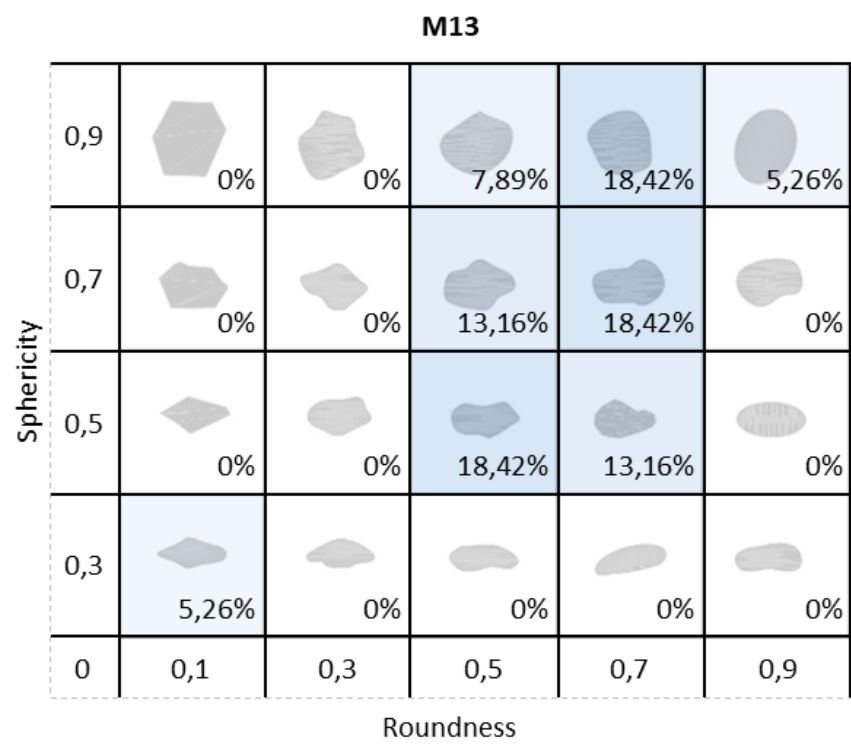






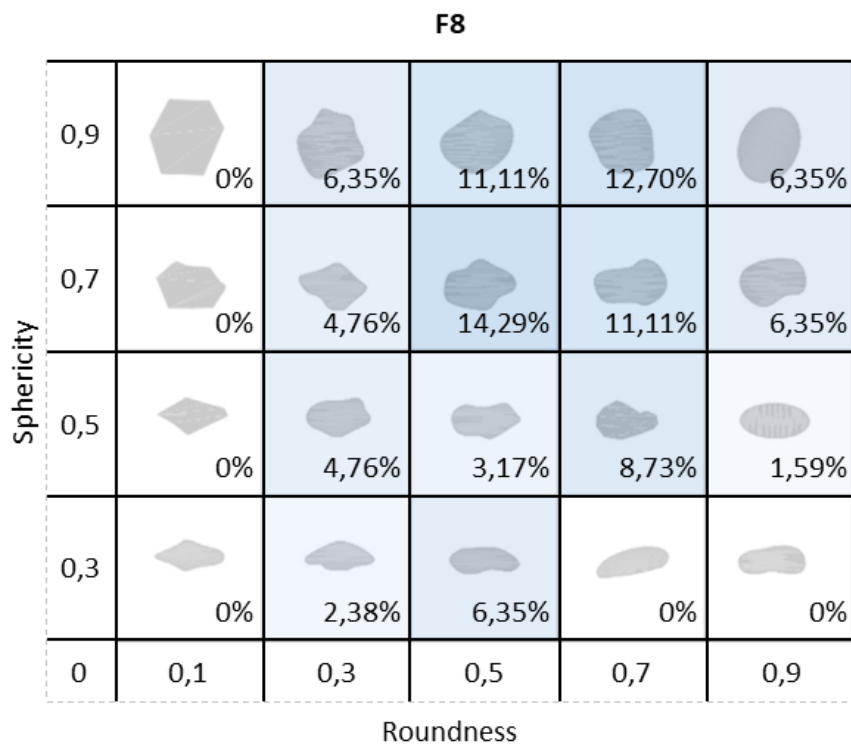
4.2.6 Injectite 7





4.3 Formations

4.3.1 Brentskardhaugen Bed





4.3.2 Carolinefjellet Formation

